Radiation therapy induced effects on lymphocyte subpopulations and prognostic value of CD69, PD-1 and PD-L1 in the peripheral blood of patients with advanced HNSCC

von

Christina Lucia Muggenthaler

Inaugural-Dissertation zur Erlangung der Doktorwürde

der Tierärztlichen Fakultät der Ludwig-Maximilians-Universität

München

Radiation therapy induced effects on lymphocyte subpopulations and prognostic value of CD69, PD-1 and PD-L1 in the peripheral blood of patients with advanced HNSCC

von Christina Lucia Muggenthaler

aus Ronsberg

München 2021

Aus dem Veterinärwissenschaftlichen Department der Tierärztlichen Fakultät der Ludwig-Maximilians-Universität München

Lehrstuhl für Tierphysiologie

Arbeit angefertigt unter der Leitung von: Univ.-Prof. Dr. Thomas W. Göbel

Angefertigt in der Klinik für RadioOnkologie und Strahlentherapie des Klinikums Rechts der Isar der Technischen Universität München (TUM) im Rahmen des Projekts *HNprädBio* des Deutschen Konsortiums für Translationale Krebsforschung (DKTK)

Leitung: Univ.-Prof. Dr. Stephanie E. Combs

Mentor: PD Dr. rer. nat. Mathias Gehrmann

Gedruckt mit Genehmigung der Tierärztlichen Fakultät

der Ludwig-Maximilians-Universität München

Dekan:	Univ.-Prof. Dr. Reinhard K. Straubinger, Ph.D.
Berichterstatter:	Univ.-Prof. Dr. Thomas W. Göbel
Korreferent:	Univ.-Prof. Dr. Benedikt Sabaß

Tag der Promotion: 17. Juli 2021

Meiner Familie & Tano

TABLE OF CONTENTS

I. List of Abbreviations

χ2	Chi-Square test
AJCC	American Joint Committee on Cancer
APCs	antigen presenting cells
APC	allophycocyanin
BSA	bovine serum albumin
CD4	cluster of differentiation on the surface of T helper cells
CD8	cluster of differentiation on the surface of cytotoxic T cells
CD69	cluster of differentiation on the surface of lymphocytes early after activation
CI	confidence interval
COX	cyclooxygenase
CPV	canine papillomavirus
CT	computed tomography
CTC	circulating tumor cell
ctDNA	circulating tumor DNA
CTLA-4	cytotoxic-T-lymphocyte associated protein 4
cTNM	clinical TNM
CTRL	control group/healthy donor
DHL	Dalsey, Hillblom and Lynn
DKTK	Deutsches Konsortium für Translationale Krebsforschung
DNA	deoxyribonucleic acid
EBV	Epstein-Barr virus
ECM	extracellular matrix
EDTA	ethylene diamine tetraacetic acid
EGFR	epidermal growth factor receptor
ELISA	enzyme-linked immunosorbent assay
FACS	fluorescence activated cell sorting
FCS	fetal calf serum
FDA	Food and Drug Administration
FeLV	feline leukemia virus
FITC	fluorescein isothiocyanate
FIV	feline immunodeficiency virus
FNA	fine-needle aspiration
FoxP3	forkhead box P3
FSC	forward scatter

xg	gravity
GERD	gastroesophageal reflux disease
gMFI	geometric mean fluorescence intensity
Gy	Gray
H2O	water
H2O2	hydrogen peroxide
H2SO4	sulphuric acid
HER-2	human epidermal growth factor receptor 2
HIV	human immunodeficiency virus
HNprädBio	short title of study 'Prospektive Radiochemotherapie-Studie bei Kopf-Hals-Plattenepithelkarzinomen im DKTK'
HNSCC	head and neck squamous cell carcinoma
HPV	human papillomavirus
HRP	horseradish peroxidase
IFN	interferon
IgG	immunoglobulin G
IL	interleukin
ILC	innate lymphoid cell
irAE	immune-related adverse event
LL	lower left
LR	lower right
M	metastasis
Mdn	median
MDSC	myeloid-derived suppressor cell
MHC	major histocompatibility complex
microRNA	micro ribonucleic acid
MRI	magnet resonance imaging
MST	median survival time
n	number
N	node
NBI	narrow band imaging
NK	natural killer
NK-like	natural killer-like
OLP	oral lichen planus
OR	odds ratios
p	significance level
p16	tumor suppressor gene p16INK4a
p53	tumor protein p53

p_{adj}	adjusted p-value
PBMC	peripheral blood mononuclear cell
PBS	phosphate buffered saline
PCR	polymerase chain reaction
PD-1	programmed cell death protein 1
PD-L1	programmed cell death ligand 1/CD274
PD-L2	programmed cell death ligand 2/CD273
PE	phycoerythrin
PerCP	peridinin-chlorophyll-protein complex
PET	positron emission tomography
PHA	phytohemagglutinin
pTNM	pathological TNM
R0	blood draw before treatment
R1	blood draw during chemoradiotherapy
R2	blood draw 3 months after chemoradiotherapy
R3	blood draw 6 months after chemoradiotherapy
R4	blood draw 12 months after chemoradiotherapy
R5	blood draw after recurrence
SCC	squamous cell carcinoma
SHP-1	Src homology region 2 domain-containing phosphatase-1
SHP-2	Src homology region 2 domain-containing phosphatase-2
SPSS	Statistical Package for the Social Sciences
SSC	side scatter
Stat1	signal transducer and activator of transcription 1
T	tumor
TCR	T cell receptor
TIL	tumor-infiltrating lymphocyte
TIM3	T cell immunoglobulin and mucin domain-containing protein 3
TME	tumor microenvironment
TNF	tumor necrosis factor
TNM	TNM classification of Malignant Tumors
Treg	regulatory T cell
UICC	Union for International Cancer Control
UL	upper left
UR	upper right
UV	ultraviolet
VEGF	vascular endothelial growth factor
z	standard score

II. List of Figures

III. List of Tables

1. Introduction

Worldwide almost 25 million patients have been diagnosed with cancer in 2017, approximately 10 million patients have died because of their cancer disease. [1, 2] Overall, men are to a little extent more likely to be diagnosed with invasive cancer during the course of their life than women [3], another source reports about a 20% elevated incidence rate in men when comparing all sorts of cancers. Worldwide cancer death rates are similarly up to 50% higher for men compared with women. In conclusion about 20% of men and 17% of women will develop cancer during their lifetime whereas 12.5% of men and 10% of women subsequently will die from the disease. [2]

Approximately 3 percent of estimated new cancer cases in 2020 have their origin at oral or pharyngeal sites, whereas 72 percent of those cases afflict male individuals. Nearly 1.8 percent of estimated cancer deaths in 2020 are related to oral or pharyngeal cancer, of which also 72 percent are male patients. [3] Incidence of developing cancer at sites of the oral cavity and pharynx in the United States is increasing among 29–49 year-old men (1.2%) and women (0.7%). [4] Global new cancer cases and deaths related to sites of the head and neck are displayed in Table 1.

Table 1: Global new cases and deaths in 2018 resulting from sites of the head and neck

	New Cases	**Deaths**
Lip and oral cavity	354,864	177,384
Nasopharynx	129,079	72,987
Oropharynx	92,887	51,005
Hypopharynx	80,608	34,984

Source: [2]

Survival rates for patients suffering from squamous cell carcinoma of the head and neck have not improved during the past fifty years regardless of major advances in oncology. [5, 6] Therefore, research on prognostic biomarkers for more individual treatment schedules remains mandatory to improve overall prognosis

for patients. This study examines the effects of radiation therapy on lymphocyte subpopulations during the course of treatment with irradiation as well as the prognostic capabilities of early activation marker CD69, immune checkpoint receptor PD-1 and its ligand PD-L1.

1.1. Squamous cell carcinoma of the head and neck (HNSCC)

Head and neck cancers emerge from parts of the upper aerodigestive tract: The lip and oral cavity, nasal cavity and paranasal sinuses, oropharynx and hypopharynx as well as pharynx and larynx. Cancer can also arise from major and minor salivary glands and lymph nodes of the head and neck. [7-9] About 90 percent of head and neck cancers are squamous cell carcinomas. [8] This typical type of head and neck cancer has its origin in the surface squamous epithelium of the mucosal lining and is categorized as malignant. [8-10] Epithelial malignancies of the head and neck show a heterogenous behavior. [9] HNSCC takes seventh place regarding cancer-related deaths, survival rates do not seem to have improved over the course of half a decade. [5, 6, 9]

1.1.1. Risk factors

Smoking and alcohol consumption

Since as early as 1988, alcohol and tobacco consumption have been well known risk factors for the development of HNSCC. [11] With almost three quarters of all cancer diseases of the upper aerodigestive tract being related to tobacco and alcohol consumption, smoking and drinking alcoholic beverages are the major contributors. Almost 30% of cases are linked to solely smoking whereas only about 1% can be related to alcohol alone. [12] Alcohol possesses carcinogenic capabilities due to enzymatic reduction to acetaldehyde, mucosal sites of the oropharynx and hypopharynx are especially at risk for cancer induction. [13] For nasopharyngeal carcinomas, risk increases for men who start smoking at an earlier age, smoke more cigarettes per day and have a longer history of smoking. Risk is highest for men with a history of daily smoking of more than 30 cigarettes over the course of more than 30 years. History of smoking is often measured in cumulative pack-years. [14]

When tobacco and alcohol consumption occur combined, the risk for HNSCC at various sites increases tremendously, especially for cancers located in the oral and pharyngeal area. [12, 13, 15] This can be explained due to a better permeation of carcinogenic tobacco components such as nitrosamines, aldehydes and polycyclic aromatic hydrocarbons into mucosal cells after solvation in alcohol. [13] Smoking and consumption of alcoholic beverages have a stronger negative effect on men than women (see Table 2). [11]

Table 2: Increased risk for oropharyngeal cancer according to cigarette and alcohol consumption

	OR for Men	**OR for Women**
Heavy smoking	7.4	-
Heavy drinking	5.8	0.0
Heavy smoking and drinking combined	37.7	107.9

Source: [11] ; Heavy smoking is defined as 40+ cigarettes per day for more than 20 years, heavy drinking is defined as 30+ drinks per week. OR = odds ratio.

Usually, patients are older than 45 years when diagnosed with HNSCC in relationship to tobacco or alcohol consumption. [15]

Also environmental tobacco smoke is recognized as a proven risk factor for HNSCC; direct smoke from cigarettes and alike as well as exhalations of smokers are categorized as environmental tobacco smoke. [16] For example, living with an active smoker – either as a child or as an adult – is correlated with increased risk for nasopharyngeal carcinoma. [14]

After quitting smoking for more than 15 years, smokers can reach risk ratios of never smokers. Even after abstaining for 2 to 14 years, risk for oral cancer decreases to a large extent. [13, 17]

Other risk factors have an important role in the development of head and neck cancer in Europe. [12] One fourth of HNSCC cases cannot be attributed to smoking or drinking alcoholic beverages. [15]

HPV

Worldwide human papillomaviruses (HPV) are cause of annually more than half a million cancer cases in women and 60,000 cancer cases in men. With cervical cancer, anogenital cancer and head and neck cancer, three major cancer sites can be related to HPV infection. 38,000 of these annual cancer cases develop in the region of the head and neck. Especially cancer incidence in the oropharynx is accounted to HPV, approximately one third of oropharyngeal squamous cell carcinoma is caused by HPV infection. [18] Also, HPV-caused cancer cases in the oral cavity and larynx occasionally occur (less than 4%). [18, 19] The number of oral infections with papillomaviruses causing oropharyngeal cancer is accelerating in several countries, especially in male individuals. [20]

Most HPV-caused oropharyngeal squamous cell carcinomas are positive for HPV16, whereas HPV18, HPV33 and HPV35 can be detected as well as HPV6, HPV11, HPV31, HPV45, HPV52 and HPV58. [18, 19] Together, HPV16 and HPV18 constitute 85% of head and neck cancer cases caused by human papillomaviruses and are referred to as high-risk HPV types. [18, 21]

Worldwide, cancers attributable to HPV infection vary vastly, with highest HPV16 prevalence in the United States, moderate prevalence in Europe and lowest prevalence in Brazil. [19] Concludingly, more developed countries are more prone to HPV-related squamous cell carcinoma of the head and neck, whereas incidence in developing countries is lower or not known. [18] In western countries oropharyngeal cancer has increased three-fold, affecting younger patients who do not particularly smoke or consume alcohol. [22, 23]

Genomic analysis reveals that HPV-positive tumors differ biologically from HPV-negative tumors. [24] Prophylaxis via HPV vaccination could prevent a large amount of cancer incidences caused by HPV, including squamous cell carcinomas of the head and neck. [18, 19]

Other risk factors

Oral microbiome: Large quantities of *Corynebacterium*, *Klingella* as well as other genera and species can be related to reduced risk for HNSCC, especially when HNSCC is linked to smoking and laryngeal cancer. [25] Also, *S. anginosus* –

predominantly located in dental plaque and the gingiva – is often detected in patients with oral squamous cell carcinoma and might be linked to HNSCC carcinogenesis, though those malignancies cannot solely be attributed to *S. anginosus* infection. [26-28]

Oral lichen planus (OLP): These premalignant lesions caused by chronic inflammatory medical conditiocmns have been suggested to promote malignant transformation to HNSCC in about 5 of 100 patients whilst causes therefore are unknown. Particularly, erythematous erosive lesions show progression to cancer. [16, 29]

Diet: Frequently consuming fresh fruits and vegetables supplies the body with antioxidants which decrease the risk for malignancies of the head and neck as well as contribute to preventing mucosal damage due to oxidative stress caused by smoking and/or alcohol consumption. [13, 16, 30] When consumed frequently, carotene-rich vegetables such as fresh tomatoes, carrots and green peppers might be the most valuable contributors of protecting antioxidants and show a risk reduction of oral and pharyngeal cancers. [16, 31] Eating preserved meats with elevated nitrite levels more frequently increases the risk for undifferentiated nasopharyngeal tumors. Supplementing the body with more vitamin C reflects a decreased risk for differentiated squamous cell carcinomas, mostly for non-smokers or ex-smokers. [32] Preferring fish and oil over meat and butter might also have protective qualities. [33]

Gastroesophageal reflux disease (GERD): It has been suggested that GERD might be causal to squamous cell carcinoma of the larynx and pharynx due to permanent mucosal damage caused by gastric fluids arising from the esophagus. [16, 34-36] Rate of diagnosing GERD is doubled for patients suffering from cancers of the larynx and pharynx compared with healthy individuals. The risk for laryngeal and pharyngeal malignancies is twice as high with a condition of GERD, though only 5 to 14 percent of laryngopharyngeal cancers can be linked to GERD. [36]

Epstein-Barr virus (EBV): Over 90 percent of grown-ups are infected with this herpesvirus, which persists life-long. [16] EBV has been linked to a number of cancers, also in the aetiology of the development of nasopharyngeal carcinoma

EBV might have its part. Depending on geographic variability, nasopharyngeal carcinoma due to EBV develops decades after first infection. [16, 37]

Genetic conditions: Some persons are genetically more susceptible to mutagens than others, this could possibly display an independent risk factor for occurrence of HNSCC in close relatives. [16] Patients suffering from Fanconi anemia – an autosomal recessive condition – have a remarkably elevated risk for several malignancies including cancer of the head and neck, particularly in the oropharynx. [16, 38] Fanconi anemia patients become diseased at a young age with HNSCC displaying aggressive behavior. [39]

Occupation: Exposition to i.e., wood dust, solvents, paint and asbestos might have an influence on the development of HNSCC in the larynx and oral cavity. [16, 40, 41]

Socioeconomic status: Most risk factors are observed in correlation to socioeconomic status. 75% of HNSCC patients have a lower socioeconomic status measured by income and education. Additionally, they are more likely to be prone to established risk factors as tobacco and alcohol consumption, poor diet and oral hygiene. [13, 42, 43]

1.1.2. Clinical symptoms and diagnosis

Clinical symptoms

Clinical symptoms may vary depending on the site of the tumor. In general, neck disease is often observed in relation to HNSCC. [13] Neck disease includes symptoms such as nonhealing ulcerative lesions, dental infection and a neck mass as well as dysphagia and odynophagia. Further signs at presentation might include sinus congestion, globus pharynges, headache, epistaxis and hemoptysis. [44]

Signs often only occur with extensive tumor volume. Common clinical symptoms of various sites of HNSCC are collectively displayed in Table 3. [13, 44, 45]

When HNSCC progresses, systemic symptoms such as weight loss, fatigue, debility and changes in neurocognitive behavior might occur. Further, secondary medical conditions such as aspiration pneumonia and obstruction of airways are possible. Symptoms that typically accompany HNSCC can be confused with benign illness,

i.e. sinusitis or bacterial pharyngitis, and lead to a delay of diagnosis. [44]

Table 3: Clinical symptoms of HNSCC in relation to the tumor site

Site of tumor	Oral cavity	Oropharynx	Hypopharynx	Nasopharynx	Larynx
Clinical symp-toms	pain	pain and feeling of lump in throat	feeling of lump in throat	nasal obstruction (unilateral)	change in voice and hoarseness
	ulcerative lesions	referred otalgia	otalgia (involvement of glossopharyn-geal nerve)	epistaxis	referred otalgia
	impaired tongue movement	impaired tongue movement	palpable neck mass	sinusitis	respiratory difficulties
	problems with dentures	reduced mobility of palate	food sticking	brain invasion (late in disease)	hemoptysis
	decreased opening of mouth		saliva accumulation in hypopharynx		dysphagia/ odynophagia

Source: [13, 44, 45]

Diagnosis

A thorough physical examination including palpation of the head and neck is conducted after anamnesis. As a next step, work up of HNSCC mainly consists of imaging techniques. [23, 46, 47] The purpose of imaging techniques is to determine the extent of the tumor, to rule out distant metastasis or another primary tumor. [44] Most of the times computed tomography (CT) is the chosen imaging method, but also magnet resonance imaging (MRI) can be selected. MRI is especially contributing to the imaging of cancer of the nasopharynx and advanced cancers of the larynx. Combined PET/CT scans might be helpful in the diagnosis of advanced stages while endoscopy might be a useful asset for early diagnosis. [23, 46, 47] Narrow band imaging (NBI) might be helpful to distinguish malignant from benign lesions when used by appraised endoscopists. [47] An X-ray of the chest aids to the assessment of distant metastases in this area. [45, 46] Moreover, a biopsy under local or general anesthesia with histopathological classification is often helpful for diagnosis. [45, 48]

The stage at diagnosis has relevant prognostic value on treatment success. [13] In almost half of HNSCC cases, the cancer has already progressed to an advanced stage until diagnosis. [49] In particular, cancers of the oropharynx and hypopharynx are presented at a late stage with nodal metastases. [45, 50] Therefore, the disease is often not curable with therapy and patients often experience recurrence or distant metastasis. [49]

1.1.3. Localization, metastasis and staging

Localization

Cancers of the head and neck mainly arise from following parts of the upper aerodigestive tract [7-9]:

lip and oral cavity	nasal cavity and paranasal sinuses	oropharynx	hypopharynx
pharynx	larynx	major and minor salivary glands	regional lymph nodes

Around three quarters of squamous cell carcinomas in the oral cavity are located either in the floor of the mouth, the tongue or the retromolar triangle. The localization in the ventral part of the mouth might be reasoned by carcinogens which primarily gravitate to the mucosal area of the mouth. Oropharyngeal tumors are mainly detected in tonsils or the associated fossa, additionally they can originate from the base of the tongue. Cancer of the minor salivary glands is found on the lateral wall of the pharynx as well as on the surface of the soft palate. [45]

Regularly, head and neck cancers behave relatively predictable. Tumors preferably spread locally and regionally. With increasing nodal enlargement and extracapsular extension HNSCC is more likely to disseminate with the blood stream. Distant metastases are not commonly detected which has a positive impact on treatment and prognosis. [23]

Metastasis

Since HNSCC patients tend to experience locoregional recurrence, a second primary tumor or even distant metastasis, almost every second patient will die in the following 5 years after diagnosis. [51] Almost 90% of patients with distant

metastatic spread are diagnosed within the first and second year, even with adjusted treatment median overall survival time clearly averages under 1 year. [52, 53]

Usually, patients are already suffering from advanced disease with metastasis to the lymph nodes; only every third patient is diagnosed with HNSCC at an early stage. [51] Diagnosis at an earlier stage is related to a better prognosis, nodal status can be identified by histopathologic examination. [51, 54]

Metastasis commonly begins by spreading to lymph nodes in the head and neck area, most probably the cervical lymph node is affected by regional metastasis. [51, 54] Smallest detectable size of metastasis is a diameter of 2mm, especially primary tumor sites of lip and tongue can be related to enlarged cervical lymph nodes. [54] Also, the depth of tumor invasion and degree of differentiation is directly related to nodal metastasis in the neck. [55] Tumors with poor differentiation are correlated with inferior distant control, whereas distant control is better for HPV-positive oropharyngeal squamous cell carcinoma compared with other types of HNSCC. Furthermore, increasing N classification in the TMN staging system as well as extranodal extension are negative factors for the emergence of distant metastasis. [52]

Distant metastases can commonly be detected in the lung, liver, bones, lymph nodes, pleura and skin. Less frequently they spread to the adrenal gland, pancreas, brain, omentum, spleen and soft tissues. [52]

Staging

Defining cancer stage is a basic component of cancer care worldwide. To ensure consistent staging, the American Joint Committee on Cancer (AJCC) staging manual describes guidelines for the staging of tumors – including malignancies of the upper aerodigestive tract. [7] The foundation for cancer staging is the TNM classification system which was first published by the Union for International Cancer Control (UICC) and united with the AJCC staging system in 1987 [56]:

T	N	M
“tumor”	“node”	“metastasis”
size of primary tumor	existence and scope of affected regional lymph nodes	existence of distant metastasis

Nowadays, TNM stage classification is composed of clinical and pathological data leading to a clinical TNM (cTNM) and a pathological TNM (pTNM) system. [7] The current eighth edition of the AJCC staging manual includes three separate chapters regarding head and neck cancers: nasopharyngeal cancer, HPV-positive oropharyngeal cancer and HPV-negative oropharyngeal cancer, to take the multitude of malignancies into account. In recent years research has led to significant changes in the scientific comprehension of HNSCC development and behavior. Thus, the prognostic relevance of newly validated cancer characteristics is taken into account. [7, 57] For example, if either p16 can be detected by immunohistochemistry or presence of high-risk HPV-DNA is confirmed, the tumor is designated as HPV-positive. HPV-positive squamous cell carcinoma of the oropharynx is connected to a better prognosis than HPV-negative tumors, leading to a mandatory test for p16 for oropharyngeal squamous cell carcinoma. [57, 58] Furthermore, involvement of cervical lymph nodes negatively affects the prognosis. [54]

1.1.4. Tumor microenvironment

Beside malignant tumor cells, cancer consists of various additional non-malignant cells located in extracellular matrix (ECM). These surroundings are labeled as the tumor microenvironment (TME). [9] As early as in the 1970s, research stated that the development of a tumor cannot be linked to the genes alone but is also affected by factors such as the primary environment and angiogenesis. [9, 59] Cancer cells interact with the tumor environment in which they are embedded - for instance by secretion of soluble factors. In order to prevail, tumors are able to create a microenvironment with immunosuppressive characteristics which enables tumor cells to escape detection by the patient’s innate and acquired immune system, mainly interfering with the function of T cells and presentation

of antigens. [9, 60] Furthermore, it has been suggested that the inflammatory process taking place in the tumor microenvironment has an unfavorable impact on tumor growth and disease progression and suppresses the patient's immune system. [9, 61] The extracellular matrix (ECM) for instance provides cytokines, chemokines and growth factors and influences the tumor cells mechanically. [9]

Cell types constantly found in the tumor microenvironment (TME) [9]:

vascular endothelial cells	pericytes	myofibroblasts	specialized cells depending on cancer site
lymphatic endothelial cells	fibroblasts	adaptive and innate immune cells	

HNSCC cancers show a broad spectrum of immune infiltration. For instance, HPV-positive HNSCC shows different immunologic behavior. In the oropharynx elevated levels of T cell infiltration as well as activation of the immune system can be detected; these findings align with the predominant localization of HPV-positive HNSCC at oropharyngeal sites due to the high proportion of lymphoid tissue. [62] The higher levels of immune infiltration in HPV-positive HNSCC might have a favorable prognosis on tumor clearance after radiation therapy. [63, 64] Smoking of tobacco can be linked to local suppression of the immune system as well as to a decline of cytotoxic effects within the tumor microenvironment. [62, 65] Lower immune infiltration can be associated with a higher risk of locoregional recurrence as well as declining overall survival. Dysfunctional T cells with multiple defects regarding activation and function can be identified in circulation and tumor infiltration. [60]

1.1.5. Therapy

For squamous cell carcinoma of the head and neck different treatment options exist, combining modalities like surgery, chemotherapy and radiation therapy. Choosing the adequate therapeutic option for each patient is dependent on the stage of the disease and site of the primary tumor. While either surgery or irradiation are sufficient for malignancies at an earlier stage (stage I and stage II), locoregionally advanced cancer (stage III or stage IV) is treated by combining chemotherapy with surgery and/or irradiation. When metastatic spread has

occurred or after initial irradiation the locoregional recurrent tumor cannot be resected, the modalities are combined for palliative therapy. [9] After performing a neck dissection, lymph nodes of the head and neck can be assessed to identify the patient's risk for neck disease. When nodal disease can be identified, patients undergo radiotherapy or chemoradiotherapy. Chemoradiation therapy is indicated as a primary or neoadjuvant therapeutic option when addressing metastases or tumor invasion in adjacent structures. [66]

Usually, chemoradiation therapy combines radiation therapy from 70 to 100 Gray (Gy) and platinum-based chemotherapeutic agents such as carboplatin or cisplatin. [66, 67] Since HPV-positive HNSCC has a favorable prognosis, treatment de-escalation for HPV-positive tumors is discussed to lead to a reduction of acute and long-term side-effects caused by irradiation. [48]

Cancer cells differ in their molecular characteristics from healthy cells. By identifying those differences, suitable targets can subsequently be addressed in therapy to induce cell death or cytostasis. Targeted therapy though is a difficult venture because of the wide range of possible targets along different growth promoting pathways. [9]

1.1.6. Prognosis

Regardless of changes in treatment, overall survival rates for patients suffering from HNSCC have not improved much over the course of time. [9] After diagnosis, 5-year relative survival measures between 60 and 70 percent for malignancies of the oral cavity and pharynx. Diagnosis at an earlier stage of disease is linked to a better prognosis whereas 5-year relative survival is poor for locoregional advanced or metastatic stage as well as for recurrent disease. [9, 68] Therefore stage at presentation is a crucial factor for the patient's prognosis with worse treatment outcome for advanced disease, especially when HNSCC is not related to HPV infection. [13, 69] Also, the extent of the tumor categorized by the TNM classification system serves as a meaningful prognostic factor. [48]

Additionally, HPV status has a strong impact on the prognosis for HNSCC regarding overall survival, especially when located at oro- and hypopharyngeal subsites. [48, 70] Patients with HPV-positive oropharyngeal carcinoma tend to be

significantly younger and have a significantly better prognosis: 5-year survival for HPV-positive HNSCC amounts to more than 70 percent whereas HPV-negative disease only measures up to a maximum of 50 percent. [22, 71] In general, HPV-positive tumors are more sensitive for radiation therapy, even though patients often have advanced stages at the time of diagnosis. [72, 73]

Mutagenesis due to tobacco consumption accounts as a negative prognostic factor for overall survival. [22, 62] Patients consuming tobacco when diagnosed with HNSCC have a worse survival rate; when comparing with never-smokers, current smokers are 70 times more likely to die whereas ex-smokers have a 40 times elevated risk for death during the follow-up period. [74]

Furthermore, choosing the suitable treatment option has an impact on the patient's prognosis. For instance, radiotherapy alone has a worse overall survival rate by contrast with cisplatin-based chemoradiotherapy. [66] Standard treatment approaches result in various tumor responses since they often do not address molecular characteristics of the heterogenous cancer types. [5] Recurrence and second primary malignancies frequently occur; about every second patient will experience recurrent or metastatic disease within a follow-up period of three years. [5, 63] Limited treatment options are leading to a median overall survival of six to seven months. [5, 75]

Regarding the tumor microenvironment, tumors with higher means of immune infiltration of adaptive immune subpopulations are linked to better overall survival. [62] For HPV-positive HNSCC, especially infiltration with T cells and CD8+ T cells has a positive impact. [62, 67] In contrast, infiltration with subpopulations of the innate immune system negatively contributes to the patient's overall survival, most probably due to inflammatory processes and angiogenesis supporting disease progression. [62] Also, hypoxia within the tumor microenvironment accounts for a negative prognostic factor since radiotherapy is less effective when lacking reactive oxygen species. [64, 76]

1.2. Squamous cell carcinoma of the head and neck (HNSCC) in small animals

Oral tumors are common among small animals and can be located at subsites of the oral cavity, tongue, gingiva, parodontium, pharynx and salivary glands. [77, 78] In dogs, oral neoplasia is the fourth most frequent cancer and accounts for five to seven percent of all tumors, while more than 60% of those tumors are categorized as malignant. [77-80] Up to one fourth of the malignant tumors are squamous cell carcinomas. Neoplasia is also frequently seen in cats, up to 10% are located at oral sites whereas nine out of ten neoplasms are categorized as malignant. Approximately 60% of these tumors are attributable to squamous cell carcinoma. [77] Oropharyngeal neoplasia is more frequently seen in dogs compared with cats with a slight sex predisposition for male dogs and a breed predisposition for, *inter alia*, German shepherds, Chow Chows, Boxers, Weimaraner, Golden retrievers and Gordon setters. [79]

Oral SCC mainly affects animals with middle or advanced age. [78, 81] At the time of diagnosis dogs most probably are around the age of 9. Larger dogs are more susceptible than small dogs with a breed predisposition for German shepherds, Shetland Sheepdogs and English springer spaniels. [77, 78, 82] Oral squamous cell carcinoma is one of the most diagnosed malignancies in cats. On average, cats are 10 to 13 years old upon diagnosis whereas no breed or sex predispositions are obvious. [77, 78, 83, 84]

Nasal tumors are rare in dogs, but frequently affect cats and most likely are categorized as squamous cell carcinoma. [78, 79] Almost 20 percent of all feline skin tumors concern the nasal planum. [78] Incidence of sinonasal SCC is elevated within advanced-aged cats and dogs, for canine patients mean age of diagnosis is around 10 years. [77, 79] Cats are about 9 to 10 years of age around the time of occurrence, mean age for SCC of the nasal planum amounts to 11 to 12 years. [77, 79, 85] Regarding feline patients, approximately 50 percent of all tumors originating from the nasal area affect the nasal planum. [77] Furthermore, over 90 percent of diagnosed nasosinal tumors are malignant. [79]

1.2.1. Risk factors

There exists no known cause for the development of canine and feline oral SCC. [77, 78, 82] Radiation therapy targeting the oral cavity may be seldomly related to tumor development in dogs. [77] White dogs, Poodles, Samoyeds and Labrador retrievers seem to have an elevated risk for squamous cell carcinoma of the tongue. [79] Environmental factors may have an impact on the development of squamous cell carcinoma of the tongue and tonsil for both species. [78] Environmental tobacco exposure has been identified as a risk factor for cancer of the nasal cavity and paranasal sinuses in dogs. [80, 86] Further, increasing p53 expression might be linked to risk of oral SCC in cats but cannot be definitively verified as a risk factor. [77, 79, 83] Additionally, the presence of papillomaviruses, feline leukemia virus (FeLV) or feline immunodeficiency virus (FIV) cannot be verified as a risk factor for cats. [77, 83, 87] In contrast, regarding feline nasal SCC positive p16 immunohistochemical staining might be connected to a more favorable prognosis. [88] Canine papillomaviruses CPV1, CPV2, CPV3, CPV9, CPV12 and CPV16 are sparsely linked to the development of malignancies in single cases. [89-93] For example, immunohistochemistry, PCR or positivity for p16 identify the presence of papillomavirus in viral pigmented plaques in cases of metastatic SCC and chromosomal integration has been discovered for the first time. [92-94] It has been noted that cats experience elevated risk for oral SCC due to wearing flea collars, disorders affecting the teeth and consuming canned cat food, especially tuna. [77, 79, 81, 83, 95]

An elevated risk for neutered cats is identified, whereas neutered males seem to be particularly affected by tumors of the nasal planum. [77] Advanced-aged cats, in particular individuals with poorly pigmented skin in the nasal planum, have a higher risk for the development of nasal malignancies, predispositions for dogs have not been identified yet. [78] The development of SCC of the nasal planum can be traced back to multiple factors, including UV radiation. Feline papillomavirus can be verified by viral DNA or overexpression of p16, a tumor suppressor gene, in almost every second SCC of the nasal planum in cats. [77, 79] Regarding sinonasal tumors and tumors of the nasal cavity, dogs with a long-headed skull seem to have an increased risk, same as for larger

breeds. [78, 79] Also, environmental causes such as exposition to second hand smoke and other pollutants may have an impact. [79] Siamese cats might have a breed predisposition for the disease. [78]

1.2.2. Clinical symptoms and diagnosis

Clinical symptoms

Often the first observed symptom is a mass, further physical symptoms include heavy salivation, bad breath, dysphagia, dental problems such as loose teeth, grooming difficulties in cats, swelling of facial areas, loss of appetite, nasal or oral bleeding and weight loss as well as lymphadenopathy of regional nodes. [77-79] Cancer masses located in the caudal parts of the mouth are seldomly detected by the owner, other cancer related symptoms are present at the time of veterinary examination. [79] Squamous cell carcinomas first resemble a pale plaque and then grow into a fleshy mass or a raised plaque with formation of a central ulcer. [77] Ulceration as well as secondary infections are very common. [77, 84] Malignancies of the tongue are seldomly diagnosed in small animals, often accounted to squamous cell carcinomas and associated with severe pain and functional disabilities. [78, 79] In cats, tumor expression of parathyroid hormone-related protein may be increased and affect bone resorption, paraneoplastic hypercalcemia has been identified in few patients. [79, 84] Typical symptoms of laryngeal malignancies include a progressively changing pitch of voice, dysphagia and exercise intolerance. [79]

Characteristic symptom for cats suffering from SCC of the nasal planum is a crusted, ulcerative lesion. [78, 85] After tumor invasion, bleeding of the lesions is common and local irritation can cause sneezing. Nares might be obstructed due to extensive tumor growth. [78] For canine patients, the nose might appear swollen and/or the nares contracted, most common symptoms include sneezing, ulceration and bleeding. [78, 96] External lesions are usually not visible since the tumor is often located in the mucous membrane. [78, 79] Symptoms for sinonasal neoplasms often occur two to three months before diagnosis and include pain, unilateral nasal discharge (mucopurulent or bloody), nose bleeding, sneezing, stridor/stertor and dyspnea due to obstructed airways, possibly epiphora and

additionally weight loss in cats. [78, 79, 97] After further progression including invasion, facial swelling, exophthalmos, blindness and neurological symptoms might become obvious. [78, 79, 97, 98]

Diagnosis

Most of the times a short general anesthesia is necessary for palpatory examination, performance of imaging techniques and biopsy. [79] For oral tumors, differentiation between neoplastic and inflammatory causes is necessary and is performed by cytologic analysis of deep tissue scraping, fine-needle aspiration or impression smears and excisional biopsy. [77, 79] Ulceration of oral tumors might complicate a definite diagnosis via cytology, immunohistochemistry then is the method of choice for definitive diagnosis and for the detection of prognostic factors leading to a suitable treatment approach. [77] Histology can confirm the presence of oral squamous cell carcinoma and divides the disease into five subtypes correlated with varying clinical behavior and prognosis. [77, 78] Imaging techniques such as radiography, CT and MRI are convenient to rule out metastatic spread and to stage tumors since oral neoplasia frequently infiltrates bony adjacent structures. [77-79] In radiographs, bone lysis is only detected at an extent of cortex destruction above 40 percent. CT and MRI aid to an improved evaluation of tumoral extension into the orbit, nasal cavity and caudal pharynx. [79] To assess metastatic spread to regional lymph nodes, fine-needle aspiration is an appropriate tool. [77-79] Excisional biopsy and histological examination of regional lymph nodes might be more powerful for the evaluation of metastasis. [99] In addition to palpation, ultrasonography might aid to the assessment of the primary tumor as well as the regional lymphonodal size though the size of lymph nodes cannot predict metastasis. [77, 79, 99] When diagnosed, squamous cell carcinomas of the oral cavity are often already staged as advanced and infiltrating surrounding structures. [77]

While radiography might be beneficial for dogs suffering from extensive tumors of the nasal planum affecting bony structures and the nasal cartilage, it is not conveniently used for cats. [78] Cytological diagnostics like scraping or fine-needle aspiration have not proven to be helpful, a biopsy is of greater use for histological assessment of the lesion and depth of invasion. [78, 79] CT and MRI might be used

to improve tumor staging and defining the localization for further treatment in dogs. [79] For sinonasal SCC, radiography is a valuable option to assess the nasal cavities and to rule out metastasis to the thorax. Other imaging techniques like CT and MRI present more detail on the tumor localization and adjacent structures. Diagnostic biopsy samples can be gained with or without endoscopy and are further analyzed histologically. [78, 79] Poor keratinization is often obvious in sinonasal squamous cell carcinomas. [77] Cytological assessment of conspicuous lymph nodes should be performed with fine-needle aspiration samples. [78, 79]

Tumors of the tongue require a biopsy and fine-needle aspiration of regional lymph nodes. Further, ultrasonography can be used to assess resectability. Metastasis to the lung should be ruled out by thoracic radiography. For laryngeal malignancies, a biopsy is performed since a too small sample size or cytologic diagnostic alone might render a false result. While radiography is able to point out the tumor's localization, CT imaging is more precise. [79]

1.2.3. Localization, metastasis and staging

Localization

Usually, canine oral SCCs affect the mandibular and maxillary gingiva, less frequently also subsites of the pharynx, soft palate and lips. [77, 82] In almost three out of four cases of canine oral SCC, infiltration of the bone is observed at the time of diagnosis. [77, 79] Oral SCC in cats usually develops at sublingual, maxillary and mandibular subsites, with sublingual oral SCC frequently developing in close proximity to the frenulum. [77] Less frequent sites of oral SCC are the pharynx, larynx, soft and hard palate as well as the lip. [77] Also, in cats, oral SCC frequently infiltrates into adjoining bones. [77, 79] Canine nasal tumors regularly extend into the nasopharynx, frontal sinuses and caudal recesses. [97] In cats, tumors of the tongue are often located in proximity to the frenulum. [79]

Metastasis

Canine oral SCC is not connected with a high rate of metastasis, less than 15 percent show metastasis to the regional lymph nodes. [77, 78, 81] In general, metastasis is reported for canine patients in approximately every fifth case, excluding tonsillar SCC, with a higher metastatic potential for caudally located

cancer. [79] For tonsillar SCC, higher metastatic rates are reported. [82] In few feline cases, metastasis to regional lymph nodes has occurred at the time of diagnosis. [77, 79] Feline oral SCC tends to metastasize only after a longer time of disease progression; management of local recurrence is a greater challenge due to restricted quality of life. [83] A secondary infection and ulceration negatively impact necrosis of adjacent structures. [77] Tumors of the tongue show aggressive behavior and often infiltrate the full thickness of the tongue at the time of diagnosis. The disease of the tongue often spreads to lymph nodes, also metastasis is frequent. [78, 81] SCC of the nasal planum in the cat slowly progresses over the course of several months, finally presenting with invasive behavior and uncommonly metastatic spread. [78, 79] For dogs, tumor progression occurs faster and also local as well as regional lymphonodal metastasis are possible. [78] Also, sinonasal malignancies tend to metastasize slowly, especially to regional lymph nodes and the lung, invasive behavior and local tumor recurrence are more frequent. [78, 79] Bone invasion is often detectable early after initial diagnosis. In dogs, laryngeal SCC tends to be locally invasive and shows metastatic behavior. [79]

Staging

For staging, often a modified human TNM classification from 1980 is used for oral tumors in small animals. On basis of variable sizes of the canine oral cavity staging leads to a disadvantage in favor of stage III tumors and prevents differentiation of prognosis between stages. Prognostic factors for small animals are not as well-known as for humans. So far, clinical staging in small animals has only shown limited advantages in defining the patient's prognosis. Histological staging based on the subtype and grade of the tumor may provide useful information for prognosis. [77]

1.2.4. Therapy

Various treatment approaches exist for canine oral SCC, such as surgery, radiotherapy, chemotherapy and photodynamic therapy as well as combination treatments. [77, 82] Most common therapeutic approaches are surgical resection (with margins of a minimum of 2cm for dogs and greater than 2cm for cats) and

radiotherapy. [79] Surgery is a very effective therapeutical approach for oral cancer. When bone infiltration has occurred, hemi-maxillectomy or mandibulectomy are necessary for the surgical approach to prevent local recurrence. [77-79] While dogs tolerate the resection of the facial bone well, cats might suffer from post-surgical morbidity. [78] After surgery, complications such as heavy salivation, nose bleeding, eating difficulty, mandibular drift and malocclusion might occur. [79]

Radiotherapy can be applied as a single modality treatment or in combination with surgery and obtains a good penetration of the canine bone. [77-79] When tumors have a too large extent to be successfully excised, radiation therapy alone is indicated. [79] Furthermore, affected regional lymph nodes can be additionally targeted. [78] Regarding feline patients, radiotherapy as a sole treatment is not sufficient for tumor control. [79] For canine and feline patients, combining surgical treatment with post-operative radiation therapy might present the most beneficial treatment. [78, 79, 100] Mucositis is a very common and painful acute side effect caused by radiotherapy and can lead to refusal to eat and drink requiring supportive care. Possible late side effects are xerostomia less clinically significant compared with humans and seldomly the development of oronasal fistulas and osteoradionecrosis. [79]

Also, cryosurgery has been described for neoplasia smaller than 2cm in diameter and without extensive bone invasion. Platinum-based chemotherapy is applied intravenously for patients suffering from more aggressive tumors such as tonsillar SCC and canine patients with metastasis. [79] For feline patients, chemotherapy alone could not provide effective outcomes and cisplatin is contraindicated. [79, 100] A protocol consisting of piroxicam and a platinum-based drug (cisplatin or carboplatin) might improve prognosis for feline and canine patients. [79]

Euthanasia is mainly chosen for reasons of the patient's discomfort and pain. Surgery including mandibulectomy or radiotherapy in combination with carboplatin-based chemotherapy are applied to extend survival times for cats. To a high percentage, feline patients need to be euthanized since the malignancy leads to systemically significant constraints such as difficulty in breathing,

dysphagia and loss of appetite. Therefore, median survival rates of cats are as short as one to two months. [77]

Regarding squamous cell carcinomas of the nasal planum, the lesion's extent should be taken into account when choosing a suitable therapy. After deep tumor invasion, solely surgery is an effective therapeutic approach. [78, 79] Functional and cosmetic reconstruction are necessary after excision, results are favorable for cats whereas tumors in dogs tend to have invaded and extended to a greater extent when diagnosing SCC of the nasal planum. [78, 79, 101] For incomplete excised tumors, post-operative radiotherapy has been applied. [78, 79] Superficial radiation techniques might lead to favorable outcomes for superficial SCCs in cats. [78] A superior recurrence free and overall survival time is reported for smaller cutaneous squamous cell carcinomas of the nasal planum. [102] For sinonasal SCC, treatment options are sparse due to adjacent critical organs and focus on local disease control. Surgery might be possible though most nasal SCCs cannot be fully addressed by surgery alone. [78, 79] Therefore, radiotherapy most of the times is the suitable treatment option, either alone or in combination with surgical cytoreduction after radiation therapy. [78, 79, 103] Radiation dosage is mostly limited because of adjacent skin, oral mucosa and eyes. [78, 79]

For tumors of the tongue, glossectomy is necessary with a minimum of 50% of the tongue remaining in the oral cavity. [78, 79] Impaired grooming function in cats leads to a decreased hair-coat hygiene. [79] Since the tongue is especially sensitive to ionizing radiation, toxic side effects are very common. [78] Laryngeal SCC might possibly be surgically removed or, when invasive behavior is obvious, treated with radiation therapy to ensure laryngeal functionality after treatment. Chemotherapy may also be a beneficial approach. [79]

1.2.5. Prognosis

All in all, the prognosis for dogs suffering from oral SCC is favorable. [79] Younger age, complete tumor excision, smaller diameter and rostral location of the malignancy are possibly linked to an improved prognosis regarding canine oral SCC. [77-79, 100, 104] For canine patients undergoing radiation therapy, the type and size of the tumor are relevant factors regarding tumor control. [79] Dogs show

a significantly improved median survival time (MST) for post-operative radiation therapy when complete excision is impossible. [105] Generally, after curative surgical therapy canine patients experience a long disease-free period of more than 2 years. [77] For dogs treated surgically, death risk declines more than 90 percent and 1-year survival amounts to over 90 percent when comparing with untreated dogs suffering from oral SCC. [106] Hence, complete surgical resection should be regarded as the gold-standard therapeutic approach. [105] Cancer recurrence mainly occurs due to incomplete surgical resection in about three out of five cases. [79]

For cats, prognosis for oral SCC is less favorable compared with dogs due to fast recurrence. Local recurrence occurs in more than 85 percent of patients. [79] Location and extent of the tumor may aid as a prognostic factor, with maxillary location of the disease linked to a better prognosis for feline patients. Immunohistological staining showing a patchy cyclooxygenase (COX)-1 pattern may also relate to an improved prognosis when comparing with diffuse COX-1 staining. Papillomavirus among small animals is less likely a prognostic factor for oral squamous cell carcinoma, even though immunohistochemical staining for p16 could aid to the prognosis of cutaneous squamous cell carcinomas in cats. [77]

The tumor size and extent of tumor invasion define the prognosis for squamous cell carcinoma of the nasal planum. When detected at an early stage without extension to the lip or tumor invasion, prognosis for feline patients is favorable, the forecast for invasive tumors should be cautiously worded. [78, 79, 85] For dogs, prognosis is fair to good, surgical approach might lead to an overall survival rate of 1 to 4 years. [78, 79, 107] Complications after planectomy such as dehiscence are common, some dogs need to undergo revision surgery. [107] Cats and dogs even show long survival time without therapy, since SCC of the nasal planum seldomly metastasizes. [79] Sinonasal SCC is linked to an unfavorable prognosis when untreated; euthanasia is often necessary within quarter to half a year due to local tumor progression. Though sinonasal SCC often cannot be cured and recurrence is frequent, after radiotherapy overall survival times without disease specific symptoms amount up to 1 year in every second patient. [78] For cats, overexpression of p16 is linked to an improved prognosis for nasal SCC. [77]

For canine patients suffering from nose bleeding, prognosis might be demeanor. [79]

Depending on the site, type and staging, for tumors of the tongue, prognosis is less favorable with frequent lymphatic invasion and regional lymphonodal metastasis up to 40% in dogs. [77-79]

1.3. Dogs and cats as animal models of human HNSCC

Different animal models have been established to study HNSCC; no animal model on its own is suitable for further analysis of HNSCC development and treatment of the disease. [108, 109] Hamster, mouse and rat (i.e. hamster cheek pouch model) are used as a traditional model for cancer development and therapeutic approach for strategic disease prevention. Utilization of genetically modified mice as in vivo models aid to examine the function of specific genes and their modification throughout the pathogenic process in humans. [108] To investigate HNSCC with infiltration of adjacent bone, mouse orthotopic models are very useful. [108, 110, 111] To develop and validate numerous novel therapeutic strategies, including immunotherapy, traditional animal models (rodents) have come to use. [108] Disappointingly, severe limitations are noted [108, 112]: Clinical responses cannot be reliably predicted and sufficient lymphonodal metastasis cannot be induced in rodents. [108]

Spontaneous development of malignancies in companion animals have a strong resemblance of clinical and molecular patterns compared with human cancer. Artificial reproduction of these common grounds in a laboratory environment appears impossible. [83] Regarding the incidence, analogic clinical behavior, therapeutic approach and cancer biology, oral SCC in cats is regarded as a meaningful and promising animal model for human HNSCC. [83, 108, 113] Similarities further concern factors such as frequent occurrence, advanced age at diagnosis, upregulation of EGFR expression, modified expression of p53, hypoxia in the tumor microenvironment, cancerous angiogenesis as well as bone invasion and osteolysis. [83, 100, 108, 113, 114] While for other species development of lingual SCC is fairly uncommon, humans and cats can suffer from this disease. [100, 108] In comparison with the lateral location of human lingual SCC,

the disease is located ventrally in cats. [108] HNSCC of cats and humans show resistant behavior towards chemotherapeutic modalities, furthermore tumor resection with adequate histological margins is hard to achieve. [100] As noted, mankind and cats have several genetic and pathophysiologic characteristics in common. Consequently, cats might present a useful spontaneous model in a veterinary clinical setting regarding HNSCC in regard of translational research for further understanding of HNSCC and novel therapeutic approaches. [83, 108, 113]

Same as for cats, spontaneous canine HNSCC presents a significant animal model for human HNSCC, since molecular characteristics including the tumor microenvironment, genetic character and pathways connected to the tumor, progression of disease, and response to administered treatments behave similarly. [115, 116] Such as infiltrative human HNSCC, poor differentiation of canine squamous cell carcinoma of the head and neck might be connected to faster tumor progression. [108] Investigation of the involvement of canine papillomaviruses, i.e. CPV1, in the tumorigenesis in spontaneous dog models might not contribute to further assessment of HPV-positive human HNSCC. [117] Results from translational studies with dogs might help to develop novel therapeutic approaches in humankind. [115, 116]

1.4. Radiation therapy

Soon after discovering radiography, ionizing radiation has been used as a therapeutic approach for cancer and some other diseases. Nowadays, every second cancer patient undergoes radiotherapy. Gray (Gy) is the measuring unit for the dose of radiation and describes the energy which is absorbed by the targeted tissue (J/kg). Ionizing radiation causes a dose dependent amount of DNA damage leading to cell death. Total radiation dosage is split into smaller fractions, often administered to patients on a daily basis. Due to sparing healthy tissue fractionation facilitates the use of a higher total radiation dosage leading to the death of an elevated number of tumor cells. On the contrary, fractionation elongates the time of radiation therapy giving an advantage to cancer cells to repopulate healthy tissue. [118] The classification of fractionation types depending on radiation dosage is outlined in Table 4.

Table 4: Fractionation of radiation dosage in radiotherapy

fractionation	hyperfractionation	standard	hypofractionation
Gy/day	< 1.8	1.8-2	> 2

Source: [118]

The biological response of tissue to radiation therapy is described by the 5 Rs. [119, 120] Since immunotherapy is gaining popularity as an additional therapeutic approach for cancer diseases, a 6th R has been proposed (see Table 5). [119]

Table 5: The Rs of radiation therapy

1	**Repair** of induced DNA damage
2	**Re-assortment** of cell cycle towards radiation-sensitive mitosis
3	**Repopulation** of tumor cells between administration of radiation
4	**Re-oxigenation** for improved radiation sensitivity
5	**Radiosensitivity** defining tumor response
6	**Reactivation** of the immune system

Source: [119]

Usually, adjacent healthy tissue limits the total radiation dosage which can be administered to the patient. Ionizing radiation can lead to well-known acute and late side effects. [118]

1.4.1. Effects of ionizing radiation

Ionizing radiation leads to damage of the DNA and stimulates the production of reactive oxygen species eventually causing cell death. Furthermore, radiotherapy activates potent immune responses directed towards the tumor. For instance, expression of major histocompatibility complex (MHC) class I is enhanced leading to an improved tumor-specific immune response. Additionally, dendritic cells experience more frequent activation as well as migration and lymphocyte

infiltration in the tumor is improved (see Table 6). [64, 67, 121]

Conversely, ionizing radiation can lead to an elevation of regulatory T cells (Treg) which help to suppress the immune response and show resistant behavior towards cisplatin. [64, 121, 122] An elevation of myeloid-derived suppressor cells (MDSCs) has a negative impact due to suppression of the immune response (see Table 6). [123] Also, immune checkpoint ligands such as PD-L1 can be expressed on cancer cells more frequently. Elevated levels of PD-L1 expression might negatively influence the patient's immune response and interfere with radiation-induced positive effects on the immune response. [64, 124]

Table 6: Radiation induced effects on tumoral immune response

positive effects	negative effects
↑ antigen cross-presentation	↑ regulatory T cells (Tregs)
↑ Type I interferon	↑ myeloid-derived suppressor cells (MDSCs)
↑ major histocompatibility complex (MHC) class I	↓ depleted and exhausted T cells and inhibited T cell reaction

Source: [64, 67]

1.4.2. Site-specific side effects in patients with HNSCC

Up to 5 out of 100 patients are affected by side effects caused by ionizing radiation during radiation therapy, whereas the radiation intensity has a large impact on the incidence of side effects. [125]

Adverse effects of ionizing radiation can be divided into acute and late side effects. Acute side effects typically appear during or in the following weeks after radiotherapy and affect tissues with high turnover rate of cells (i.e., mucosa or skin) leading to diseases such as hematopoietic cytopenia, mucositis and desquamation. [118, 126] Acute side effects commonly disappear within weeks or months after therapy, but enormous toxicity might lead to late side effects. [126, 127]

After a longer period of time, radiation therapy can cause ulceration, fibrosis, atrophy, neural or vascular damage or even dysfunction of organs. [118, 126] Late

side effects develop months or even years after radiation therapy and mainly affect tissues with a lower cell turnover rate. Late side effects normally show a progressive behavior and have a life-long impact on the patient's well-being and quality of life. [126] Additionally, ionizing radiation can cause mutations of the DNA leading to the development of further malignancies. Radiation-induced cancer usually emerges years after treatment with radiation. [118]

Mucositis is a very common side effect of radiotherapy targeting the head and neck; more than 60% of HNSCC patients experience enormous mucositis while undergoing chemoradiotherapy. About half of those patients cannot finish their scheduled therapy because of the severe side effects of mucositis including pain from inflammation and ulceration, nutritional difficulties and intense secretions potentially leading to nausea, vomiting and gagging. [126-128] Bacteremia and sepsis can be a secondary side effect since pathogens can enter the bloodstream at sites of ulceration. [128]

Since minor and major salivary glands are sensitive to radiation, another frequently seen side effect is xerostomia. The lack of saliva has an influence on nutritional intake, swallowing function, taste, dental health and the ability to speak properly. [126, 128] Patients experience xerostomia early after receiving as little as a few radiotherapy fractions and also, xerostomia is often a late side effect profoundly impacting the patient's life. [126, 127] Another late side effect caused by ionizing radiation is hypothyroidism, becoming obvious in approximately every fifth patient only after five to ten years after therapeutic radiation. [127] Further potential late side effects are loss of hearing, trismus and thinning of mucosal tissue. [126, 127]

Radiation dermatitis refers to an inflamed skin due to radiation toxicity. It usually develops in the following few weeks after the beginning of radiotherapy. A progressing erythema can develop into patchy desquamation and in few cases into stronger desquamation and ulceration. Almost every HNSCC patient undergoing radiotherapy is affected by radiation dermatitis to a certain degree; severe manifestations are rare. [128]

Lymphedema and fibrosis might result after surgery or radiotherapy possibly leading to chronic inflammation and loss of function. Since lymphedema and fibrosis might persist as a late side effect, early treatment of the condition should be focused. [44]

Additionally, HNSCC patients often are psychologically affected and distressed while undergoing radiation therapy. Up to 50% might show symptoms referring to depression and anxiety. Depression is linked to a bigger extent of malnutrition and is regarded as a risk factor for recurrence and a decrease in overall survival. [128]

In some cases, radiotherapeutic treatment needs to be interrupted due to toxicity responses. Those cases especially can be linked to oropharyngeal tumors and malignancies with increased T stage. [129] Late side effects can be linked to patients of older age, laryngeal or hypopharyngeal tumors and neck dissection following chemoradiotherapy. [126] Patients affected by severe radiosensitivity are more likely to experience grave morbidity after radiation therapy. [130] Death which can be related to chemoradiotherapy in HNSCC is reported to be one of the three major causes of a patient's death. [126]

1.4.3. Effects of radiation therapy on lymphocytes

Lymphocytes rank among white blood cells. Even though they have a similar appearance they account for different functions of the immune system. B cells, T cells and innate lymphoid cells (ILCs) such as natural killer cells (NK cells) produce a certain set of antibodies and cytokines. NK cells are able to impart direct elimination of malignant cells. T cells can be subdivided into NK-like T cells, γδ T cells, CD8+ and CD4+ T cells. CD8+ T cells are able to exert either cytotoxic or cytolytic behavior to get rid of malignant cells. [131]

Radiotherapy is linked to an improvement of the anti-tumor immunity by stimulating T cell-mediated immunity. Otherwise, it is related to the elevation of regulatory T cells (Tregs) leading to a suppression of the anti-tumor response of the immune system. [132]

Especially the components of the hematopoietic system are sensitive to ionizing radiation. Radiation not only induces cell death of malignant cells but also of lymphocytes. [131] Primarily NK cells, naïve T cells (with a greater effect on

CD4+ T cells) and B cells are affected by radiosensitivity while NK-like T cells, T memory cells and regulatory T cells (Tregs) are withstanding to a greater extent. [131, 133] Subpopulations of T cells fall after radiation therapy. [134-137] CD4+ and CD8+ T cell counts are affected as well as the CD4+/CD8+ T cell ratio which shows a decline. [134-136] In particular, the decrease of CD4+ T helper cells is pronounced. [136, 138] Also, the level of B cells declines subsequently to radiation therapy. [135-137] One year after undergoing radiation therapy, patients still present with declined levels of lymphocyte subpopulations. [135, 139]

Additionally to ionizing radiation, other factors might add to the long-lasting immunosuppression after undergoing radiotherapy. [138] Whereas healthy donors present low levels of Tregs, this fraction shows a double increase for patients with head and neck squamous cell carcinoma. After radiotherapy, Tregs remain increased for the duration of one month. [136] NK cells remain unaffected by disease or radiation therapy or even show an increase. [136, 138]

The number of lymphocytes might have an influence on the prognosis for HNSCC patients. [140, 141] Regulatory T cells as well as tumor-infiltrating lymphocytes (TILs) and dendritic cells might have an impact on the prognosis. [140] Additionally, patients with lower lymphocyte numbers at baseline have a decreased overall survival rate. [142]

1.5. Immune checkpoint inhibitors in the treatment of HNSCC

Before the 19th century, the patient's immune system has been identified as an important factor of the initial development and progression of malignancies. In recent years, immunotherapy has gained popularity as a considerable cancer treatment modality. Treatment options of the immunotherapeutic field such as monoclonal antibodies targeted at tumor antigens, cell-based dendritic vaccines and immune checkpoint inhibitors have recently been approved by the Food and Drug Administration (FDA), a central U.S. authority. [143] Approved immune checkpoint inhibitors targeting PD-1 in HNSCC cases are enlisted in Table 7.

Immune checkpoint inhibitors show promising results for many malignancies and mainly interfere with programmed cell death protein 1 (PD-1), programmed cell death ligand 1 (PD-L1) and cytotoxic-T-lymphocyte associated protein 4

(CTLA-4). [143, 144] Forementioned checkpoint inhibitors interact with the regulation of T cells, which are fundamentally supporting the patient's immune response, i.e. regarding the destruction of tumor cells. [144] To ensure adequate T cell activation, a balance between inhibitory and co-stimulatory signals is crucial. [9] T cells are activated through co-stimulatory molecules and interaction with the T cell receptor, immune checkpoints consequently monitor and modulate the immune response's intensity and length of time. [145] After T cell activation, expression of CTLA-4 is induced and impedes further co-stimulation after reaching a certain threshold while upregulation of PD-1 adversely affects the signaling regarding the T cell receptor which binds to the antigen. [144]

For the functioning of immune checkpoint pathways, a receptor, i.e. PD-1, and a related ligand, such as PD-L1, need to correspond. [145] Immune checkpoints are able to suppress the immune response in order to ensure self-tolerance and to avoid autoimmunity and damage in peripheral tissues caused by T cell reaction. [146] Tumor cells take advantage of the mechanism of immune checkpoints to evade detection and elimination by the patient's immune system. [145, 146] Especially for squamous cell carcinomas of the head and neck, immune checkpoints serve tumor cells as a mechanism to escape detection by the immune system by interfering with T cell activation and functioning. [146] Consequently, the goal for immunotherapy is not only to initiate an immune response but also to interfere with tumoral inhibitory pathways regarding T cell response. [144] For the treatment of HNSCC, immunotherapy is an eligible modality due to the large immune infiltration. Depending on the aetiology of HNSCC, the extent of immune infiltration and activation varies greatly and needs to be taken into consideration to define suitable targeted immunotherapies. [62]

Certain side effects can be related to immune checkpoint inhibitors, they are described as immune-related adverse events (irAEs). [145-147] Generally, PD-1 inhibitors show less toxicity compared with regular chemotherapy. [63, 146, 147] irAEs might manifest at different organ systems, i.e., leading to endocrinologic diseases, hepatitis, colitis and pneumonitis. Anti-PD-1 therapy should also be implied for suitable patients with advanced age, co-morbidities, lung metastases or even controlled diseases like HIV and Hepatitis C. [147]

The immune response modulation initiated by immune checkpoint inhibitors often demonstrates a long-lasting effect protecting patients against tumor progression. [143, 144, 148] For HNSCC, only up to every fifth patient can show a valuable response. [148] Therefore, combining additional immune checkpoint inhibition with anti-cancer treatment modalities might produce a greater response rate. [143] To identify patient groups for whom the treatment with immune checkpoint inhibitors is likely to produce a viable tumor response is a key element for future therapeutic approach. [143, 144, 148] Therefore, immunologic and translational biomarkers can aid to prognostic and predictive patient stratification. [143, 144]

Table 7: Approved immunotherapies for HNSCC

immune checkpoint inhibitor	**targeted immune checkpoint**	**indication**	**year of approval - institute**
Nivolumab Pembrolizumab	PD-1	Recurrent HNSCC refractory to platinum-based therapy	2016 - FDA
Nivolumab	PD-1	Recurrent HNSCC refractory to platinum-based chemotherapy	2017 - European Commission
Pembrolizumab	PD-1	Monotherapy for recurrent or metastatic HNSCC with PD-L1 expression ≥ 50% tumor proportion score and progression despite platinum-based chemotherapy	2017 - European Commission
Pembrolizumab (monotherapy and in combination with platinum and fluorouracil)	PD-1	First-line therapy for metastatic or unresectable recurrent HNSCC; Monotherapy for patients with PD-L1 positive score ≥ 1	2019 - FDA

Source: [147]

1.6. Prognostic biomarkers for HNSCC

Different types of biomarkers can contribute to diagnosing malignancies and making decisions regarding cancer therapy (see Table 8). [149] Prognostic biomarkers contribute to the monitoring of cancerous disease regarding cancer research, patient care and tumor control, i.e., by defining the patient's presumable outcome at the time of diagnosis as well as the probability of disease recurrence or survival until tumor-related death after treatment. [149-151] Therefore, prognostic biomarkers have a potent role for treatment decision and scheduling for treatment intensity by target-orientedly stratifying patient subgroups. Also, during therapy patients might experience certain events which might be identified by biomarkers and affect the decision-making. [149]

Table 8: Types of biomarkers and their definition

type of biomarker	definition of benefit
diagnostic biomarker	identification of tumor disease
prognostic biomarker	improved or unfavorable outlook of tumor disease regardless of therapeutic approach
predictive biomarker	prediction of specific therapy outcome; often simultaneously serving as a therapeutic target
companion diagnostic biomarker	diagnostic, prognostic or predictive biomarker to stratify patient subgroups for individual therapeutic approach

Source: [149, 150, 152]

Clinical utility is a key factor for the benefit of a prognostic biomarker, which means the assay needs to be reproducible ensuring the same quality. [150] Difficulties regarding prognostic biomarkers include the ensurance of the quality and performance of laboratory assays as well as the quality of statistical analysis and research publication. [149] HPV positivity has been linked to a greater radiosensitivity turning p16 status into a prognostic biomarker leading to the consideration of adjustments in radiotherapeutic approach. [64, 153-156] Also, Protein death ligand 1 (PD-L1) detected by immunohistochemistry is among new promising prognostic intra-tumoral biomarkers for HNSCC. [48, 157, 158] Other biomarkers with a high prognostic potential are EGFR overexpression as well as

mutation of p53, which is connected to a poor prognosis regarding overall survival. [48, 150, 159] Further understanding of the tumor microenvironment of HNSCC might lead to finding new potential prognostic biomarkers. [155]

Regularly, HNSCC is diagnosed at a late stage by endoscopy, biopsy of tumor tissue samples and/or fine-needle aspiration (FNA). [160] These diagnostic approaches cannot factor the heterogeneity of HNSCC, are substantially affected by the malignancy's location, constitute a more invasive surgical procedure, are more cost-intensive in comparison with a simple peripheral blood draw and cannot be regularly repeated. [160-162] Up to date, no feasible prognostic biomarkers exist to properly identify residual tumor burden after treatment. [162] Gaining information from easily accessible sources like blood or saliva, referred to as liquid biopsies, might allow to predict tumor recurrence at earlier stages during the follow-up period since frequency of imaging techniques is limited due to potential side effects. [48, 148, 163] Potential prognostic biomarkers which can be detected in patient's blood samples are either circulating tumor cells (CTCs), tumor antigens, tumor-associated autoantibodies or microRNAs. [48, 163, 164] HPV ctDNA can be identified in plasma samples of patients with HPV-positive oropharyngeal squamous cell carcinoma and might lead to an earlier diagnosis of small-sized tumors as well as aid to monitor the behavior of disease. [165] PD-L1 expression can also be discovered upon CTCs in the peripheral blood of HNSCC patients with locally advanced disease. Increased PD-L1 expression after a definitive therapeutic approach can be related to an elevated risk for disease progression and death in comparison with lower PD-L1 expression upon CTCs. These findings might help to stratify patients for PD-1-targeted immunotherapies. [166] This is an enormous advantage since early therapeutic approach of recurrent disease is crucial for the patient's prognosis. [148]

1.7. Early activation marker CD69

1.7.1. The role of early activation marker CD69

The lymphocyte antigen CD69, an early activation marker, is a type 2 membrane-bound glycoprotein associated with the NK-gene complex and can be detected on cells of the hematopoietic system, such as platelets, neutrophil

and eosinophil granulocytes, Langerhans cells of the epidermis and lymphocytes. [167-169]

To respond properly to infectious agents, cellular components of the immune system adequately need to be able to be activated and proliferate. After initiation of the immune response by antigenic and mitogenic stimulation, certain surface antigens are expressed on activated lymphocytes with CD69 being the earliest one. [170] While expression of CD69 is upregulated very early after initial stimulation by a variety of stimuli on NK cells, B cells and T cells through engagement with the T cell receptor (TCR/CD3) within a maximum of four hours, the surface antigen can almost not be found on resting lymphocytes. [168, 169, 171-173] Upregulation of CD69 on NK cells occurs faster than on T cells, ultimate activation levels show the same results for both cell types. [172] Highest expression rates can be measured 18 to 48 hours after stimulation. [173] Levels of CD69 begin to decrease four to six hours after activation. [171] 72 hours after activation, CD69 expression decreases close to background levels. [173]

The early activation marker CD69 is involved in the regulation of several significant pathways. CD69 might be additionally involved with the migration of activated lymphocytes and the release of cytokines, leading to a lymphonodal retention of T cells. Therefore, CD69+ T cells are more commonly detected in inflamed tissue or lymph nodes when comparing with the circulating blood stream. [171]

Due to its rapidly upregulated expression on CD8+ and CD4+ T cells as well as on T cells in the periphery of inflammatory processes, CD69 serves as an established early indicator of T cell activation. [169, 173] Cell phenotypes as well as the level of CD69 expression on lymphocytes and lymphocyte subsets can be easily measured by flow cytometry with the use of specific monoclonal antibodies (mAbs) with a high amount of sensitivity. [168-170, 173]

1.7.2. Early activation marker CD69 in relation to HNSCC

For migration and presence of T cells in inflamed tissues, it is essential that T cells are activated and the surface marker CD69 is upregulated. [174] Progression of cancerous disease can be related to increased expression of CD69 on CD4+ and

CD8+ T cells, decreased tumor-infiltration of T cells (TILs) as well as to the exhaustion of CD8+ T cells leading to an impaired anti-tumor immunity. [174, 175] Tumor-infiltrating lymphocytes (TILs) are able to contribute to the production of anti-tumoral cytokines. A treatment with an antibody targeted against CD69 can enhance the anti-tumor response and delay disease progression by increasing the levels of tumor-infiltrating CD8+ and CD4+ T cells. Therefore, CD69 might serve as a potential target for an immunotherapeutic approach of tumor disease. [174]

For squamous cell carcinoma of the larynx, high levels of early activation markers are expressed on the surface of T cells whereas late activation markers show a decreased expression. This might lead to regulatory dysfunction and a restricted immune response. Elevated levels of CD69-expressing CD4+ and CD8+ T cells can be linked to significantly fewer secretion of IL-10 and IFN-γ detectable in peripheral blood. [175] For patients suffering from squamous cell carcinoma of the head and neck, decreased cytotoxicity of lymphocytes regarding malignant cells can be related to a reduced secretion of IL-12, TNF-α and IFN-γ since secretion of these cytokines is relevant for cytotoxic NK cell and T cell activity. [176] Additionally, increased levels of activated T cells in the peripheral blood are correlated with worse prognosis regardless of the TNM stage. Likewise, elevated levels of early activation marker CD69 are associated with inferior prognosis with worse overall survival. [177]

1.8. The PD-1/PD-L1 pathway

1.8.1. The PD-1 receptor

The programmed cell death protein 1 (PD-1) is a transmembrane protein receptor of the Ig family which can be found superficially as a monomer on CD4-/CD8-negative αβ and γδ T cells, activated T cells, NK cells, B cells, NK-like T cells, dendritic cells, macrophages as well as on monocytes. [178-182] As a negative regulator of the immune system, PD-1 can be accounted to the CD28/CTLA-4 family while its function regarding the inhibition of T cell activation differs from CTLA-4. [178, 181-184] PD-1 occupies many functions in relation to T cells including activation, exhaustion and tolerance. The PD-1/PD-L1 pathway is an important regulatory mechanism to prevent autoimmunity by suppressing

activation of self-reactive CD8+ and CD4+ T cell responses ensuring self-tolerance in tissues. [178, 179, 181] Additionally, the receptor has the ability to interfere with effector functions of NK cells and B cells when expressed on their surface. [181] Due to the obstruction of the signaling of the T cell receptor through a co-inhibitory pathway, PD-1 seemingly prevents the T cells from responding leading to restricted anti-tumor immunity. [180-183, 185] After the activation of T cells, rising PD-1 expression can be measured within 24 hours and disappears when the stimulating antigen is absent. [179, 181] Ongoing stimulation of T cells by an antigen (i.e. tumor or chronic infection) directs to a permanently high expression of PD-1 leading to T cell exhaustion. [178, 181, 185] Tumors are able to evade immune surveillance by various immune escape mechanisms, by facilitating the expression of co-inhibitory molecules (i.e., PD-1 and PD-L1), among other things. [181] When comparing with healthy subjects, patients suffering from cancer of the head and neck experience an elevated expression of PD-1 on certain lymphocyte subpopulations. [186] Elevated expression of PD-1 upon innate-type B cells might additionally lead to the suppression of B cell expansion and hinder them from developing into immunoglobulin G (IgG) expressing plasma cells. Consequently, innate humoral immune responses can be downregulated. [178]

1.8.2. The ligands PD-L1 and PD-L2

PD-L1 (CD274) and PD-L2 (CD273), the two ligands of the PD-1 receptor, also might have the ability to inhibit T cell response. [178, 180-182] After stimulation by proinflammatory cytokines like TNF-α, VEGF and interferons, PD-L1 is expressed on the surface of mainly antigen presenting cells (APCs) like dendritic cells, macrophages, T cells, B cells and further cells (i.e. fibroblasts, stromal and parenchymal cells, epithelial and vascular endothelial cells). [178-181] Additionally, tumor cells express PD-L1 on their surface to evade immune surveillance, enhance tumor growth and restrict secretion of IFN-γ. [178, 180, 181, 183]

In comparison with PD-L2, PD-L1 is more frequently detected. Stimulating the expression of PD-L1 and PD-L2 might represent a mechanism of negative feedback to lower T cell activity in order to prevent increased immune tissue damage. [181] When binding to their receptor PD-1, the ligands induce the recruitment of

tyrosine phosphatase SHP-1 and SHP-2. [178, 181] Consequently, phosphorylation of the T cell receptor signaling molecules decreases resulting in a diminished activation of T cells and production of cytokines finally leading to decreased T cell cytotoxicity. [179-181, 187] Furthermore, production of regulatory T cells (Tregs) is promoted by the PD-1/PD-L1 pathway. [181] Levels of Tregs show a reduction upon treatment with immune checkpoint inhibitors targeting the PD-1/PD-L1 pathway. [63] The two ligands PD-L1 and PD-L2 are found to interact with each other to a small extent. The impact of this interaction on the immune checkpoint and response of the immune system has not been defined yet. [188]

1.8.3. The prognostic relevance of PD-1 and PD-L1 for HNSCC

For HNSCC, expression of PD-1 on CD8+ T cells infiltrating the tumor is favorable for tumor growth. Around 50 percent of patients suffering from HNSCC express PD-L1 in the TME. [180] Active smokers generally show a lower PD-L1 expression within the TME. [65] Prognostic value of PD-L1 expression for the patients' overall survival is still under investigation since several studies have produced opposing results. [155, 189] HPV status measured by p16, PD-1 and PD-L1 expression are correlated. According to some studies, patients with a higher expression level of PD-1 and PD-L1 are associated with improved overall survival and decreased likelihood of experiencing tumor recurrence. [190, 191] Contrary to studies regarding other tumor types, elevated levels of PD-L1 expression can be associated with an improved prognosis for HPV-positive HNSCC whereas elevated levels on exosomes are linked to progression of disease. [180] Another study regarding HNSCC identifies high PD-L1 expression as a negative prognostic factor for overall survival independent of other prognostic factors (i.e., lymphonodal involvement, tumor size, surgical margin status, distant metastases and extranodal involvement). Elevated PD-L1 expression can also be linked to the likelihood of developing distant metastasis. [192]

1.8.4. Immunotherapy targeting the PD-1/PD-L1 pathway

Immunotherapy by targeting the PD-1/PD-L1 pathway with antibodies, known as an immune checkpoint blockade, results in favorable clinical outcomes regarding different cancerous malignancies with response rates up to 50 percent. [181, 182]

Blocking the PD-1/PD-L1 pathway results in improved cytokine release, T cell proliferation and cytotoxicity effectuating an ameliorated anti-tumor response. Also, the elevation of glucose concentration in the TME leads to a production of increased IFN-γ levels. An increased mutational tumor burden can be linked to an improved immune checkpoint inhibitor response while an active smoking status decreases the likelihood of a positive benefit. [65, 181] Patients suffering from recurrent or metastatic HNSCC with higher PD-L1 expression levels demonstrate an improved response rate , but also patients with poor PD-L1 expression can benefit from treatment with immune checkpoint inhibitors. [155]

Nivolumab, a monoclonal antibody directed against PD-1, demonstrated improved outcomes for classical Hodgkin's lymphoma, non-small-cell lung carcinoma, metastatic renal cell carcinoma and unresectable or metastatic melanoma or HNSCC leading to its approval by the FDA. [181, 182] Pembrolizumab, another immunotherapeutic drug, obtained the FDA's approvement in 2016 as a therapeutic approach for metastatic or recurrent HNSCC following platinum-based chemotherapy. [182] Positive response rates with an improvement of overall survival rates can be observed for both nivolumab and pembrolizumab regardless of the HNSCC's HPV status. [180, 182] The combination of blocking CTLA-4 and PD-1, approved by the FDA for unresectable or metastatic melanoma, or combination of either immune checkpoint inhibitor with other therapeutic approaches can possibly ameliorate response rates and therapy outcomes. [181, 193] Prediction of a patient's response to immune checkpoint therapy remains a great challenge. [184] Side effects of PD-1/PD-L1 immune checkpoint inhibition are of a more pathologically chronic nature and fainter when comparing with other immune checkpoint inhibitors. [178, 180, 181]

1.9. Aim of the study

The striving for a more personalized approach of cancer care requires knowledge of the molecular structure of a tumor as well as of the tumor microenvironment, also allowing for a reduction of treatment related side effects and toxicity. After proper risk assessment, personalized cancer care ensures choosing the most beneficial therapy and screening strategy for the patient while saving healthcare costs and meaningful treatment time. [9] Figure 1 displays the key elements of

personalized cancer care. Assessment of the patient's prognosis is also critical for cancer management since some patients are more likely to experience recurrence and therefore have the need for an intensified therapeutic approach and cancer screening. A reduced risk of recurrence might allow for de-escalation strategies to achieve less systemic side effects. [9]

Figure 1: Key elements of personalized cancer care

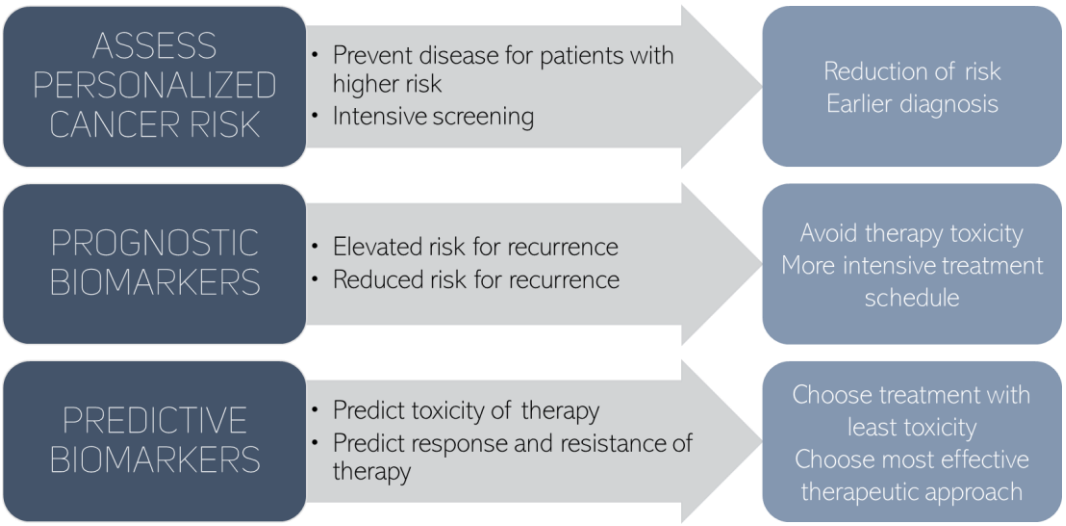

Source: [9]

In this study, we observe patients with locally advanced HNSCC within a time frame of two years in order to investigate the impact of radiation-induced effects on lymphocyte subpopulations (T cells, NK cells, B cells and NK-like T cells) in consideration of prognosis for tumor recurrence. Further, we want to validate the prognostic impact of three potential biomarkers (CD69, PD-1 and PD-L1) on locoregional control for locally advanced HNSCC. Findings might lead to a more precise definition of risk groups and a more suitable patient stratification for individualized radiation dosage de-escalation as well as for therapeutic approach with immune checkpoint inhibitors targeting CD69 and/or the PD1-/PD-L1 pathway.

2. Materials and Methods

2.1. Materials

2.1.1. Basic laboratory equipment

Table 9: Basic laboratory equipment

Equipment	Manufacturer
Heraeus Multifuge 3S-R Centrifuge	Thermo Electron Corporation, Waltham, MA, USA
Heraeus Fresco 17 Centrifuge	Thermo Electron Corporation, Waltham, MA, USA
Vortex mixer MS1 Minishaker	IKA®, Staufen, Germany
Vortex-Genie 2	Scientific Industries, Bohemia, NY, USA
Heater MR Hei-Standard	Heidolph Instruments, Schwabach, Germany
Pipet Aid Pipetboy	Integra Biosciences, Hudson, NH, USA
Pipettes pipetman (1-10µL, 10-100µL, 20-200µL, 100-1000µL)	Gilson, Middleton, WI, USA
Pipettes Lambda Plus (0.1-2µL, 0.5-10µL, 20-200µL, 100-1000µL)	Corning Incorporated, Corning, NY, USA
Pipettes Lambda (0.5-10µL, 20-200µL)	Corning Incorporated, Corning, NY, USA
Multiple pipettes 30-300µL (Research plus/Reference 2)	Eppendorf AG, Hamburg, Germany
Multiple dispenser	Eppendorf AG, Hamburg, Germany
Precision scale	Kern & Sohn GmbH, Balingen, Germany
FACS Calibur flow cytometer	BD Biosciences, San Jose, CA, USA
ELx808™ Absorbance Microplate Reader	BioTek, Winooski, VT, USA

2.1.2. Consumable supplies

Table 10: Consumable supplies

Equipment	Manufacturer
Disposable latex gloves	Ansell LTD, Brussels, Belgium
EDTA KE tubes	unknown
FACS tubes 5mL	Sarstedt, Nümbrecht, Germany
Disposable pipette (1mL/2mL/5mL/10mL/25mL/50mL)	Greiner Bio-One, Frickenhausen, Germany
Eppendorf tubes (0.5mL/1.5mL)	Eppendorf AG, Hamburg, Germany
Eppendorf Tips epT.I.P.S.® (Reloads 0.1-10µL, Standard/Bulk 2-200µL, Standard 20-300µL)	Eppendorf AG, Hamburg, Germany
Disposable pipette tips (200µL/1000µL)	Sarstedt, Nümbrecht, Germany
Disposable pipette tips (Capillaries and Pistons)	Gilson, Middleton, WI, USA
Combitips advanced® 25mL	Eppendorf AG, Hamburg, Germany
Reagent reservoir 4870 50mL	Corning Incorporated, Corning, NY, USA
Cellstar® tubes (15mL/50mL)	Greiner Bio-One, Frickenhausen, Germany
SafeSeal micro tubes (0.5mL/1.5mL/2mL)	Sarstedt, Nümbrecht, Germany
Costar 3590 96 Well EIA/RIA Plate	Corning Incorporated, Corning, NY, USA
Plate sealers Easyseal™ Transparent 79x135mm	Greiner Bio-One, Frickenhausen, Germany
Disposal bags	Sarstedt, Nümbrecht, Germany
Paper towels	Mobiloclean® Handelsgruppe GmbH + Co. KG., Munich, Germany

2.1.3. Kits

Table 11: ELISA kits

Kit	Catalog No.	Manufacturer
DuoSet® ELISA Development System Human PD-1	DY1086	R&D Systems
DuoSet® ELISA Development System Human PD-L1/B7-H1	DY156	R&D Systems

2.1.4. Chemicals and reagents

Table 12: Chemicals and reagents

Equipment	Manufacturer	Catalog No./Part No.
Alkopharm 70	L. Brüggemann KG, Heilbronn, Germany	
FBS Supreme, South America origin, heat inactivated 45min at 56°C	PAN-Biotech GmbH, Aidenbach, Germany	P30-3031
Bovine Serum Albumin (BSA)	Sigma-Aldrich, Steinheim, Germany	A7030-100G
Dulbecco's Phosphate Buffered Saline (PBS)	Sigma-Aldrich, Steinheim, Germany	D8537-500ML
FACS lysing solution	BD Biosciences	349202
FoxP3 buffer set A	BD Biosciences	51-9005451
FoxP3 buffer set B	BD Biosciences	51-9005450
BD FACSFlow™	BD Biosciences	342003
FACS Rinse	BD Biosciences	340346
FACS Clean	BD Biosciences	340345
Triton® X-100	Sigma-Aldrich, Steinheim, Germany	T8787-250ML
Human PD-1 Standard	R&D Systems	842904
Human B7-H1 Standard	R&D Systems	843766

Streptavidin-HRP	R&D Systems	890803
Color Reagent A (H2O2)	R&D Systems	DY999
Color Reagant B (Tetramethylbenzidine)	R&D Systems	DY999
Sulphuric acid	Sigma-Aldrich, St. Louis, MO, USA oder Steinheim, Germany	339741-100ML
Millipore water		

2.1.5. Buffers and solutions

Table 13: Buffers and solutions

Equipment	Concentration	Manufacturer
FACS Buffer	FCS 1:9 in PBS	
FACS lysing buffer	FACS lysing solution 1:9 in H2O	BD Biosciences
Buffer A	Component A 1:10 in H2O	BD Biosciences
Buffer C	Component B 1:50 in buffer A	BD Biosciences
Wash buffer	0.05% Triton® X-100 in PBS	
Reagent diluent	1% BSA in PBS	
Substrate solution	1:1 mixture of Color Reagent A and Color Reagent B	R&D Systems
Stop Solution	2 N H2SO4	

2.1.6. Antibodies

Table 14: Antibodies

Antibody	Company	Catalog No./Part No.
IgG1-FITC	BD Biosciences	345815
IgG1-PE	BD Biosciences	345816
IgG1-PerCP	BD Biosciences	345817

IgG1-APC	Caltag/Invitrogen	MG105
CD94-FITC	BD Biosciences	555888
CD56-FITC	BD Biosciences	345811
CD4-FITC	BD Biosciences	555346
CD8-FITC	BD Biosciences	555366
CD56-PE	BD Biosciences	345812
CD19-PE	BD Biosciences	555413
CD16-PE	BD Biosciences	555407
NKG2D-PE	R&D Systems	FAB139P
NKp30-PE	Beckman Coulter	PN IM 3709
NKp46-PE	Beckman Coulter	PN IM 3711
CD8-PE	BD Biosciences	555367
FoxP3-PE	BD Biosciences	560046
CD3-PerCP	BD Biosciences	345766
CD45-APC	Caltag/Invitrogen	MHCD4505
CD69-APC	BD Biosciences	340560
CD56-APC	BD Biosciences	555518
CD25-APC	BD Biosciences	340907
Human PD-1 Capture Antibody	R&D Systems	842902
Human PD-1 Detection Antibody	R&D Systems	842903
Human B7-H1 Capture Antibody	R&D Systems	843764
Human B7-H1 Detection Antibody	R&D Systems	843765

2.1.7. Software

Table 15: Software

Software	Version	Manufacturer
BD CellQuest™ Pro	6.0 MacApp® R15.1	BD Biosciences
Gen5	11	BioTek, Winooski, VT, USA
Microsoft® Excel for Mac	16.39	Microsoft
IBM SPSS Statistics	26	IBM

2.2. Methods

2.2.1. Collection of patient databases

This project is part of the prospective multicentric observational cohort study *HNprädBio* of the Deutsches Konsortium für Translationale Krebsforschung (DKTK) which focuses on the validation of the prognostic impact of potential biomarkers on locoregional control of locally advanced head and neck cancer. This study of the DKTK is registered at ClinicalTrials.gov under the registration number NCT02059668. Launch of the study took place in March 2014 and total enrollment of 550 participants was estimated.

Validation of certain biomarkers to predict the effect of chemoradiotherapy in patients with cancer of the head and neck is the aim of the study. Enrolled patients suffer from locally advanced squamous cell carcinoma of the oral cavity, oropharynx or hypopharynx. Their treatment schedule is equal to the standard of care according to the center of treatment. The *HNprädBio* study consists of two patient groups: Patients who receive primary chemoradiotherapy and patients who receive adjuvant chemoradiotherapy. This project only focuses on patients who are treated with primary approach.

2.2.1.1. Inclusion criteria

Patients with locally advanced squamous cell carcinoma of the oral cavity, oropharynx or hypopharynx are included in the study design if they meet all of the defined inclusion criteria (see Table 16).

Table 16: Inclusion criteria

Inclusion criteria for *HNprädBio*
HNSCC stage 3 or 4 without distant metastases
Able to take part regularly in the aftercare of cancer treatment
Scheduled irradiation dose: 69-72 Gy
Scheduled time of treatment: 38-54 days
Scheduled simultaneous chemotherapy with cisplatin *(scheduled cumulative dosage is a minimum of 180mg/m^2 of the body surface, partitioned into several single dosages)*
General condition according to WHO 0-2
Written consent of the patient

2.2.1.2. Exclusion criteria

If one of the criteria in Table 17 is met, patients are excluded from the DKTK study.

Table 17: Exclusion criteria

Exclusion criteria for *HNprädBio*
Distant metastases
Contraindication for cisplatin-based chemotherapy
Induction chemotherapy
Scheduled irradiation dose: < 69 Gy and > 72 Gy
Scheduled time of treatment: < 38 days or > 54 days
Prior irradiation in the area of the head and neck, if there is risk in overlapping of radiation treatment volume
Additional tumor disease, if treatment is necessary at the time or probably within the following 2 years or if this tumor disease has impact on the prognosis of the patient
Other diseases or conditions which reduce the survival probability to less than 2 years or interfere with the aftercare in this 2-year timeframe
Pregnancy or lactation
Patient is not able to give consent or written consent is missing

2.2.1.3. Patient database

Starting in 2014, blood samples are gained from patients suffering from locally advanced HNSCC. All DKTK facilities taking part in the multicenter study supply blood samples. Hence blood samples are collected at the Ludwig-Maximilian's university hospital in Munich, Charité university hospital in Berlin, University Hospital Carl Gustav Carus in Dresden, university hospital in Heidelberg, university hospital in Frankfurt, university hospital in Essen, university hospital in Freiburg and university hospital in Tübingen besides the Klinikum Rechts der Isar in Munich. Blood samples are scheduled to be taken at five and six different time points, respectively: Before treatment (R0), during chemoradiotherapy (R1), 3 months after chemoradiotherapy (R2), 6 months after chemoradiotherapy (R3), 12 months after chemoradiotherapy (R4) and in case recurrence or metastases are suspected (R5). Patients are surveilled over a time frame of two years. Blood from healthy donors is taken at one time point (see Figure 2).

Figure 2: Overview of time points of blood draw

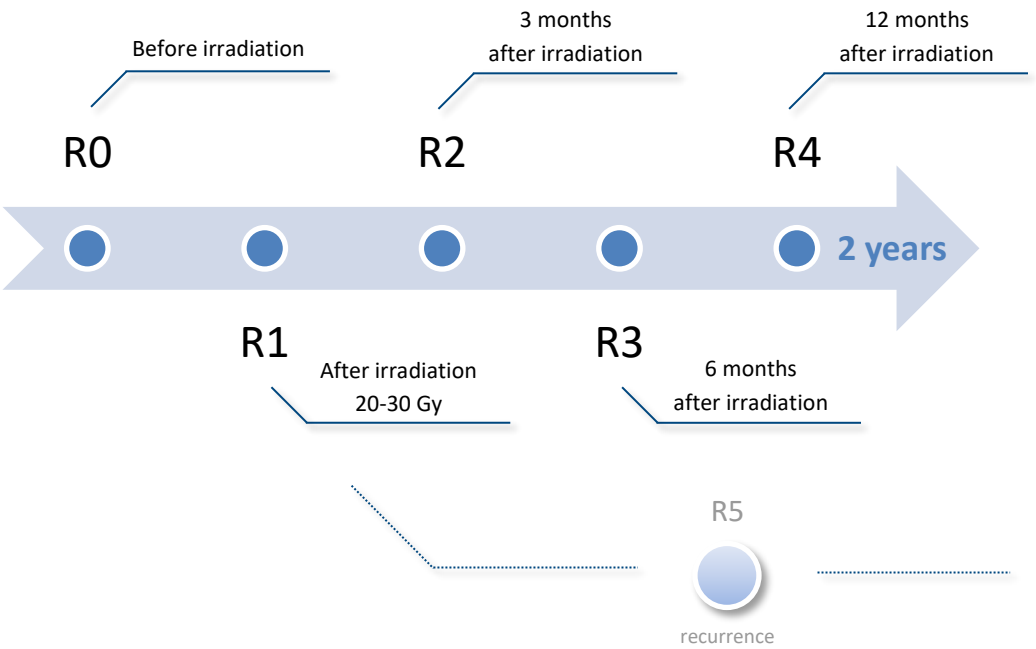

Whole blood samples are collected in EDTA KE tubes, sent by DHL Express to the Klinikum Rechts der Isar in Munich and further regularly prepared for analysis one day after blood draw. For plasma separation EDTA blood is centrifuged at 1,500xg

for 15min at 4°C. Plasma samples are stored in 500µL aliquots at -80°C, whereas 1.5mL of EDTA blood is used for FACS analysis.

Many HNSCC patients do not reliably keep their radiation and aftercare appointments. Additionally, some patients sadly pass away during treatment or aftercare. Therefore, only a partial data set can be gained for some patients. Consequently, patients are chosen for analysis after FACS acquisition according to the completion of at least four blood draws in case of no recurrence. All patients who experienced recurrence of HNSCC are included. This results in a total number of 117 blood sample donors: Patients with no tumor recurrence (n = 80), patients with tumor recurrence (n = 27) and healthy donors (CTRL) (n = 10) (see Table 18).

Table 18: Blood sample donors

	No recurrence	**Recurrence**	**CTRL**
Number of samples	80/107 (75%)	27/107 (25%)	10

CTRL = healthy blood donors

As a next step, samples which are indicative of poor lysis are manually excluded after FACS analysis. For the recurrence group, R4 samples are not further included in the analysis since the sample size of 5 is too small to be comparative. The small sample size might be an indicator that recurrence often occurs before the R4 time point of treatment aftercare. An overview of the distribution of samples across patient groups and time points of blood draw is outlined in Table 19.

Table 19: Number of samples for each time point of blood draw

	Time point	**No recurrence**	**Recurrence**
Number of samples	R0	71	22
	R1	71	16
	R2	66	20
	R3	71	13
	R4	75	-
	R5	-	26

2.2.2. Analysis of the immune phenotype with FACS

Multi-color fluorescence activated cell sorting (FACS) analysis is a popular biotechnological method which allows to rapidly count and sort cells depending on their expression of specific cell surface molecules. Antibodies specific to the cell surface molecule are used to detect a certain cell population in solution. Detection antibodies are conjugated with a fluorophore. Light scatter and fluorescence intensity are measured as the suspended cells are passing through a laser light beam. Counting and differentiation between the cell populations is hence possible by combining several suitable detection antibodies. [194, 195] Consequently, differences in the circulating immune cell composition of healthy donors and HNSCC patients can be explored by FACS analysis.

2.2.2.1. FACS acquisition

The amount and density of receptors on individual subgroups of lymphocytes are measured as well as the expression of the early activation marker CD69 on certain cell types using EDTA blood samples. FACS (FACS Calibur flow cytometer, BD Biosciences) is performed the day after the blood draw with 1.4mL EDTA blood. 100µL EDTA blood is pipetted into each of the 14 test tubes. Then detection antibodies are added to the test tubes in certain combinations (see Table 20). After incubation for 15 minutes in the dark at room temperature, tubes are washed by adding 2mL of 10% FCS in Dulbecco's Phosphate Buffered Saline Sigma (PBS) (FACS buffer) and centrifugation at 500xg for 5 minutes at room temperature. Afterwards 2mL of lysing buffer solution (1:9 dilution of BD lysing Solution Cat. 349202 with millipore H2O) are pipetted into each tube and incubated for 10 minutes at room temperature without exposition to light. After centrifugation at 500xg for 5 minutes at room temperature, the tubes are washed again with 3mL of FACS buffer. Then 500µL of FACS buffer are added to tubes 1-11 for resuspension of the pellet before performing flow cytometry up to a count of 50,000 cells within the following hour. Furthermore, tubes 12-14 are stained separately to characterize regulatory T cells. To fixate the cells, they are incubated for 10 minutes with 2mL of buffer A solution (1:10 dilution of component A with H2O).

Table 20: Overview of antibody combinations in tubes 1-14 for FACS analysis of EDTA blood from HNSCC patients and healthy donors

Tube	Specificity	Antibody	Company	Catalog No.	Volume in µL
1	**Isotype control**	IgG1-FITC	BD	345815	5
		IgG1-PE	BD	345816	5
		IgG1-PerCP	BD	345817	5
		IgG1-APC	Caltag/Invitrogen	MG105	1
2	**T cells**	CD94-FITC	BD	555888	5
	NK cells	CD56-PE	BD	345812	5
		CD3-PerCP	BD	345766	10
		CD45-APC	Caltag/Invitrogen	MHCD4505	1
3	**B cells**	CD56-FITC	BD	345811	5
	T cells	CD19-PE	BD	555413	20
	NK cells	CD3-PerCP	BD	345766	10
		CD45-APC	Caltag/Invitrogen	MHCD4505	1
4	**T cells**	CD56-FITC	BD	345811	5
	NK cells	CD16-PE	BD	555407	10
		CD3-PerCP	BD	345766	10
		CD45-APC	Caltag/Invitrogen	MHCD4505	1
5	**T cells**	CD56-FITC	BD	555518	5
	NK cells	NKG2D-PE	R&D Systems	FAB139P	10
		CD3-PerCP	BD	345766	10
		CD69-APC	BD	340560	5
6	**T cells**	CD56-FITC	BD	345811	5
	NK cells	NKp30-PE	BC	PN IM 3709	10
		CD3-PerCP	BD	345766	10
		CD69-APC	BD	340560	5
7	**T cells**	CD56-FITC	BD	345811	5
	NK cells	NKp46-PE	BC	PN IM 3711	10
		CD3-PerCP	BD	345766	10
		CD69-APC	BD	340560	5
8	**T cells**	CD94-FITC	BD	555888	5
	NK cells	NKG2D-PE	R&D Systems	FAB139P	10
		CD3-PerCP	BD	345766	10
		CD56-APC	BD	555518	10
9	**T cells**	CD94-FITC	BD	555888	5
	NK cells	NKp30-PE	BC	PN IM 3709	10
		CD3-PerCP	BD	345766	10
		CD56-APC	BD	555518	10
10	**T cells**	CD94-FITC	BD	555888	5
	NK cells	NKp46-PE	BC	PN IM 3711	10
		CD3-PerCP	BD	345766	10
		CD56-APC	BD	555518	10
11	**CD4+**	CD4-FITC	BD	555346	20
	T cells	CD8-PE	BD	555367	20
	CD8+	CD3-PerCP	BD	345766	10
	T cells	CD45-APC	Caltag/Invitrogen	MHCD4505	1

12	**Isotype control**	IgG1-FITC	BD	345815	5
		IgG1-PE	BD	345816	5
		IgG1-PerCP	BD	345817	5
		IgG1-APC	Caltag/Invitrogen	MG105	1
13	**CD4+ Treg**	CD4-FITC	BD	555346	20
		FoxP3-PE	BD	560046	20
		CD3-PerCP	BD	345766	10
		CD25-APC	BD	340907	5
14	**CD8+ Treg**	CD8-FITC	BD	555366	20
		FoxP3-PE	BD	560046	20
		CD3-PerCP	BD	345766	10
		CD25-APC	BD	340907	5

Afterwards the tubes are centrifugated at 500xg for 5 minutes at room temperature and washed with 3mL FACS buffer. 0.5mL of buffer C solution (1:50 dilution of component B with buffer A) serve to permeabilize the cells during incubation for 30 minutes. Following two washing steps with 2mL FACS buffer and centrifugation at 500xg for 5 minutes, tubes 12-14 are stained with PE-conjugated antibodies (Treg transcription factor FoxP3-PE and IgG1-PE as a negative control). After two washing steps and addition of 500µL FACS buffer for pellet resuspension tubes 12-14 are analyzed by FACS acquisition.

2.2.2.2. Analysis of FACS data

After FACS acquisition, the data is saved as listmode data according to the standard formatting Flow Cytometry Standard and consequently analyzed with BD CellQuest™ Pro Software Version 6.0. In a Forward versus side scatter (FSC vs SSC) dot plot a scatter gate (R 1) is laid upon the lymphocytes. Cell debris and cell aggregates are left out of further analysis, only cells in the lymphocyte gate are included (see Figure 3). Histograms are used to display the isotype control (tube 1) of the four different fluorescent channels (FITC, PE, APC and PerCP). Overlapping populations and background noise are identified by a marker (M1) for each fluorescent channel as seen in Figure 4.

Figure 3: FACS gating of lymphocytes within peripheral blood (EDTA)

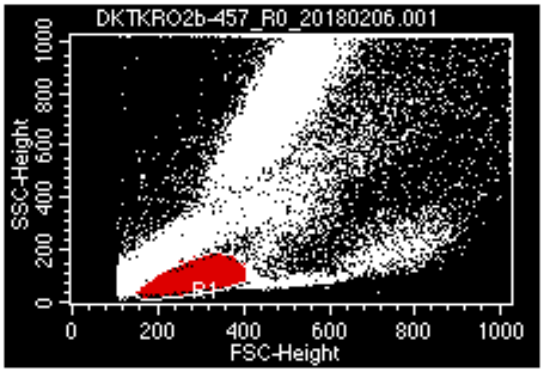

X-axis: forward scatter, Y-axis: side scatter. Lymphocytes are gated as R1.

Figure 4: Histogram of the isotype control with marker M1 for the PE fluorescent channel (tube 1)

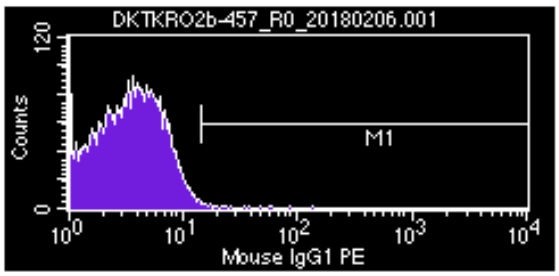

X-axis: intensity of expression of mouse IgG1-PE, Y-axis: counts of cells which stain positive for mouse IgG1-PE. M1 is placed as a marker to identify overlapping of fluorescent channels and background noise.

By means of the lymphocytes defined by gate R1, regions within lymphocyte subpopulations are defined for tubes 2-10. Outputs are displayed in form of percentage of total count of lymphocytes (% Gated) within the four quadrants. The quadrants are arranged so that the upper left quadrant (UL) displays NK cells, the upper right quadrant (UR) displays NK-like T cells and the lower right quadrant (LR) displays T cells. T cells are defined by expression of CD3. NK cells are defined by CD56 positivity, whereas NK-like T cells display both CD56 and CD3 upon their cell surface (see Figure 5). For tube 3 an additional dot plot displays B cells in the UL quadrant identified by the CD19 cell surface marker, as displayed in Figure 6. Additional histograms are used for tubes 5-7 to display the expression of early activation marker CD69 on NK cells, T cells and NK-like T cells after placing regions upon the forementioned lymphocyte subsets (see Figure 7).

The forementioned lymphocyte subpopulations are defined as regions in dot plots and CD69 APC is displayed separately within a histogram for each tube and each of those cell types. Outputs gathered are percentage of CD69+ cells (% Gated) and geometric mean fluorescence intensity (gMFI) of CD69+ cells (see Figure 8).

Figure 5: Dot plot of NK cells, T cells and NK-like T cells (tube 2-10)

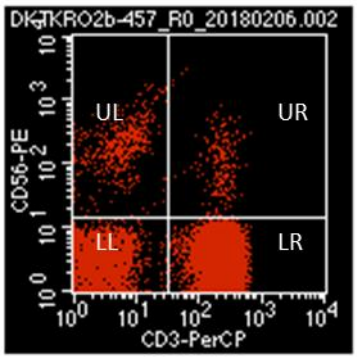

X-axis: cells which stain positive for CD3-PerCP, Y-axis: cells which stain positive for CD56-PE, UL: quadrant with NK cells, UR: quadrant with NK-like T cells, LR: quadrant with T cells, LL: quadrant with cells excluded by isotype control

Figure 6: Dot plot of B cells and T cells (tube 3)

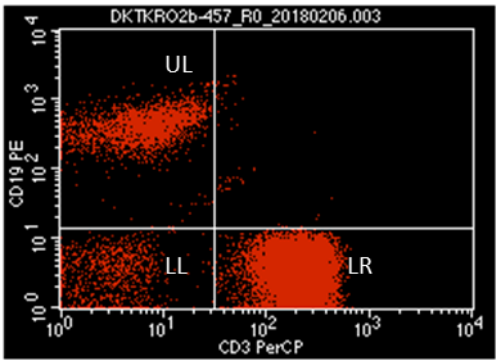

X-axis: cells which stain positive for CD3-PerCP, Y-axis: cells which stain positive for CD19-PE, UL: quadrant with B cells, LR: quadrant with T cells, LL: quadrant with cells excluded by isotype control

Figure 7: Placement of FACS regions for lymphocyte subpopulations (tubes 5-7): NK cells, T cells and NK-like T cells

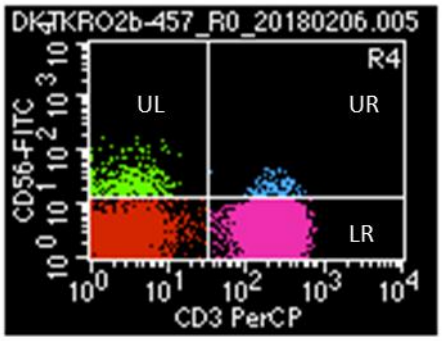

X-axis: cells which stain positive for CD3-PerCP, Y-axis: cells which stain positive for CD56-PE, UL: quadrant with NK cells, UR: quadrant with NK-like T cells, LR: quadrant with T cells

Figure 8: Histogram of CD69 positivity with marker M1 for the APC fluorescent channel

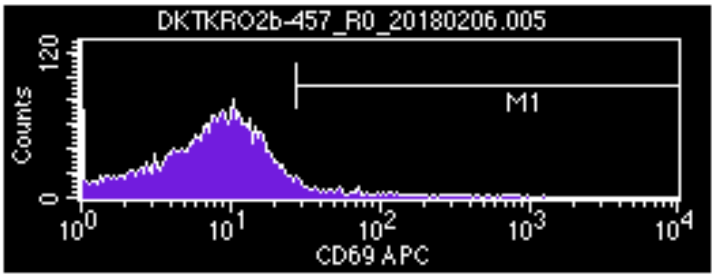

X-axis: intensity of expression of CD69-APC upon a specified lymphocyte subpopulation, Y-axis: counts of cells which stain positive for CD69-APC. M1 is placed as a marker to factor out overlapping of fluorescent channels and background noise based on the isotype control for the APC fluorescent channel.

The results are manually transferred to an Excel sheet. Obtained data is summarized in Table 21. Mean value of % Gated (NK cells, T cells, NK-like T cells; tube 2-10) and CD69+ gMFI (tube 5-7) is calculated for each lymphocyte subpopulation for further analysis. APC isotype % Gated is deducted from CD69+ % Gated values, subsequently mean value of CD69+ % Gated is calculated for NK cells, T cells and NK-like T cells (tube 5-7). To improve the comparability between the blood samples, lymphocyte subpopulations are calculated so that NK cells, T cells, NK-like T cells and B cells add up to 100 percent. The obtained values are used for further statistical analysis.

Table 21: Obtained data from FACS analysis

value	tube
Isotype PE M1 (% Gated)	1
Isotype FITC M1 (% Gated)	1
Isotype APC M1 (% Gated)	1
Isotype PerCP M1 (% Gated)	1
NK cells (% Gated)	2-10
T cells (% Gated)	2-10
NK-like T cells (% Gated)	2-10
B cells (% Gated)	3
CD69+ NK cells (% Gated)	5-7
CD69+ T cells (% Gated)	5-7
CD69+ NK-like T cells (% Gated)	5-7
CD69+ gMFI for NK cells	5-7
CD69+ gMFI for T cells	5-7
CD69+ gMFI for NK-like T cells	5-7

2.2.3. Detection of soluble immune checkpoints with ELISA

Enzyme-linked immunosorbent assays (ELISA) are used to detect specific molecules in body fluids. The immunoassay is based on the key-lock principle. For this study, a sandwich ELISA-technique is deployed. Two different antibodies are needed which both bind to the antigen at distinct locations. First, an ELISA plate is coated with a capture antibody which is subsequently immobilized. A blocking solution is added to block free binding positions. Diluted patient samples and standards of prospected antigens are added. The antigen consequently binds to the capture antibody. Afterwards an added enzyme-marked detection antibody binds to the antigen. The concentration of the emerging complex can ultimately be measured by a color reaction. [196, 197] In this study two different ELISA setups serve to determine the level of soluble human PD-1 and human PD-L1 in plasma samples of patients and healthy donors.

The day before the experiment the wash buffer and reagent diluent are prepared. To obtain the wash buffer 250µL of Triton® X-100 are added per 500mL of PBS. For the reagent diluent 1g of bovine serum albumin is dissolved per 100mL PBS by using a heater (Heater MR Hei-Standard).

2.2.3.1. Programmed cell death protein 1 (PD-1)

Human PD-1 concentration in the samples is measured with the DuoSet® ELISA Development System Human PD-1 from R&D Systems. The manufacturer's protocol is strictly followed. The day before the experiment the capture antibody is diluted in PBS to obtain the working concentration of 1µg/mL. Each well of a Costar 3590 96 Well EIA/RIA Plate is coated with 100µL of the diluted capture antibody. The plate is sealed with Plate sealers Easyseal™ Transparent 79x135mm and incubated over night at 26°C without exposition to light.

The following day the 96-well plate is washed three times by filling each well with 300µL wash buffer and subsequently eliminating fluids by pouring out into the sink and tapping out on clean paper towels (equals one washing step). Afterwards each well is blocked by adding 300µL of the reagent diluent (1% BSA solution) and incubating for at least one hour at 26°C without light exposition after sealing. During this time Human PD-1 Standard is diluted in reagent diluent to receive a seven-point standard curve with concentrations between 156 and 10,000pg/mL. The patients' plasma samples and a control plasma sample of a healthy donor are diluted in a ratio of 1:4 in reagent diluent. 100µL of each sample and the seven standard concentrations are applied in duplicates to the plate after a washing step. Empty wells are filled with 100µL of reagent diluent. The plate is then sealed and placed in the incubator at 26°C for two hours. Following the incubation another washing step follows. The detection antibody is diluted in reagent diluent to the working concentration of 200ng/mL and hence 100µL are added to each well. The plate is then sealed and incubated in the incubator at 26°C for two hours. After a washing step 100µL of Streptavidin-HRP diluted in reagent diluent to the working concentration of a 200-fold dilution are added to the 96 wells. Afterwards the plate is sealed and incubated in the incubator at 26°C for 20 minutes. Another washing step follows the incubation. Then Color Reagent A (H_2O_2) and Color Reagent B (Tetramethylbenzidine) are mixed in equal parts.

100µL of this Substrate Solution are pipetted into each well, the plate is sealed and incubated at 26°C for 20 minutes without exposition to light. Consequently, 50µL of Stop Solution (2 N H2SO4) are added to every well. Immediately afterwards the optical density is measured at 450 and 570nm with the ELx808™ Absorbance Microplate Reader.

2.2.3.2. Programmed cell death ligand 1 (PD-L1)

DuoSet® ELISA Development System Human PD-L1/B7-H1 from R&D Systems is used to measure human PD-L1 concentration in the plasma samples. The manufacturer's protocol is strictly followed. The capture antibody is diluted in PBS to the working concentration of 4µg/mL one day before the experiment. 100µL of the diluted capture antibody are given into each well of a Costar 3590 96 Well EIA/RIA Plate. Plate sealers Easyseal™ Transparent 79x135mm are used to seal the plate during incubation over night at 26°C without exposition to light.

First, the 96-well plate is washed three times with 300µL wash buffer after incubation. The fluids are eliminated by pouring out into the sink and tapping out on clean paper towels (equals one washing step). For the purpose of blocking, 300µL of the reagent diluent (1% BSA solution) are added to each well. After applying a plate sealer, the plate is incubated for a minimum of one hour at 26°C without exposition to light. Concurrently, Human PD-L1 Standard is diluted in reagent diluent to gain a seven-point standard curve with concentrations between 156 and 10,000pg/mL. Also, the plasma samples of patients and healthy donors are diluted in reagent diluent in a ratio of 1:4. A sample of a healthy donor is used as a control plasma sample. Following another washing step 100µL of the diluted samples and the seven standard concentrations are pipetted in duplicates into the plate's wells. 100µL of reagent diluent fills the remaining empty wells. The plate is incubated at 26°C for two hours after attaching a plate sealer. After a washing step the detection antibody is diluted in reagent diluent to the working concentration of 50ng/mL. 100µL of diluted detection antibody are added to each well, then the plate is sealed and incubated at 26°C for two hours without exposition to light. Another washing step follows. 100µL of a 200-fold dilution of Streptavidin-HRP in reagent diluent are given to each of the 96 wells. The plate is sealed and rests for 20 minutes in the incubator at 26°C. After a washing step Color Reagent A (H2O2)

and Color Reagent B (Tetramethylbenzidine) are equally mixed, afterwards 100µL of this Substrate Solution are given into every well. The plate is sealed and incubated for 20 minutes at 26°C without any light exposure. 50µL of Stop Solution (2 N H2SO4) are given to each well. An ELx808™ Absorbance Microplate Reader is used to instantly measure the optical density at 450 and 570nm.

2.2.3.3. Analysis of ELISA data

After gaining the results for the absorbance at 450nm and 570nm, the results are transferred to Microsoft Excel. The 570nm readings are hence subtracted from the 450nm readings to correct for optical imperfections in the plate. Mean value of the empty wells is calculated. This blank value is subtracted from the results of the other wells. Subsequently, the standard curve is drawn to obtain the formula to calculate the concentrations of the patients' and healthy donors' samples. Since the plasma samples are diluted 1:4, the calculated concentration values are multiplicated by 4. As a last step, mean values of the duplicates are calculated to obtain final results for PD-1 and PD-L1 plasma concentration. Measuring range of both ELISA protocols is specified with 157-10,000pg/mL.

2.2.4. Statistical analysis

Statistical analysis is performed using the IBM SPSS statistical analysis software (free trial software package for iOS, Version 1.0.0.1508, SPSS Inc., Chicago, IL, USA). A 95% confidence interval (95% CI) is assumed, statistical significance is determined by two-tailed p-values with $p \leq 0{,}05$ ($p \leq 0.05$ = *, $p \leq 0.01$ = **, $p \leq 0.001$ = ***). Due to a very small sample size of 5 patients, R4 samples of the recurrence group are not further included in the analysis, instead R4 and R5 samples are brought together to time point R4/R5 for an improved comparability.

Statistical analysis is put together by nonparametric univariate and multivariate analysis. To detect potential differences, measured data of different time points of blood draw (R0, R1, R2, R3, R4/R5) is compared using Wilcoxon Signed Ranks test and Related-Samples Friedman's Two-Way Analysis of Variance by Ranks for related samples. Analysis of independent samples to determine significances between patient groups (CTRL, No Recurrence, Recurrence) consists of

Mann-Whitney U test and Independent-Samples Kruskal-Wallis test. Subsequently, Post-hoc-tests (Dunn-Bonferroni) are performed for significant results of the Related-Samples Friedman's Two-Way Analysis and Independent-Samples Kruskal-Wallis test. Simple bar graphs express the differences throughout time progression as well as in comparison within different patient groups.

3. Results

The study's patient collective consists of 107 patients suffering from HNSCC of whom 27 experience a recurrence within the observational period and 10 healthy donors (control group, CTRL), as portrayed in Table 18. Age and gender as well as general constitution of all participants are unknown. Patients undergo radiation therapy in combination with cisplatin-based chemotherapy, healthy donors are untreated. Disease- and treatment-related effects on lymphocyte subpopulations, expression of early activation marker CD69 on certain lymphocyte subpopulations as well as expression of immune checkpoint PD-1 and its ligand PD-L1 are consequently investigated in the peripheral blood within a follow-up period of 2 years.

3.1. Radiation therapy induced effects on lymphocyte subpopulations

To obtain improved comparability between patient samples, lymphocyte subpopulations are adjusted so that NK cells, T cells, NK-like T cells and B cells consistently add up to 100 percent. For the control group, solely one blood sample is taken. Mean percentage of NK cells is under 10 percent, while T cells add up to almost 70 percent. NK-like T cells sum up to 3.5 percent and mean percentage of B cells is around 19 percent (see Figure 9).

Figure 9: Composition of lymphocyte subpopulations within the CTRL group

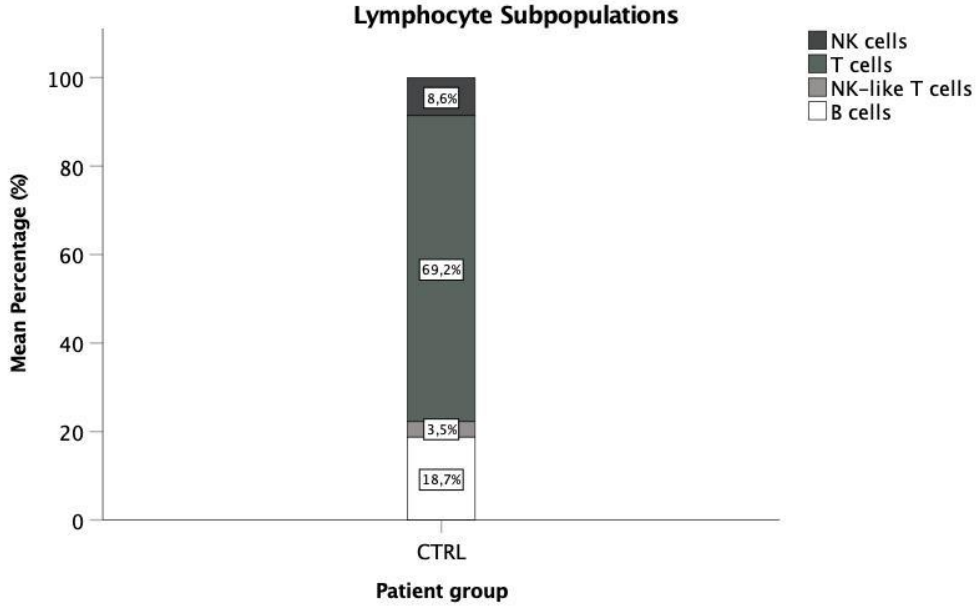

For patients without recurrence five blood samples are scheduled to be taken in total: Before treatment (R0), during chemoradiotherapy (R1), 3 months after chemoradiotherapy (R2), 6 months after chemoradiotherapy (R3) and 12 months after chemoradiotherapy (R4). Mean percentage of NK cells amounts to approximately 12 percent before radiation therapy. Consecutively after undergoing radiotherapy, mean percentage of NK cells levels up to around 20 percent. Before and during radiation therapy, T cells account for a mean percentage over 70 percent, after radiation therapy the percentage shrinks to around 60 percent and continuously sinks to under 60 percent one year after irradiation. NK-like T cells sum up to almost 5 percent before radiotherapy and are elevated during irradiation and in the following time (6.2% to 7.3%). Before undergoing therapy, mean percentage of B cells of patients without recurrent disease is situated around 11 percent. During irradiation, the percentage shrinks to 6 percent and consecutively recovers after therapy (7.5% to 13.2%) (see Figure 10).

Figure 10: Composition of lymphocyte subpopulations within the No Recurrence group

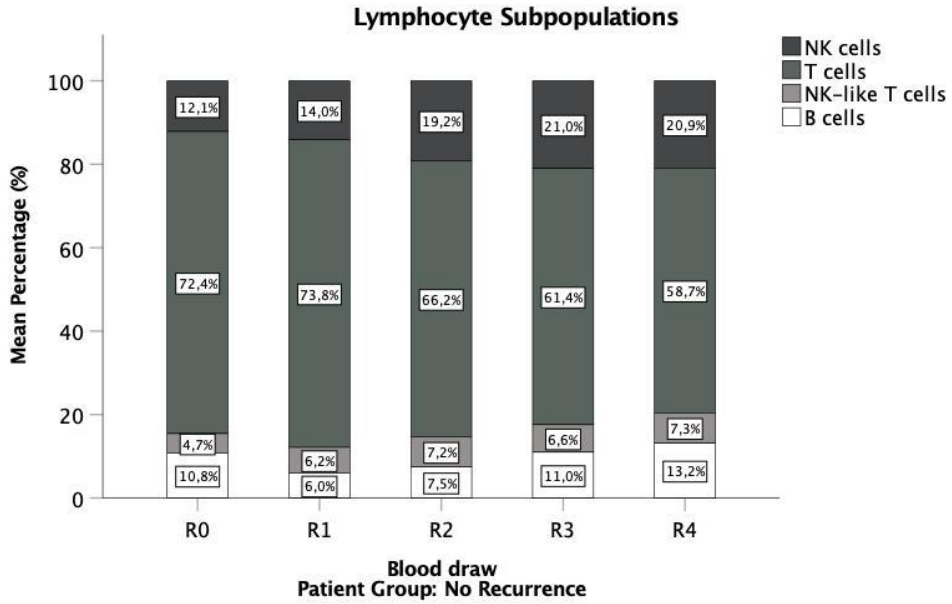

For patients experiencing recurrent disease five blood samples are used for further analysis: Before treatment (R0), during chemoradiotherapy (R1), 3 months after chemoradiotherapy (R2), 6 months after chemoradiotherapy (R3) and in case of recurrence (R5). Mean percentage of NK cells accounts for about 12 percent

before patients undergo therapy. During irradiation mean percentage of NK cells rises to approximately 14 percent and consecutively after treatment to percentages between 17.7 and 22.7 percent. Mean percentage of T cells accounts for almost 69 percent before radiotherapy, after irradiation the percentage shrinks to 59 percent. After recurrence mean percentage of T cells is located at 55 percent. NK-like T cells amount to over 6 percent before radiotherapy and are especially elevated during irradiation (10.4%). After the treatment they account for 8.1% to 9.4%. Patients suffering from recurrent disease initially show a mean percentage of B cells of 12.6 percent. During radiotherapy, the percentage sinks to 8.8 percent, after the treatment B cells recover and amount to percentages from 12.4% to 14.2% (see Figure 11).

Figure 11: Composition of lymphocyte subpopulations within the Recurrence group

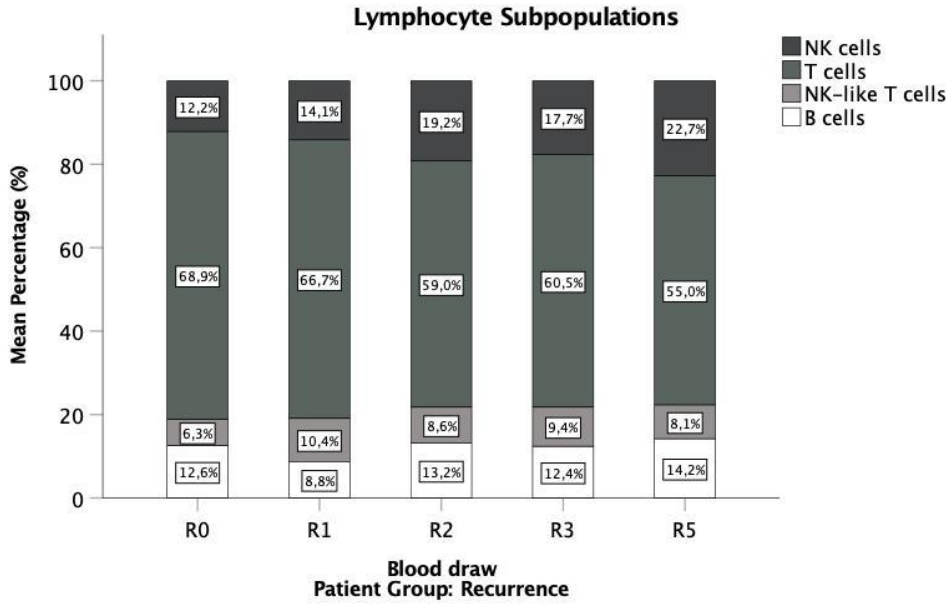

In conclusion, patients suffering from HNSCC present with a higher NK cell and NK-like T cell mean percentage in comparison with healthy donors. Furthermore, mean percentage of B cells is notably reduced in patients with head and neck cancer. HNSCC patients show similar progression within the lymphocyte subpopulations regardless of tumor recurrence.

3.1.1. NK cells

When analyzing data between groups for each time point (R0, R1 R2, R3, R4/R5), Kruskal-Wallis test is used to show differences in the mean percentage (%) of NK cells from time point R2 to R4/R5 (R2: $\chi 2 = 13.429$, $p = 0.001$, R3: $\chi 2 = 15.121$, $p = 0.001$, R4/R5: $\chi 2 = 16.839$, $p \leq 0.001$). A subsequent Dunn-Bonnferroni test confirms that the mean percentage (%) of NK cells is significantly higher for the No Recurrence group (R2: $z = -3.617$, $p = 0.001$, R3: $z = -3.882$, $p = \leq 0.001$, R4: $z = -3.869$, $p \leq 0.001$) and Recurrence group (R2: $z = -3.133$, $p = 0.005$, R3: $z = -2.573$, $p = 0.03$, R5: $z = -3.912$, $p \leq 0.001$) compared with healthy donors (CTRL) (see Figure 12).

Figure 12: Variances between patient groups in the mean percentage of NK cells for all blood draws R0 to R4/R5 analyzed by multivariate analysis (*p ≤ 0.05, **p ≤ 0.01, ***p ≤ 0.001)

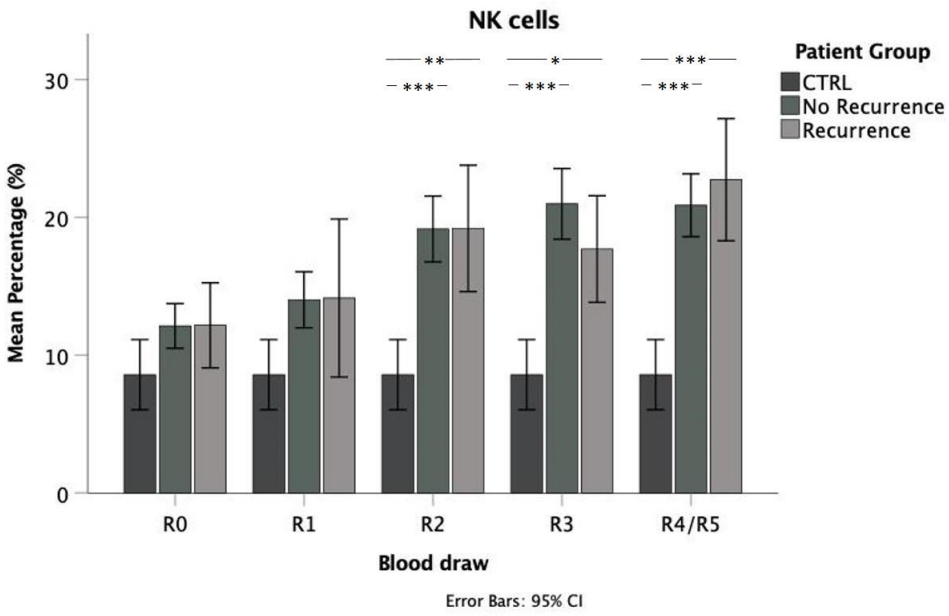

Performing univariate analysis, at time point R1 percentage of NK cells is higher for the No Recurrence group (Mdn = 12.26%, Mann-Whitney-U-Test: $z = -2.254$, $p = 0.024$) in relation to healthy donors (Mdn = 8.84%). Regarding time points R2 to R4/R5, both No Recurrence (R2: Mdn = 18.39%, Mann-Whitney-U-Test: $z = -3.565$, $p \leq 0.001$, R3: Mdn = 20.05%, Mann-Whitney-U-Test: $z = -3.762$, $p \leq 0.001$, R4: Mdn = 20.37%, Mann-Whitney-U-Test: $z = -3.942$, $p \leq 0.001$) and Recurrence group (R2: Mdn = 17.85%, Mann-Whitney-U-Test: $U = 26.500$, $p = 0.001$, R3: Mdn = 19.78%, Mann-Whitney-U-Test: $U = 16.000$, $p = 0.002$,

R5: Mdn = 23.10%, Mann-Whitney-U-Test: z = -3.673, p ≤ 0.001) show a higher NK cell percentage compared with CTRL (Mdn = 8.84%) (see Figure 13).

Figure 13: Variances between patient groups in the mean percentage of NK cells for all blood draws R0 to R4/R5 analyzed by univariate analysis (*p ≤ 0.05, **p ≤ 0.01, ***p ≤ 0.001)

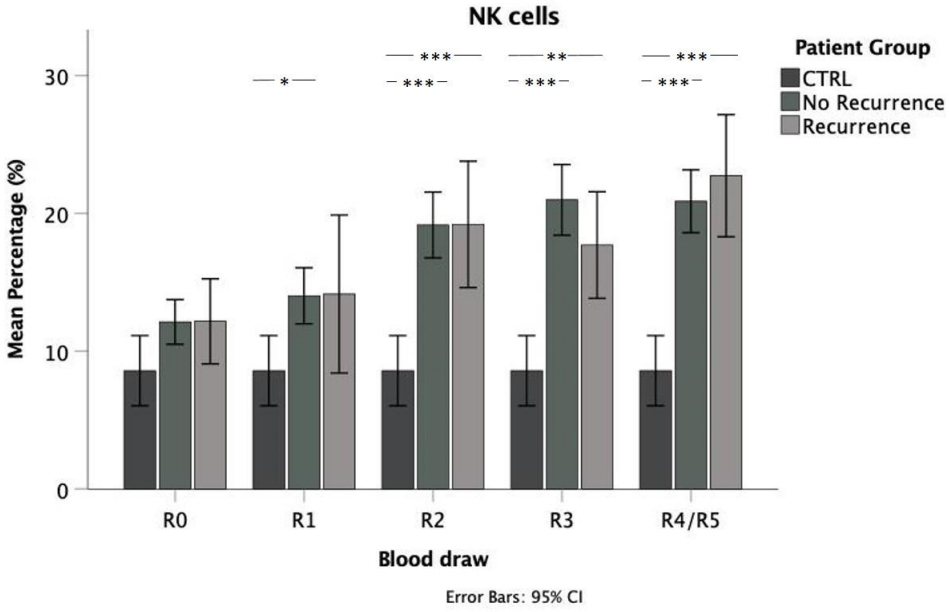

Looking at the changes over the time points of blood draw, mean percentage of NK cells differs significantly within the No Recurrence group (Friedman test: χ^2= 45.872, p ≤ 0.001, n = 47). A Dunn-Bonnferroni Post-hoc test confirms significant elevation of the NK cell mean percentage when comparing time point R0 with time point R2 (z = -1.468, p_{adj} ≤ 0.001), time point R3 (z = -1.766, p_{adj} ≤ 0.001) and time point R4 (z = -1.851, p_{adj} ≤ 0.001). The same observation is made when comparing time point R1 with time point R3 (z = -1.000, p_{adj} = 0.022) and time point R4 (z = -1.085, p_{adj} = 0.009) (see Figure 14). Regarding the Recurrence group, the Friedman Test is renounced in regard of a too small valid sample size of 4.

The Wilcoxon test aids to determine significant differences in the mean percentage of NK cells between single time points in the peripheral blood of patients. Regarding the No Recurrence group, mean percentage of NK cells grows continuously over time progression. Significant differences between time point R0 (Mdn = 11.29%) and time point R1 (Mdn = 12.26%, z = -2.258, p = 0.024, n = 144), time point R2 (Mdn = 18.39%, z = -5.874, p ≤ 0.001, n = 139), time point R3

(Mdn = 20.05%, z = -5.989, p ≤ 0.001, n = 144) and time point R4 (Mdn = 20.37%, z = -6.159, p ≤ 0.001, n = 148) are confirmed with Wilcoxon test as well as differences between time point R1 (Mdn = 12.26%) and time point R2 (Mdn = 18.39%, z = -3.849, p ≤ 0.001, n = 137), time point R3 (Mdn = 20.05%, z = -3.898, p ≤ 0.001, n = 142) and time point R4 (Mdn = 20.37%, z = -4.564, p ≤ 0.001, n = 146). Additionally, a significant elevation of NK cell percentage can be spotted between time point R2 (Mdn = 18.39%) and time point R4 (Mdn = 20.37%, z = -2.503, p = 0.012, n = 141). Merely a trend towards a higher mean percentage at time point R3 (Mdn = 20.05%, z = -1.887, p = 0.059, n = 137) in comparison with time point R2 (Mdn = 18.39%) is noted (see Figure 15).

Figure 14: Variances between time points of blood draw in the mean percentage of NK cells for the No Recurrence group analyzed by multivariate analysis (*p ≤ 0.05, **p ≤ 0.01, ***p ≤ 0.001)

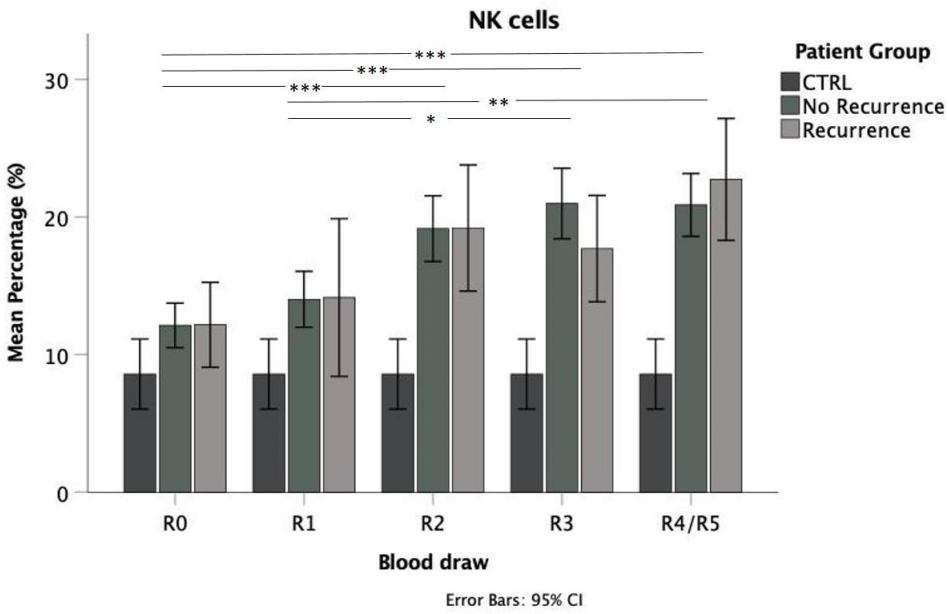

Analyzing the Recurrence group, the mean percentage of NK cells is accordingly growing throughout time progression. In comparison with time point R0 (Mdn = 10.84%), mean percentages at time point R1 (Mdn = 11.43%, z = -2.480, p = 0.013, n = 38), time point R2 (Mdn = 17.85%, z = -3.070, p = 0.002, n = 42) and time point R5 (Mdn = 23.10%, z = -3.782, p ≤ 0.001, n = 48) differ significantly. Further significances can be detected between time point R5 (Mdn = 23.10%) and time point R1 (Mdn = 11.43%, z = -3.154, p = 0.002, n = 42), time point R2 (Mdn = 17.85%, z = -2.938, p = 0.003, n = 46) and time point R3 (Mdn = 19.78%,

z = -3.040, p = 0.002, n = 39) (see Figure 16).

Figure 15: Variances between time points of blood draw in the mean percentage of NK cells for the No Recurrence group analyzed by univariate analysis (*p ≤ 0.05, **p ≤ 0.01, ***p ≤ 0.001)

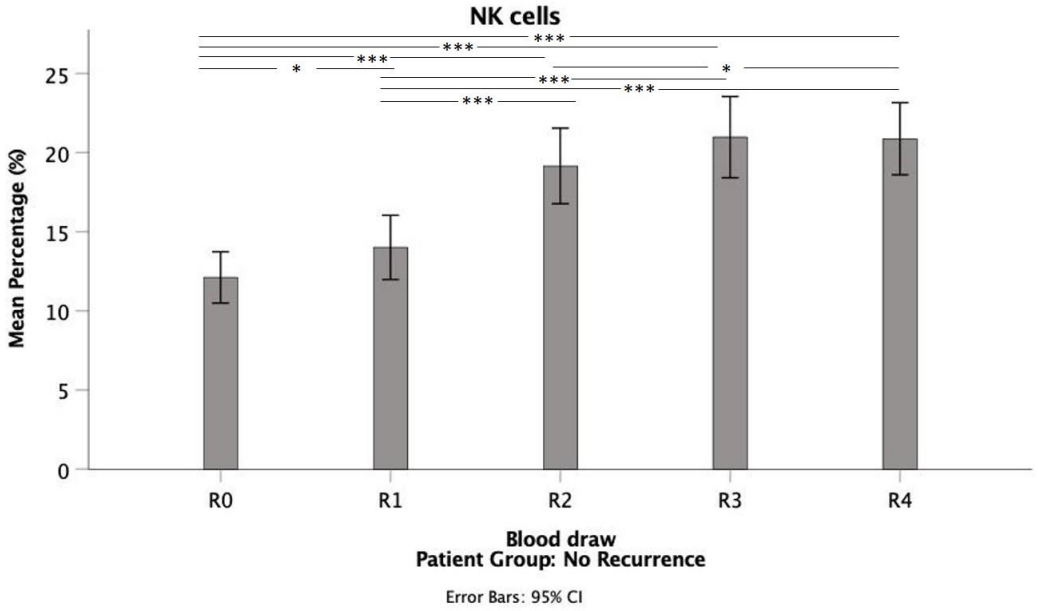

Figure 16: Variances between time points of blood draw in the mean percentage of NK cells for the Recurrence group analyzed by univariate analysis (*p ≤ 0.05, **p ≤ 0.01, ***p ≤ 0.001)

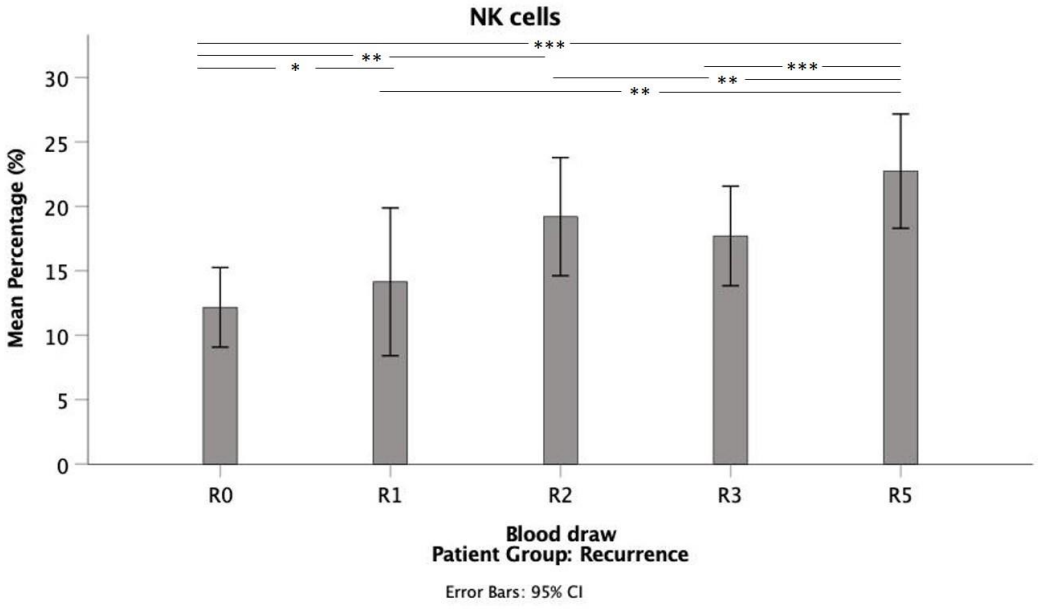

Consecutively, mean percentage of NK cells shows higher values for HNSCC patients after irradiation therapy in comparison with healthy donors.

Furthermore, the percentage grows over time within the No Recurrence group as well as in the Recurrence group.

3.1.2. T cells

As a following step, we investigated the mean percentages of T cells. Kruskal-Wallis test shows that the mean percentage (%) of T cells differs significantly for time points R2, R3 and R4/R5. (R2: χ^2 = 9.067, p = 0.011, R3: χ^2 = 6.811, p = 0.033, R4/R5: χ^2 = 14.040, p = 0.001). A following Dunn-Bonnferroni Post-hoc test is conducted. At time point R2, mean percentage of the Recurrence group is lower when comparing with the No Recurrence (z = 2.658, p = 0.024) and CTRL group (z = 2.565, p = 0.031). For time point R3, mean percentage (%) is lower within the No Recurrence compared with the CTRL group (z = 2.515, p = 0.036), while at time point R4 mean percentage (%) is lower for both No Recurrence (z = 3.187, p = 0.004) and Recurrence group (z = 3.731, p = 0.001) compared with healthy donors (see Figure 17).

Figure 17: Variances between patient groups in the mean percentage of T cells for all blood draws R0 to R4/R5 analyzed by multivariate analysis (*p ≤ 0.05, **p ≤ 0.01, ***p ≤ 0.001)

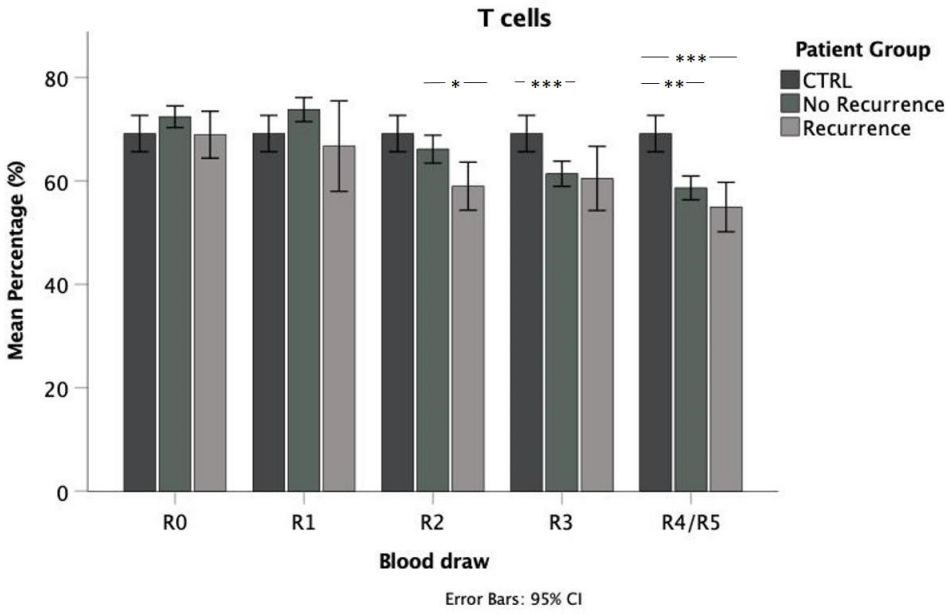

T cells are significantly reduced in patients of the No Recurrence group (Mdn = 74.60%, Mann-Whitney-U-Test: z = -1.974, p = 0.024) compared with healthy donors (Mdn = 71.34%) at time point R1. For time point R2, the Recurrence

group (Mdn = 59.94%) reveals a lower T cell percentage compared with patients without recurrent disease (Mdn = 66.885%, Mann-Whitney-U-Test: z = -2.622, p = 0.009) and the CTRL group (Mdn = 71.335%, Mann-Whitney-U-Test: U = 39.000, p = 0.006). T cell percentage is higher for CTRL (Mdn = 71.34%) at time point R3 and R4/R5 in comparison with No Recurrence (R3: Mdn = 62.45%, Mann-Whitney-U-Test: z = -2.498, p = 0.012, R4: Mdn = 59.09%, Mann-Whitney-U-Test: z = -3.383, p = 0.001) and Recurrence (R3: Mdn = 64.78%, Mann-Whitney-U-Test: U = 28.000, p = 0.021, R5: Mdn = 54.12%, Mann-Whitney-U-Test: z = -3.179, p = 0.001) (see Figure 18).

After initiation of radiation therapy, the mean percentage of T cells shrinks significantly within the No Recurrence group (Friedman test: χ^2= 79.319, p ≤ 0.001, n = 47). A Dunn-Bonnferroni Post-hoc test confirms significant differences for time point R0 in relation to time point R2 (z = 1.021, p_{adj} = 0.017), time point R3 (z = 1.830, p_{adj} ≤ 0.001) and time point R4 (z = 2.426, p_{adj} ≤ 0.001). Significant decline is also ascertained for time point R3 (z = 1.574, p_{adj} ≤ 0.001) and time point R4 (z = 2.170, p_{adj} ≤ 0.001) in comparison with time point R1. In relation to time point R2, T cells show a lower mean percentage at time point R4 (z = 1.404, p_{adj} ≤ 0.001) (see Figure 19). For the Recurrence group, Friedman test cannot deliver significant information due to the small valid sample size of 4.

According to the Wilcoxon test, the mean percentage of T cells sinks continuously after radiation therapy regarding patients without recurrence. Significant differences can be reported for time point R0 (Mdn = 72.37%) in comparison with time point R2 (Mdn = 66.89%, z = -5.066, p ≤ 0.001, n = 139), time point R3 (Mdn = 62.45%, z = -6.391, p ≤ 0.001, n = 144) and time point R4 (Mdn = 59.09%, z = -7.009, p ≤ 0.001, n = 148). When comparing time point R1 (Mdn = 74.60%) with time point R2 (Mdn = 66.89%, z = -4.438, p ≤ 0.001, n = 137), time point R3 (Mdn = 62.45%, z = -5.787, p ≤ 0.001, n = 142) and time point R4 (Mdn = 59.09%, z = -6.608, p ≤ 0.001, n = 146) the decline is also significant. Same conclusion can be drawn between time point R2 (Mdn = 66.89%) in relation to time point R3 (Mdn = 62.45%, z = -4.715, p ≤ 0.001, n = 137) and time point R4 (Mdn = 59.09%, z = -5.376, p ≤ 0.001, n = 141) as well as between time point R3 (Mdn = 62.45%) and time point R4 (Mdn = 59.09%, z = -2.986, p = 0.003, n = 146) (see Figure 20).

Figure 18: Variances between patient groups in the mean percentage of T cells for all blood draws R0 to R4/R5 analyzed by univariate analysis (*p ≤ 0.05, **p ≤ 0.01, ***p ≤ 0.001)

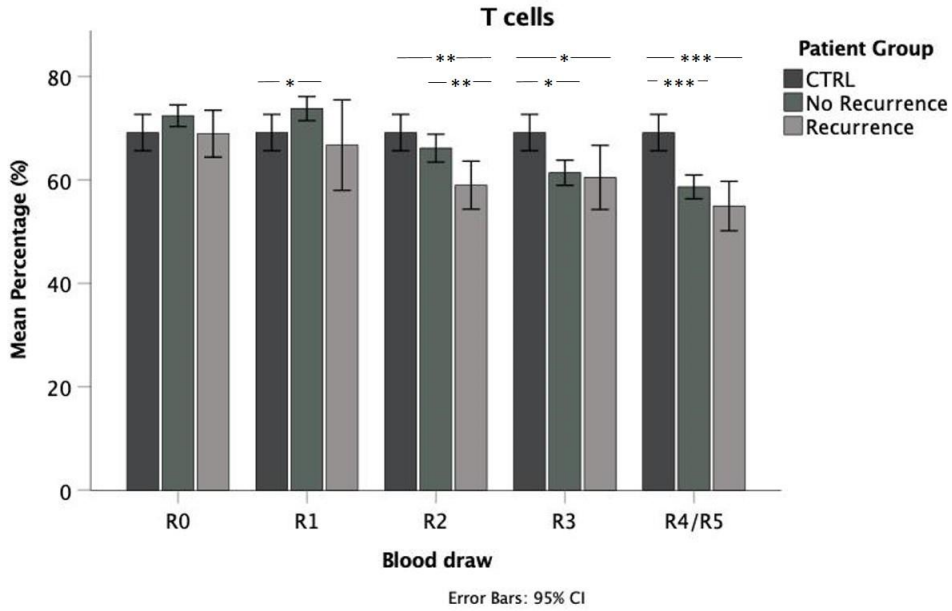

Figure 19: Variances between time points of blood draw in the mean percentage of T cells for the No Recurrence group analyzed by multivariate analysis (*p ≤ 0.05, **p ≤ 0.01, ***p ≤ 0.001)

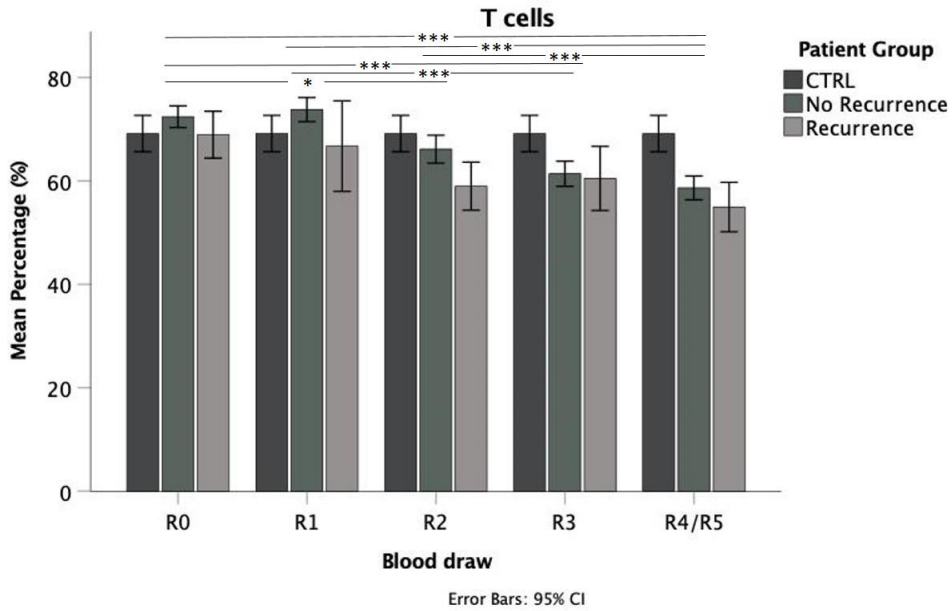

T cells are also sinking subsequently over the course of time in the peripheral blood of patients experiencing tumor recurrence. Significant differences become obvious between time point R0 (Mdn = 73.06%) and time point R2 (Mdn = 59.95%, z = -2.983, p = 0.003, n = 42), time point R3 (Mdn = 64.78%, z = -2.191, p = 0.028, n = 35) and time point R5 (Mdn = 54.12%, z = -3.945, p ≤ 0.001, n = 48).

Furthermore, significant results between time point R5 (Mdn = 54.12%) and time point R1 (Mdn = 70.12%, z = -2.844, p = 0.004, n = 42), time point R2 (Mdn = 59.95%, z = -3.219, p = 0.001, n = 46) and time point R3 (Mdn = 64.78%, z = -3.110, p = 0.002, n = 39) exist (see Figure 21).

Figure 20: Variances between time points of blood draw in the mean percentage of T cells for the No Recurrence group analyzed by univariate analysis (*p ≤ 0.05, **p ≤ 0.01, ***p ≤ 0.001)

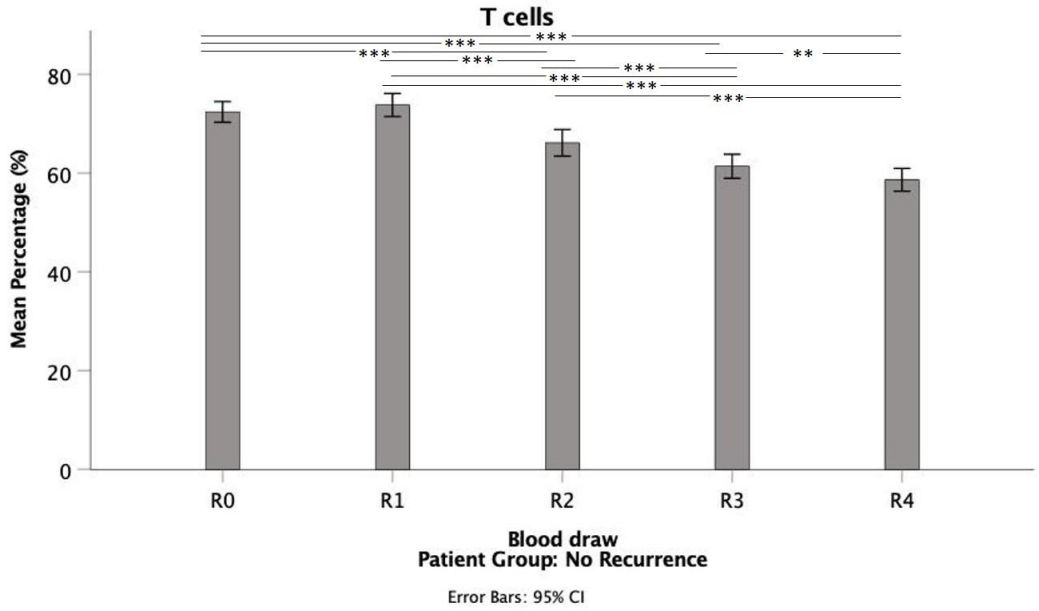

Figure 21: Variances between time points of blood draw in the mean percentage of T cells for the Recurrence group analyzed by univariate analysis (*p ≤ 0.05, **p ≤ 0.01, ***p ≤ 0.001)

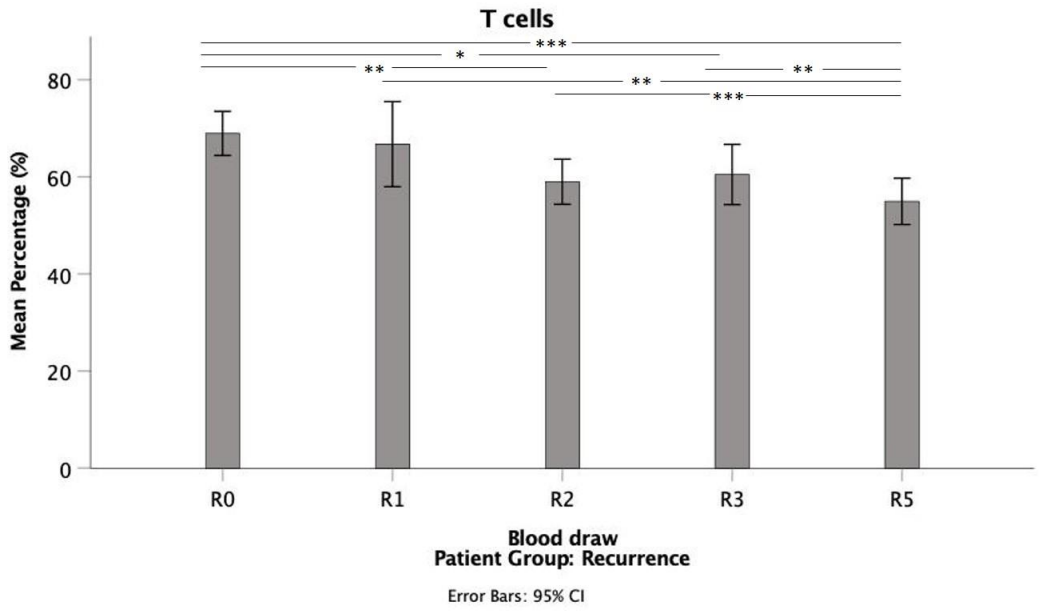

In conclusion, initial T cell percentages are similar throughout all patient groups. The mean percentage of T cells begins to sink following radiation therapy within patients suffering from HNSCC.

3.1.3. NK-like T cells

Considering NK-like T cells, solely a trend for differences between groups is obvious for time point R1 (χ^2 = 5.758, p = 0.056) for analysis with Kruskal-Wallis test (see Figure 22).

Figure 22: Variances between patient groups in the mean percentage of NK-like T cells for all blood draws R0 to R4/R5 analyzed by multivariate analysis (*p ≤ 0.05, **p ≤ 0.01, ***p ≤ 0.001)

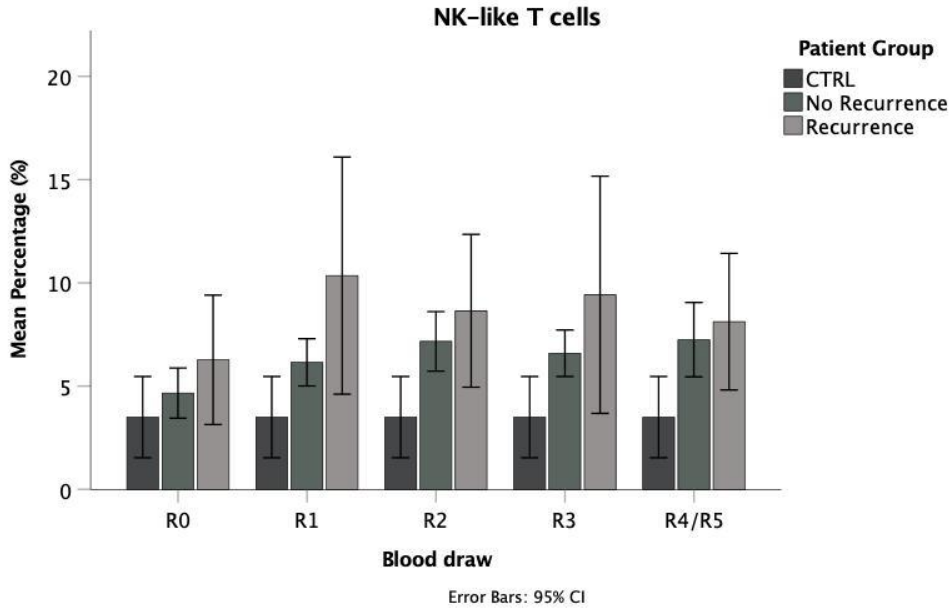

NK-like T cells are significantly elevated for patients suffering from recurrence (Mdn = 7.98%, Mann-Whitney-U-Test: U = 35.000, p = 0.017) when comparing with the control group (Mdn = 2.21%) at time point R1. At time point R2 mean percentage is significantly higher for the No Recurrence group (Mdn = 4.74%, Mann-Whitney-U-Test: z = -2.236, p = 0.025) and showing a higher trend for the Recurrence group (Mdn = 5.68%, Mann-Whitney-U-Test: U = 56.000, p = 0.055) in relation to CTRL (Mdn = 2.21%). Patients without recurrence experience a significantly higher NK-like T cell percentage at time point R3 (Mdn = 4.87%, Mann-Whitney-U-Test: z = -2.283, p = 0.022) and a higher trend at time point R4 (Mdn = 4.62%, Mann-Whitney-U-Test: z = -1.910, p = 0.056) in comparison with

CTRL (Mdn = 2.21%) (see Figure 23).

Figure 23: Variances between patient groups in the mean percentage of NK-like T cells for all blood draws R0 to R4/R5 analyzed by univariate analysis (*p ≤ 0.05, **p ≤ 0.01, ***p ≤ 0.001)

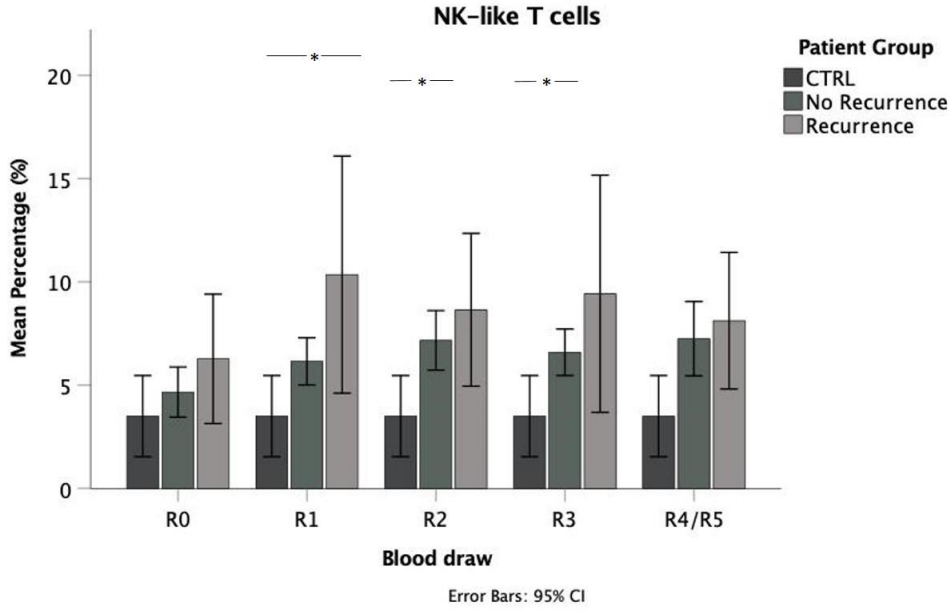

Performing a Friedman test ($\chi^2 = 51.762$, $p \leq 0.001$, $n = 47$), a significantly higher NK-like T cell mean percentage can be observed for individuals of the No Recurrence group throughout all following time points (R1: $z = -2.000$, $p_{adj} \leq 0.001$, R2: $z = -1.979$, $p_{adj} \leq 0.001$, R3: $z = -1.681$, $p_{adj} \leq 0.001$, R4: $z = -1.255$, $p_{adj} = 0.001$) in comparison with initial values at time point R0 (see Figure 24). The valid sample size of 4 is too small to draw a meaningful conclusion with the Friedman test for the Recurrence group.

Similar to the Friedman test, the Wilcoxon test displays significant differences for the No Recurrence group between time point R0 (Mdn = 3.89%) in comparison with time point R1 (Mdn = 5.08%, $z = -5.848$, $p \leq 0.001$, $n = 144$), time point R2 (Mdn = 4.74%, $z = -5.395$, $p \leq 0.001$, $n = 139$), time point R3 (Mdn = 4.87%, $z = -5.727$, $p \leq 0.001$, $n = 144$) and time point R4 (Mdn = 4.62%, $z = -5.072$, $p \leq 0.001$, $n = 148$) (see Figure 25).

Cases of recurrence show a similar behavior, mean percentages of NK-like T cells vary significantly between time point R1 (Mdn = 7.98%, $z = -2.856$, $p = 0.004$, $n = 38$), time point R2 (Mdn = 5.68%, $z = -2.765$, $p = 0.006$, $n = 42$), time point R3

(Mdn = 4.37%, z = -2.395, p = 0.017, n = 35), time point R5 (Mdn = 4.84%, z = -3.068, p = 0.002, n = 48) on basis of time point R0 (Mdn = 3.57%) (see Figure 26).

Figure 24: Variances between time points of blood draw in the mean percentage of NK-like T cells for the No Recurrence group analyzed by multivariate analysis (*p ≤ 0.05, **p ≤ 0.01, ***p ≤ 0.001)

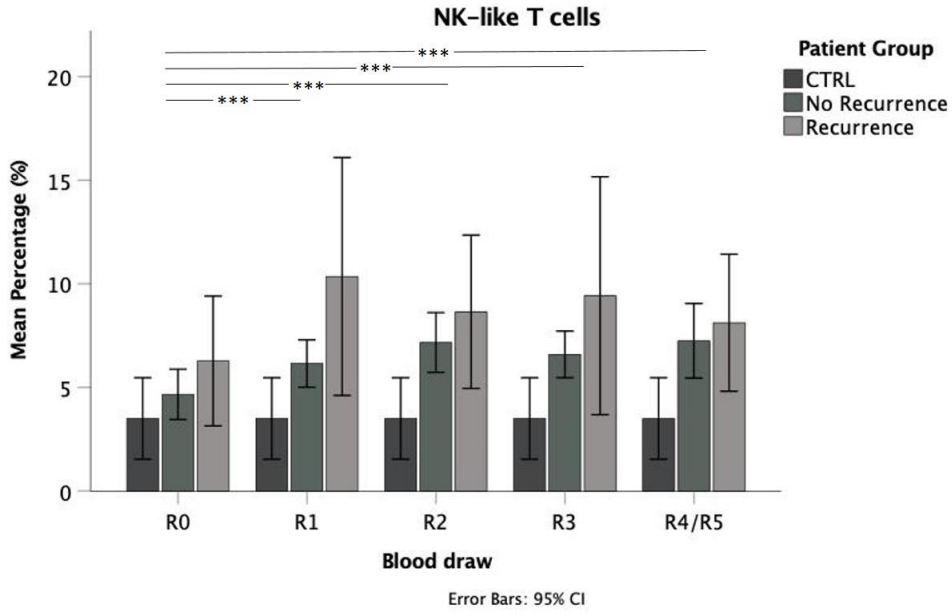

Figure 25: Variances between time points of blood draw in the mean percentage of NK-like T cells for the No Recurrence group analyzed by univariate analysis (*p ≤ 0.05, **p ≤ 0.01, ***p ≤ 0.001)

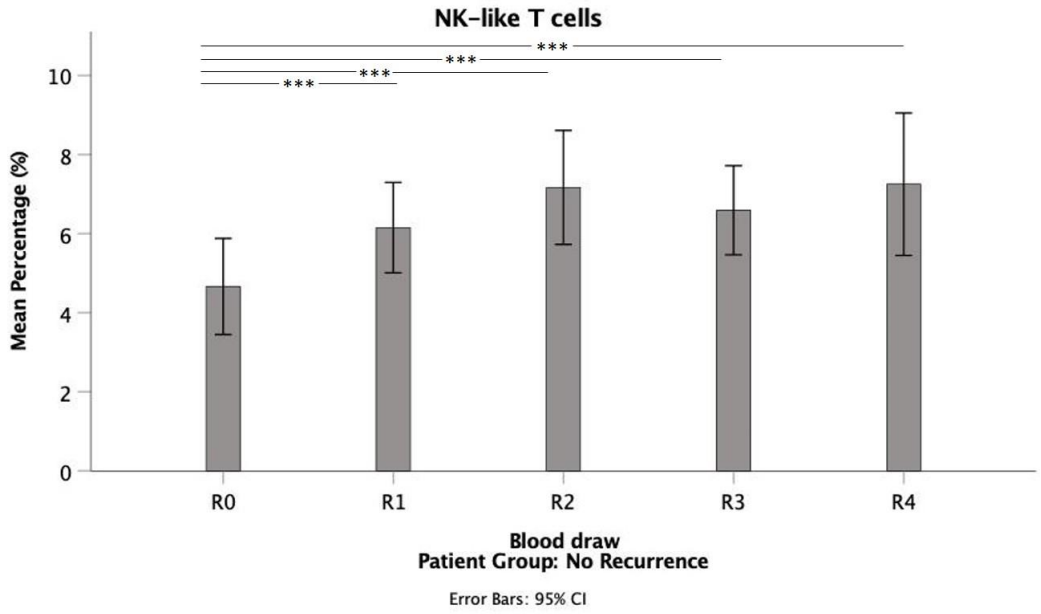

Figure 26: Variances between time points of blood draw in the mean percentage of NK-like T cells for the Recurrence group analyzed by univariate analysis (*p ≤ 0.05, **p ≤ 0.01, ***p ≤ 0.001)

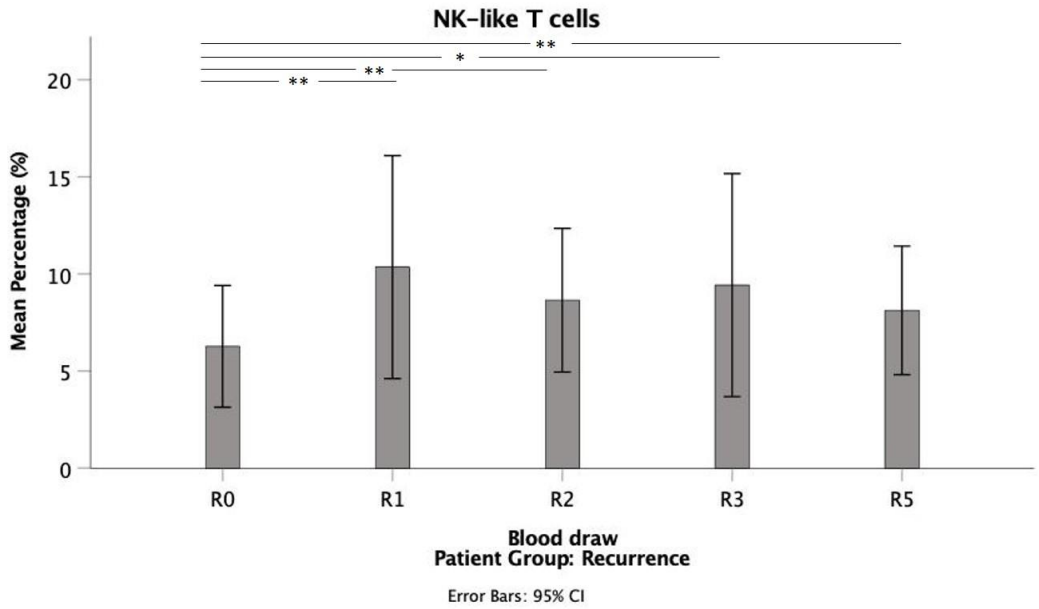

After radiation therapy, levels of NK-like T cells are significantly higher within patients without recurrence in comparison with healthy donors. For patients suffering from recurrence a similar observation is shown in the graphs even though a statistical significance can only be defined for the blood draw R1 during radiation therapy. In relation to initial values, the mean percentage of NK-like T cells is elevated at all following blood draws after initiating irradiation.

3.1.4. B cells

Next, we analyzed the mean percentage of B cells which demonstrate a different development. Performing a Kruskal-Wallis test significant differences between the patient groups can be determined (R0: χ^2 = 11.751, p = 0.003, R1: χ^2 = 22.571, p ≤ 0.001, R2: χ^2 =19.570, p ≤ 0.001, R3 χ^2 = 10.092, p = 0.006). At time point R4/R5 mean percentage (%) of B cells is not significantly different between groups. A Dunn-Bonnferroni Post-hoc test reveals that for time point R0 the mean percentage of B cells in the CTRL group is significantly higher when comparing with the No Recurrence group (z = 3.386, p = 0.002) and Recurrence group (z = 2.970, p = 0.009). For time point R1, there is the same observation (No Recurrence: z = 4.304, p ≤ 0.001, Recurrence: z = 4.526, p ≤ 0.001). Regarding time point R2 this significant difference is only obvious between the CTRL and No Recurrence group (z = 4.131, p ≤ 0.001), as well as for time point R3 (z = 3.173, p = 0.005). For time

point R3 the Recurrence group shows a trend to a lower mean percentage (%) compared with the CTRL group (z = 2.342, p = 0.057) (see Figure 27).

Figure 27: Variances between patient groups in the mean percentage of B cells for all blood draws R0 to R4/R5 analyzed by multivariate analysis (*p ≤ 0.05, **p ≤ 0.01, ***p ≤ 0.001)

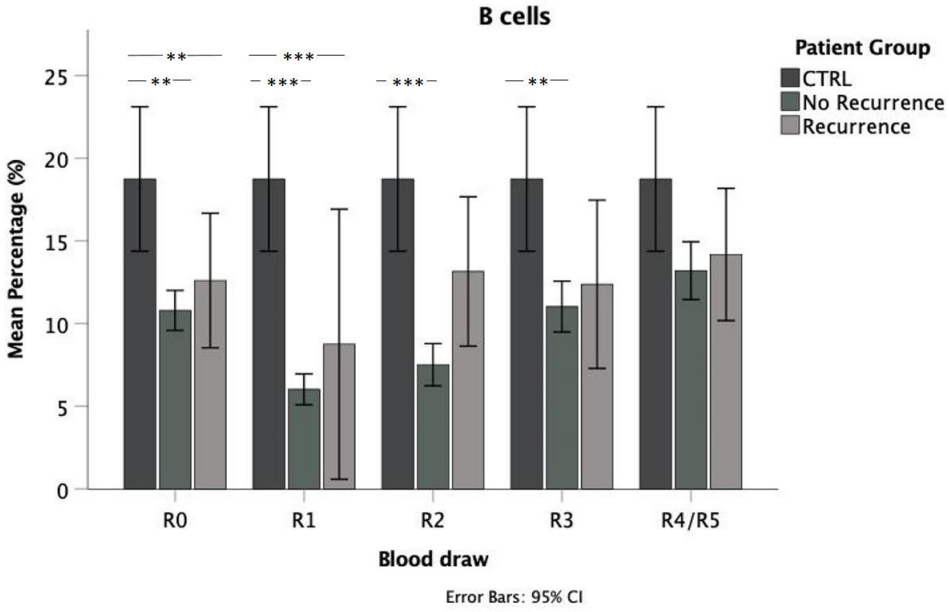

Mean percentage (%) of B cells is significantly reduced for the No Recurrence (Mdn = 10.35%, Mann-Whitney-U-Test: z = - 3.511, p ≤ 0.001) and Recurrence group (Mdn = 9.56%, Mann-Whitney-U-Test: z = - 2.561, p = 0.010) when comparing with the CTRL group (Mdn = 19.21%) for time point R0. The same observation can be drawn for time point R1 (No Recurrence: Mdn = 5.26%, Mann-Whitney-U-Test: z = - 4.759, p ≤ 0.001, Recurrence: Mdn = 4.14%, Mann-Whitney-U-Test: U = 16.000, p ≤ 0.001, CTRL: Mdn = 19.21%, Mann-Whitney-U-Test: z = - 3.511, p ≤ 0.001). Regarding time point R2 mean percentage of B cells is significantly reduced for the No Recurrence group (Mdn = 5.79%) when comparing with the Recurrence (Mdn = 11.74%, Mann-Whitney-U-Test: z = - 2.203, p = 0.028) and CTRL group (Mdn = 19.21%, Mann-Whitney-U-Test: z = - 4.241, p ≤ 0.001). For time point R3 only for the No Recurrence group (Mdn = 10.37%, Mann-Whitney-U-Test: z = - 3.259, p = 0.001) a significantly lower B cell percentage can be ascertained while the Recurrence group (Mdn = 8.85%, Mann-Whitney-U-Test: U = 34.000, p = 0.057) shows a trend towards a lower percentage when comparing with healthy donors

(Mdn = 19.21%). At time point R4 B cells are reduced for the No Recurrence group (Mdn = 12.22%, Mann-Whitney-U-Test: z = - 2.292, p = 0.022) compared with CTRL (Mdn = 19.21%) (see Figure 28).

Figure 28: Variances between patient groups in the mean percentage of B cells for all blood draws R0 to R4/R5 analyzed by univariate analysis (*p ≤ 0.05, **p ≤ 0.01, ***p ≤ 0.001)

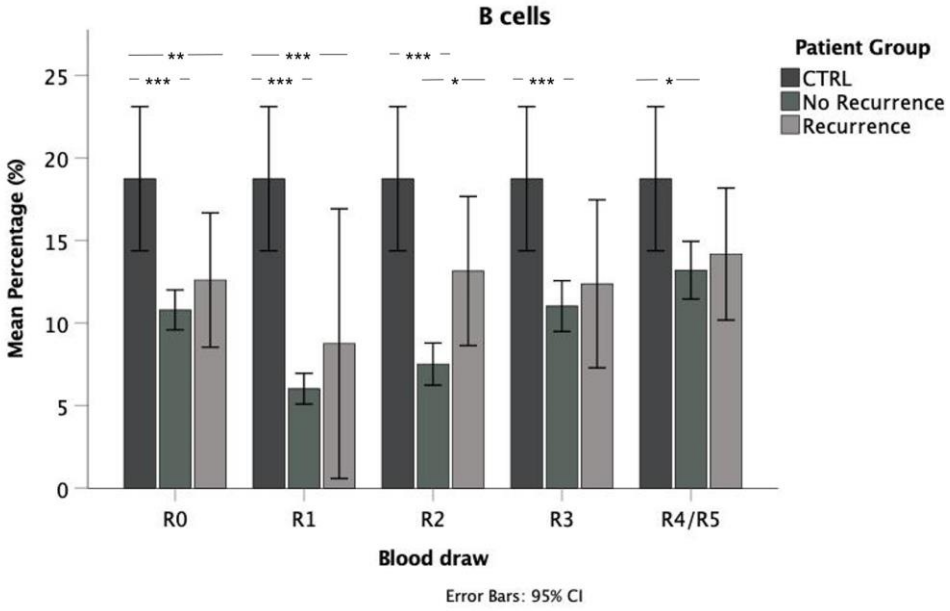

After radiation therapy, mean percentage of B cells significantly declines in the No Recurrence group before the number of B cells recovers starting at time point R2 (Friedman test: $\chi^2 = 71.506$, $p \leq 0.001$, n = 47). Dunn-Bonnferroni Post-hoc test confirms this observation comparing time point R0 with time point R1 (z = 1.574, $p_{adj} \leq 0.001$) and time point R2 (z = 1.170, $p_{adj} = 0.003$) as well as comparing time point R1 with time point R3 (z = -1.574, $p_{adj} \leq 0.001$) and time point R4 (z = -2.404, $p_{adj} \leq 0.001$). Also, a significant increase for B cells can be stated between time point R2 and time point R3 (z = -1.170, $p_{adj} = 0.003$) as well as between time point R2 and time point R4 (z = -2.000, $p_{adj} \leq 0.001$) (see Figure 29). Regarding the Recurrence group, the valid sample size of 4 is too small to draw a proper conclusion with the Friedman test.

When comparing the mean percentage of B cells for each blood draw within the No Recurrence group, the Wilcoxon test confirms the observations from the Friedman test. Significances are observed between time point R0 (Mdn = 10.35%) and time point R1 (Mdn = 5.26%, z = -6.596, p ≤ 0.001, n = 144), time point R2

(Mdn = 5.79%, z = -3.978, p ≤ 0.001, n = 139) and time point R4 (Mdn = 12.22%, z = -3.752, p ≤ 0.001, n = 148) as well as between time point R1 (Mdn = 5.26%) and time point R2 (Mdn = 5.79%, z = -2.370, p = 0.018, n = 137), time point R3 (Mdn = 10.37%, z = -5.591, p ≤ 0.001, n = 142) and time point R4 (Mdn = 12.22%, z = -6.698, p ≤ 0.001, n = 146). Additionally, significant differences are obvious between time point R2 (Mdn = 5.79%) and following blood draws (R3: Mdn = 10.37%, z = -4.970, p ≤ 0.001, n = 137, R4: Mdn = 12.22%, z = -5.642, p ≤ 0.001, n = 141) and time point R3 (Mdn = 10.37%) and time point R4 (Mdn = 12.22%, z = -4.398, p ≤ 0.001, n = 146) (see Figure 30).

Figure 29: Variances between time points of blood draw in the mean percentage of B cells for the No Recurrence group analyzed by multivariate analysis (*p ≤ 0.05, **p ≤ 0.01, ***p ≤ 0.001)

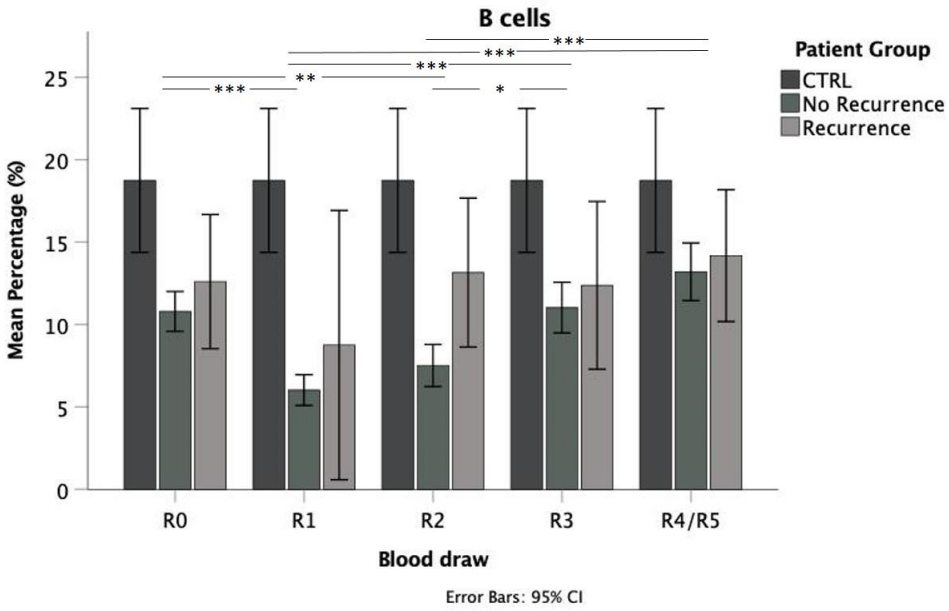

For patients with recurrence significances are less frequently detected. Merely significant results between time point R0 (Mdn = 9.56%) and time point R1 (Mdn = 4.14%, z = -2.040, p = 0.041, n = 38) as well as between time point R2 (Mdn = 11.74%) and time point R5 (Mdn = 13.11%, z = -2.374, p = 0.018, n = 46) can be reported (see Figure 31).

Figure 30: Variances between time points of blood draw in the mean percentage of B cells for the No Recurrence group analyzed by univariate analysis (*p ≤ 0.05, **p ≤ 0.01, ***p ≤ 0.001)

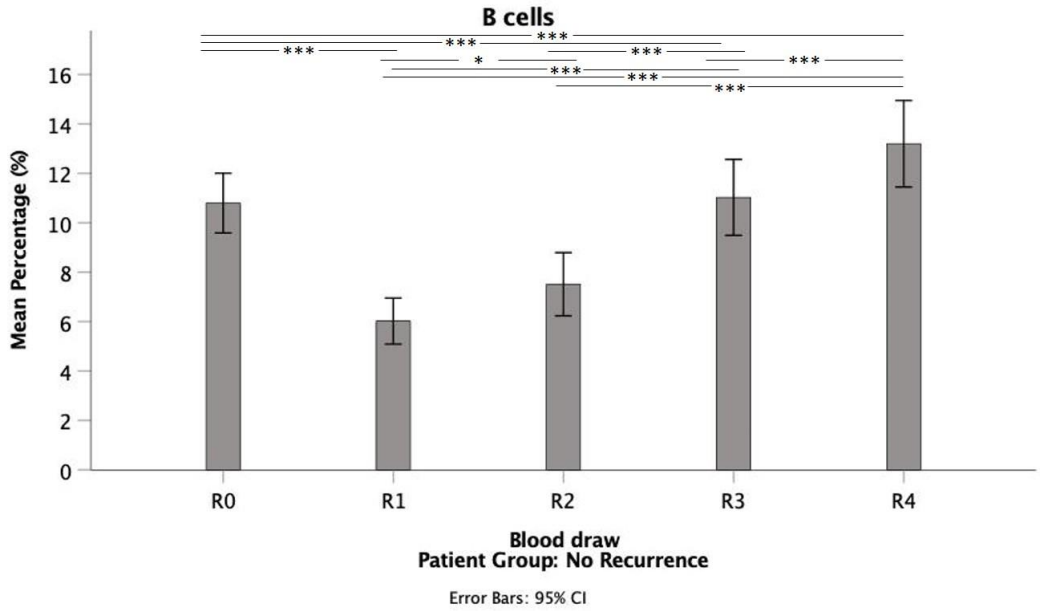

Figure 31: Variances between time points of blood draw in the mean percentage of B cells for the Recurrence group analyzed by univariate analysis (*p ≤ 0.05, **p ≤ 0.01, ***p ≤ 0.001)

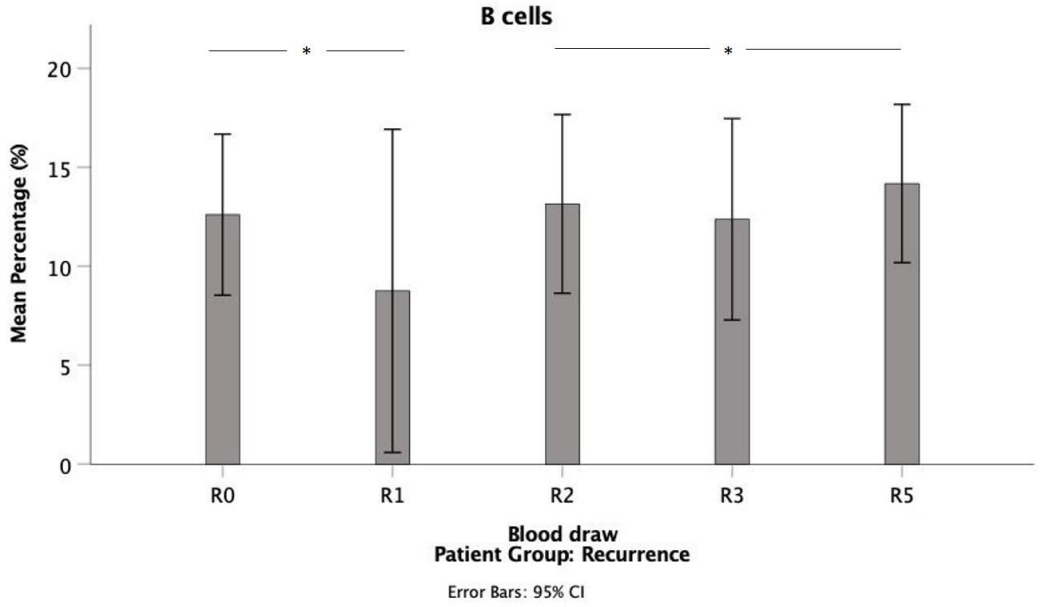

Initial percentages of B cells are significantly lower within tumor patients compared with healthy donors. After initiating radiation therapy, B cells further sink. Following the treatment, mean percentage of B cells starts to recover within patients without recurrence. For patients with recurrence, the changes over time are not as distinct. B cell levels of healthy individuals cannot be reached at the final

blood draws R4 and R5 for patients suffering from HNSCC. We are not solely interested in the lymphocytes' behavior after irradiation but also in the evaluation of potential prognostic biomarkers. Therefore, we explored the expression percentage and intensity of CD69 upon the surface of lymphocytes.

3.2. Early activation marker CD69 as a potential prognostic biomarker

3.2.1. NK cells

Percentage of CD69+ NK cells

Kruskal-Wallis test and Mann-Whitney-U-Test cannot confirm any significances between patient groups concerning the mean percentage of CD69+ NK cells. Looking at the changes over the time points of blood draw, mean percentage of CD69+ NK cells differs significantly within the No Recurrence group (Friedman test: $\chi 2 = 11.449$, $p = 0.022$, $n = 45$). A Dunn-Bonnferroni Post-hoc test solely states a higher trend for time point R1 compared with time point R0 ($z = -2.800$, $p_{adj} = 0.051$) (see Figure 32). Regarding the Recurrence group, the valid sample size of 4 is too small to draw a proper conclusion with the Friedman test.

Figure 32: Variances between time points of blood draw in the mean percentage of CD69+ NK cells for the No Recurrence group analyzed by multivariate analysis (*p ≤ 0.05, **p ≤ 0.01, ***p ≤ 0.001)

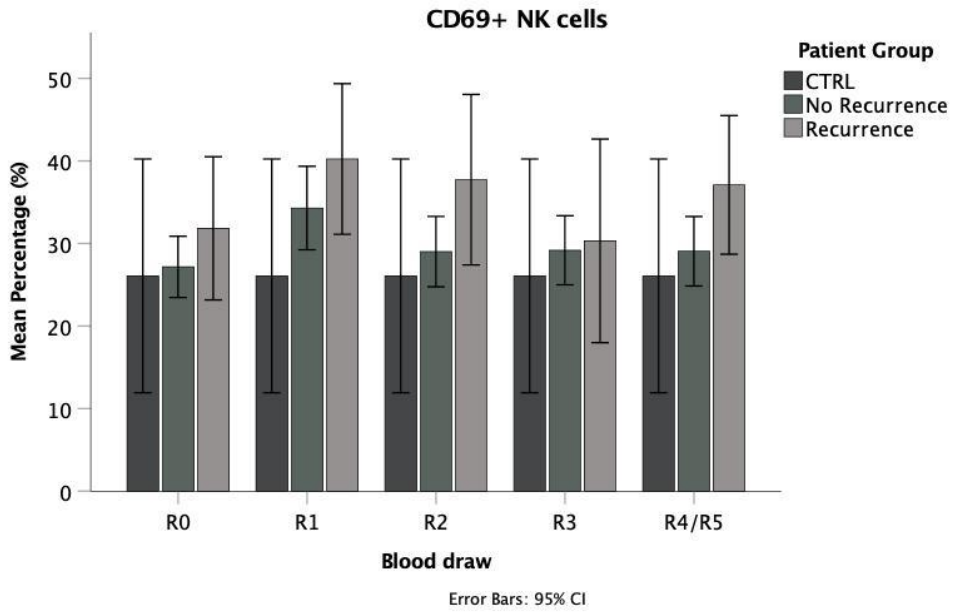

Analyzing the No Recurrence group with a Wilcoxon test, mean percentage of CD69+ NK cells is higher for blood draw R1 (Mdn = 29.69%) compared with time point R0 (Mdn = 23.91%, z = -2.891, p = 0.004, n = 144) and time point R3 (Mdn = 26.19%, z = -2.515, p = 0.012, n = 141) (see Figure 33).

Figure 33: Variances between time points of blood draw in the mean percentage of CD69+ NK cells for the No Recurrence group analyzed by univariate analysis (*p ≤ 0.05, **p ≤ 0.01, ***p ≤ 0.001)

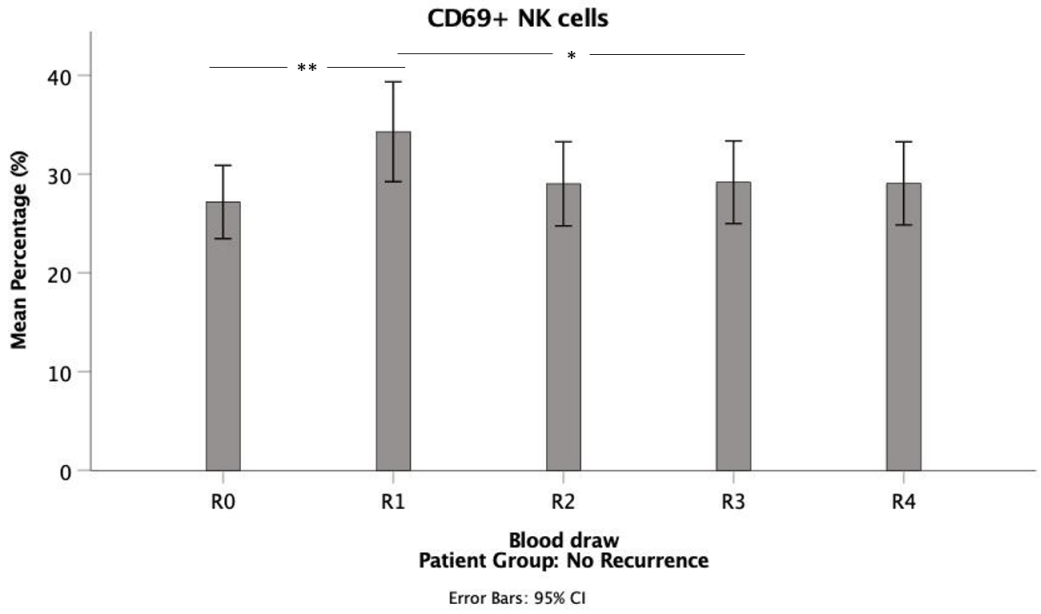

For the Recurrence group, Wilcoxon test confirms merely a significantly higher CD69+ NK cell mean percentage for time point R1 (Mdn = 44.41%, z = -2.291, p = 0.022, n = 38) compared with time point R0 (Mdn = 27.02%) (see Figure 34).

Ultimately, CD69+ NK cells present with an elevation during radiation therapy within HNSCC patients. After radiation therapy, levels fall to the initial mean percentage within patients without recurrence.

Figure 34: Variances between time points of blood draw in the mean percentage of CD69+ NK cells for the Recurrence group analyzed by univariate analysis (*p ≤ 0.05, **p ≤ 0.01, ***p ≤ 0.001)

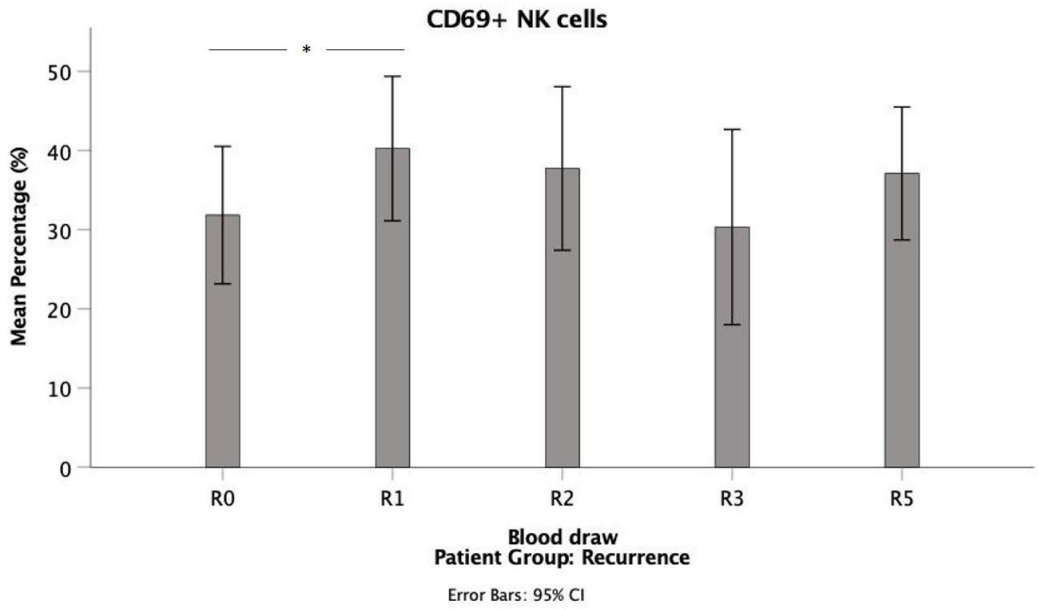

Geometric mean fluorescence intensity (gMFI) of CD69 on NK cells

A Kruskal-Wallis test cannot confirm any significant results regarding the CD69 gMFI of NK cells. With univariate analysis (Mann-Whitney-U test) a trend towards a higher CD69 gMFI within the Recurrence group can be stated (Mdn = 31.60%, Mann-Whitney-U-Test: z = -1.895, p = 0.058) in comparison with the CTRL group (Mdn = 22.21%) at time point R1 (see Figure 35).

Comparing time points of blood draw, significant differences within the No Recurrence group become obvious. (Friedman test: χ^2= 9.991, p = 0.041, n = 45). Elevation of the CD69 gMFI from time point R0 to time point R1 (z = -3.067, p_{adj} = 0.022) is confirmed by a Dunn-Bonnferroni Post-hoc test (see Figure 36). The valid sample size of 4 is too small to draw a meaningful conclusion with the Friedman test for the Recurrence group.

Comparing the first blood draw R0 (Mdn = 14.59%) with time point R1 (Mdn = 22.21%, z = -4.462, p ≤ 0.001, n = 144), time point R2 (Mdn = 21.18%, z = -2.848, p = 0.004, n = 139), time point R3 (Mdn = 20.19%, z = -2.493, p = 0.013, n = 143) and time point R4 (Mdn = 20.28%, z = -2.742, p = 0.006, n = 147) within the No Recurrence group via Wilcoxon test, the CD69 gMFI of NK cells shows a significant lower initial value (see Figure 37).

Figure 35: Variances between patient groups in the geometric mean fluorescence intensity of CD69+ NK cells for all blood draws R0 to R4/R5 analyzed by univariate analysis (*p ≤ 0.05, **p ≤ 0.01, ***p ≤ 0.001)

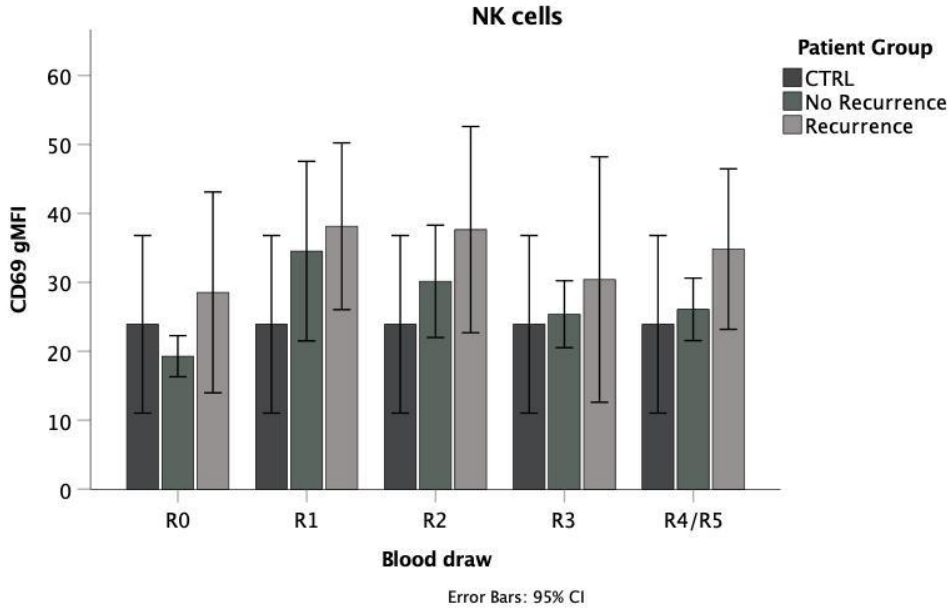

Figure 36: Variances between time points of blood draw in the geometric mean fluorescence intensity of CD69+ NK cells for the No Recurrence group analyzed by multivariate analysis (*p ≤ 0.05, **p ≤ 0.01, ***p ≤ 0.001)

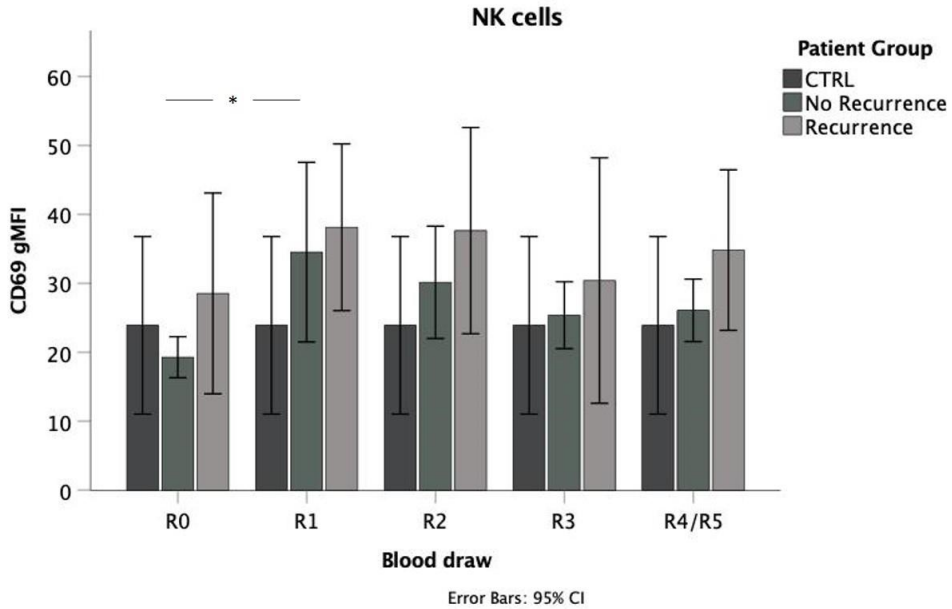

Figure 37: Variances between time points of blood draw in the geometric mean fluorescence intensity of CD69+ NK cells for the No Recurrence group analyzed by univariate analysis (*p ≤ 0.05, **p ≤ 0.01, ***p ≤ 0.001)

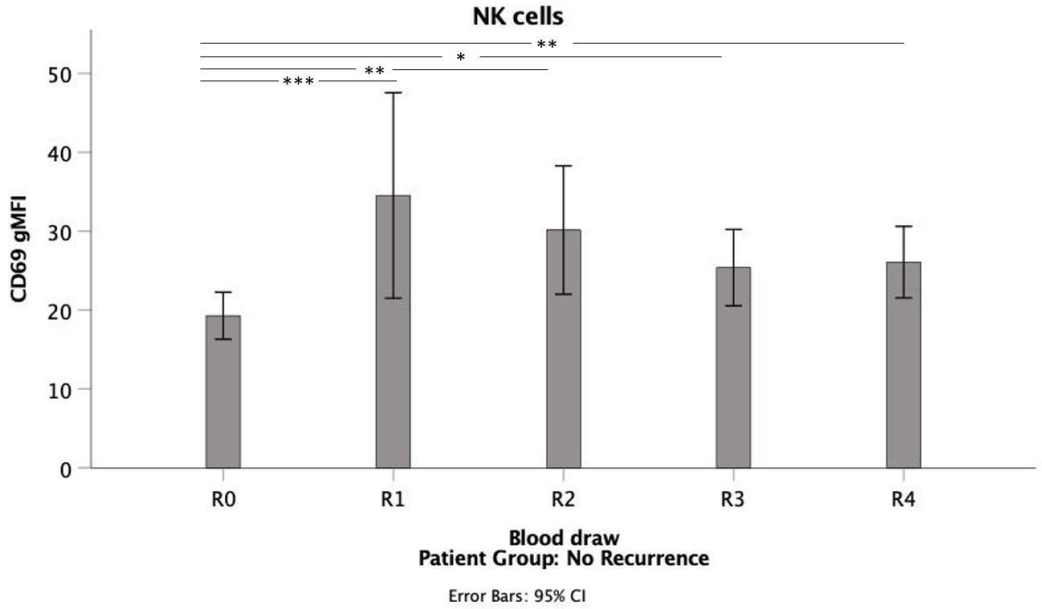

Regarding the Recurrence group, Wilcoxon test can solely reveal a significant elevation of CD69 gMFI at time point R1 (Mdn = 31.60%, z = -2.291, p = 0.022, n = 38) in comparison with time point R0 (Mdn = 21.19%) (see Figure 38).

Figure 38: Variances between time points of blood draw in the geometric mean fluorescence intensity of CD69+ NK cells for the Recurrence group analyzed by univariate analysis (*p ≤ 0.05, **p ≤ 0.01, ***p ≤ 0.001)

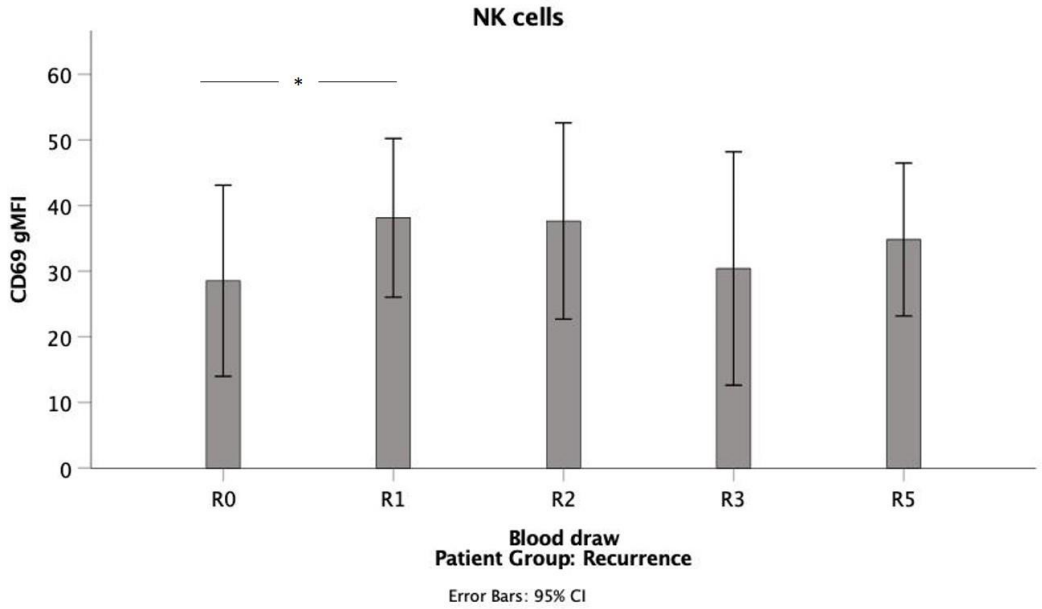

Within patients without recurrence, the geometric mean fluorescence intensity (gMFI) of CD69+ NK cells initially presents with lower values in relation to all following blood draws. gMFI is especially high during radiation therapy, this can also be confirmed to a lesser extent for patients suffering from recurrence.

3.2.2. T cells

Percentage of CD69+ T cells

In addition to CD69 expression on NK cells, we investigate the expression profile on T cells. Kruskal-Wallis test shows that the mean percentage of CD69+ NK cells differs significantly between patient groups for time point R2, R3 and R4/R5. (R2: $\chi^2 = 6.569$, $p = 0.037$, R3: $\chi^2 = 14.772$, $p = 0.001$, R4/R5: $\chi^2 = 13.224$, $p = 0.001$). A following Dunn-Bonnferroni Post-hoc test is conducted and reveals a significant difference between healthy donors and patients experiencing recurrent disease ($z = -2.517$, $p = 0.036$) for time point R2. For time point R3 mean percentage of the control group is lower in comparison with patients without recurrence ($z = -3.427$, $p = 0.002$) while at time point R4/R5 the No Recurrence group ($z = -2.650$, $p = 0.024$) and the Recurrence group ($z = -3.616$, $p = 0.001$) display a higher mean percentage in relation to healthy donors (see Figure 39).

Figure 39: Variances between patient groups in the mean percentage of CD69+ T cells for all blood draws R0 to R4/R5 analyzed by multivariate analysis (*p ≤ 0.05, **p ≤ 0.01, ***p ≤ 0.001)

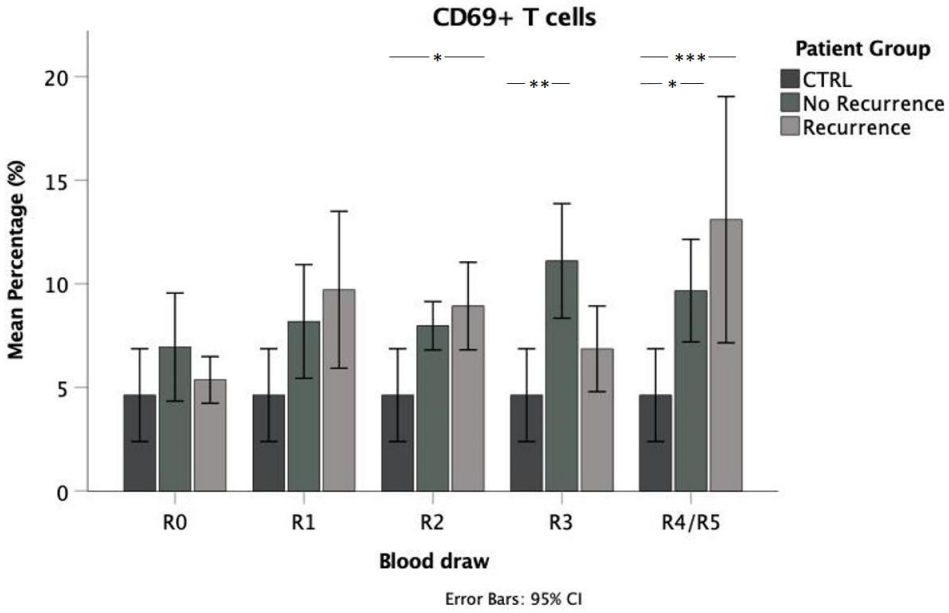

Univariate analysis reveals a higher CD69+ T cell mean percentage for the No Recurrence group (Mdn = 7.37%, Mann-Whitney-U-Test: z = -2.205, p = 0.027) and the Recurrence group (Mdn = 7.92%, Mann-Whitney-U-Test: U = 42.000, p = 0.010 in relation to the CTRL group (Mdn = 4.89%) at time point R2. For time point R3, the same result can be stated when comparing the No Recurrence group (Mdn = 8.89%, Mann-Whitney-U-Test: z = -3.433, p = 0.001) with the CTRL group (Mdn = 4.89%). Also, the No Recurrence group (Mdn = 8.89%, Mann-Whitney-U-Test: z = -2.193, p = 0.028) shows a significantly higher mean percentage compared with the Recurrence group (Mdn = 5.93%). Regarding the final blood draws R4 and R5, the No Recurrence group (Mdn = 8.13%, Mann-Whitney-U-Test: z = -2.762, p = 0.006) and Recurrence group (Mdn = 10.62%, Mann-Whitney-U-Test: z = -3.285, p = 0.001) have a higher CD69+ T cell mean percentage in relation to healthy donors (Mdn = 4.89%). Additionally, at the time of blood draw R5 the Recurrence group (Mdn = 10.62%, Mann-Whitney-U-Test: z = -2.051, p = 0.040) displays higher values in comparison with the No Recurrence group at blood draw R4 (Mdn = 8.13%) (see Figure 40).

Figure 40: Variances between patient groups in the mean percentage of CD69+ T cells for all blood draws R0 to R4/R5 analyzed by univariate analysis (*p ≤ 0.05, **p ≤ 0.01, ***p ≤ 0.001)

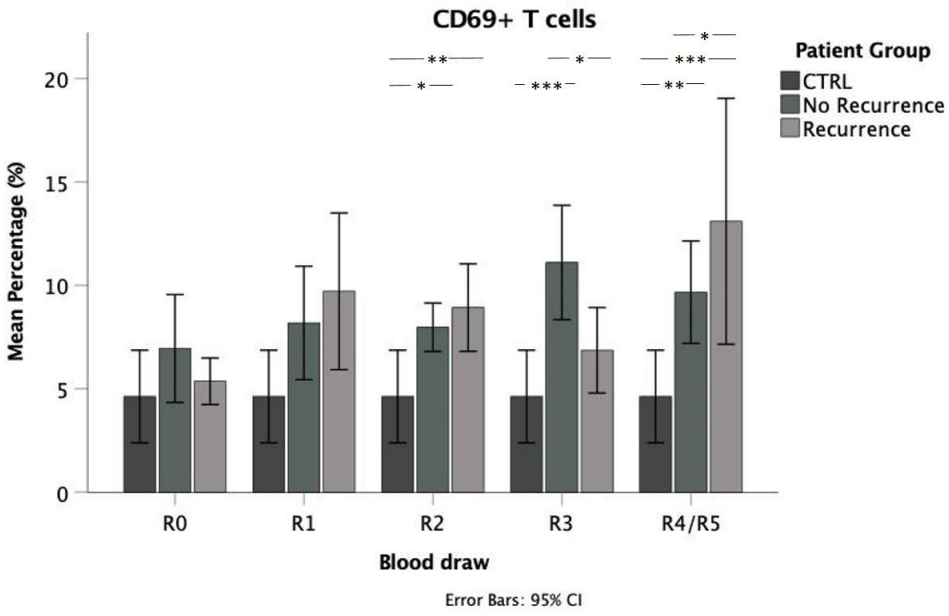

For CD69+ T cells, multivariate analysis confirms significant changes over the time points of blood draw within the No Recurrence group (Friedman test: χ^2= 28.213,

$p \leq 0.001$, n = 45). Elevation of the mean percentage over the course of time is confirmed by a Dunn-Bonnferroni Post-hoc test when comparing initial blood draw R0 with time point R2 (z = -2.867, $p_{adj} = 0.041$), time point R3 (z = -5.000, $p_{adj} \leq 0.001$) and time point R4 (z = -3.867, $p_{adj} = 0.001$) (see Figure 41). The valid sample size of 4 is too small to draw a meaningful conclusion with the Friedman test for the Recurrence group.

Figure 41: Variances between time points of blood draw in the mean percentage of CD69+ T cells for the No Recurrence group analyzed by multivariate analysis
(*p ≤ 0.05, **p ≤ 0.01, ***p ≤ 0.001)

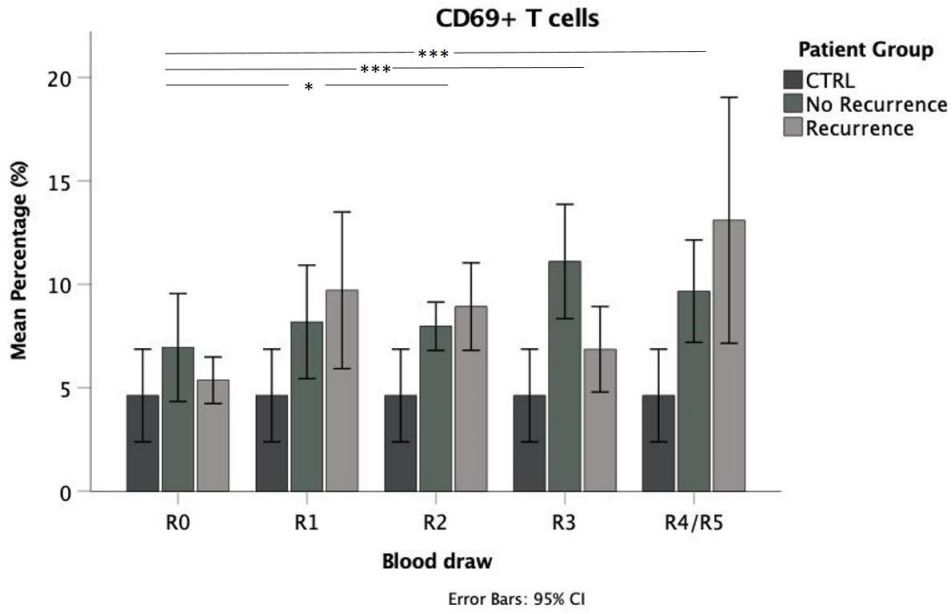

Mean percentage of CD69+ T cells is growing subsequently to the initial blood draw until the third blood draw within the No Recurrence group. Conducted by a Wilcoxon test, statistical significances confirm higher values for time point R1 (Mdn = 5.47%, z = -2.186, p = 0.029, n = 143), time point R2 (Mdn = 7.37%, z = -3.029, p = 0.002, n = 138), time point R3 (Mdn = 8.89%, z = -5.022, $p \leq 0.001$, n = 142) and time point R4 (Mdn = 8.13%, z = -4.219, $p \leq 0.001$, n = 146) compared with initial blood draw R0 (Mdn = 4.58%). In comparison with time point R1 (Mdn = 5.47%), time points R3 (Mdn = 8.89%, z = -3.625, $p \leq 0.001$, n = 141) and R4 (Mdn = 8.13%, z = -2.895, p = 0.004, n = 145) present with a higher CD69+ T cell mean percentage. Ultimately, the same growth is stated for time point R3 (Mdn = 8.89%, z = -2.578, p = 0.010, n = 136) in relation to time point R2

(Mdn = 7.37%) (see Figure 42).

Figure 42: Variances between time points of blood draw in the mean percentage of CD69+ T cells for the No Recurrence group analyzed by univariate analysis (*p ≤ 0.05, **p ≤ 0.01, ***p ≤ 0.001)

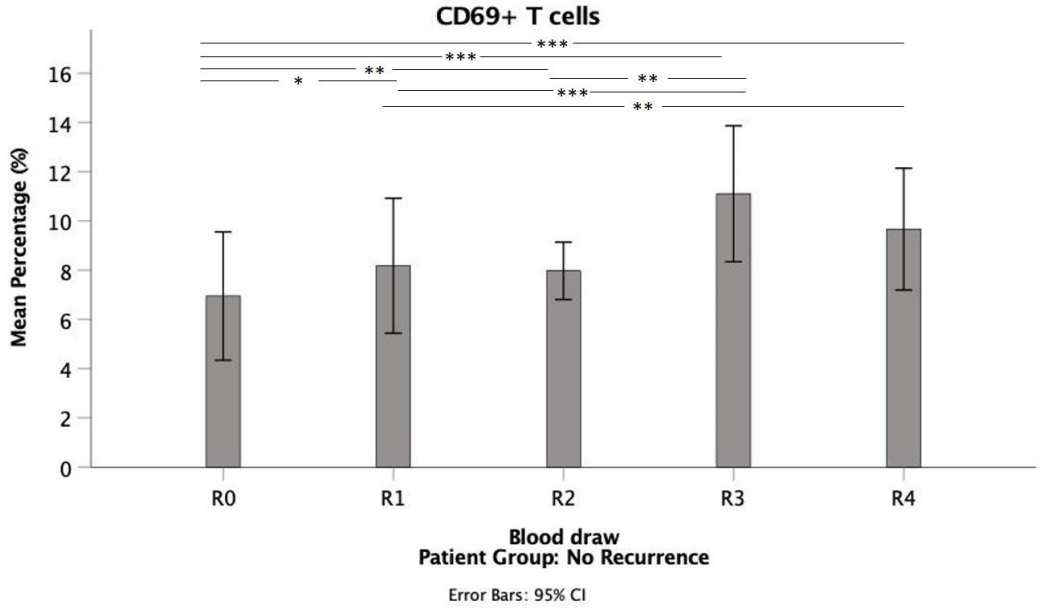

A significantly higher mean percentage of CD69+ T cells is stated by the Wilcoxon test for the Recurrence group when comparing time point R0 (Mdn = 5.48%) with time point R2 (Mdn = 7.92%, z = -3.288, p = 0.001, n = 42) and time point R5 (Mdn = 10.62%, z = -3.977, p ≤ 0.001, n = 48). Additionally, mean percentage presents higher values for time point R5 (Mdn = 10.62%, z = -2.271, p = 0.023, n = 39) in relation to time point R3 (Mdn = 5.93%) (see Figure 43).

In summary, mean percentage of CD69+ T cells is higher for patients suffering from head and neck cancer in relation to healthy individuals. Comparing the final blood draws R4 and R5, CD69+ T cells present with a higher mean percentage for patients experiencing tumor recurrence. Initial values are lower in comparison with consecutive blood draws, especially regarding patients without recurrence.

Figure 43: Variances between time points of blood draw in the mean percentage of CD69+ T cells for the Recurrence group analyzed by univariate analysis (*p ≤ 0.05, **p ≤ 0.01, ***p ≤ 0.001)

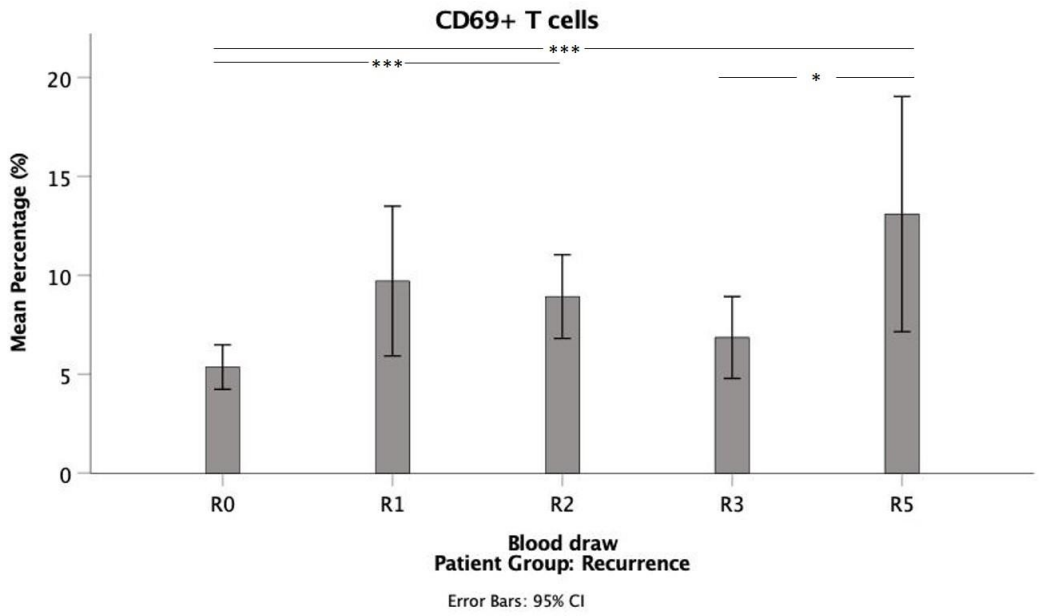

Geometric mean fluorescence intensity (gMFI) of CD69 on T cells

Performing a Kruskal-Wallis test, differences in the CD69 gMFI of T cells between patient groups are detected at time point R3 ($\chi 2 = 6.015$, $p = 0.049$) and time point R4/R5 ($\chi 2 = 7.642$, $p = 0.022$). A subsequent Dunn-Bonnferroni Post-hoc test cannot confirm any significances between the groups concerning blood draw R3, for blood draw R4/R5 CD69 gMFI of T cells is higher within the Recurrence group ($z = -2.763$, $p = 0.017$) in comparison with the control group (see Figure 44).

At time point R3, a significantly elevated geometric mean fluorescence intensity can be stated for patients without recurrence (Mdn = 10.86%, Mann-Whitney-U-Test: $z = -2.015$, $p = 0.044$) in relation to healthy donors (Mdn = 8.17%). The same observation is made for blood draw R4 (No Recurrence: Mdn = 11.60%, Mann-Whitney-U-Test: $z = -2.376$, $p = 0.018$, CTRL: Mdn = 8.17%). Additionally, when comparing patients suffering from recurrence with healthy donors (Mdn = 8.17%), a higher CD69 gMFI can be detected for the Recurrence group (Mdn = 12.83%, Mann-Whitney-U-Test: $z = -2.437$, $p = 0.015$) at time point R5 (see Figure 45).

Figure 44: Variances between patient groups in the geometric mean fluorescence intensity of CD69+ T cells for all blood draws R0 to R4/R5 analyzed by multivariate analysis (*p ≤ 0.05, **p ≤ 0.01, ***p ≤ 0.001)

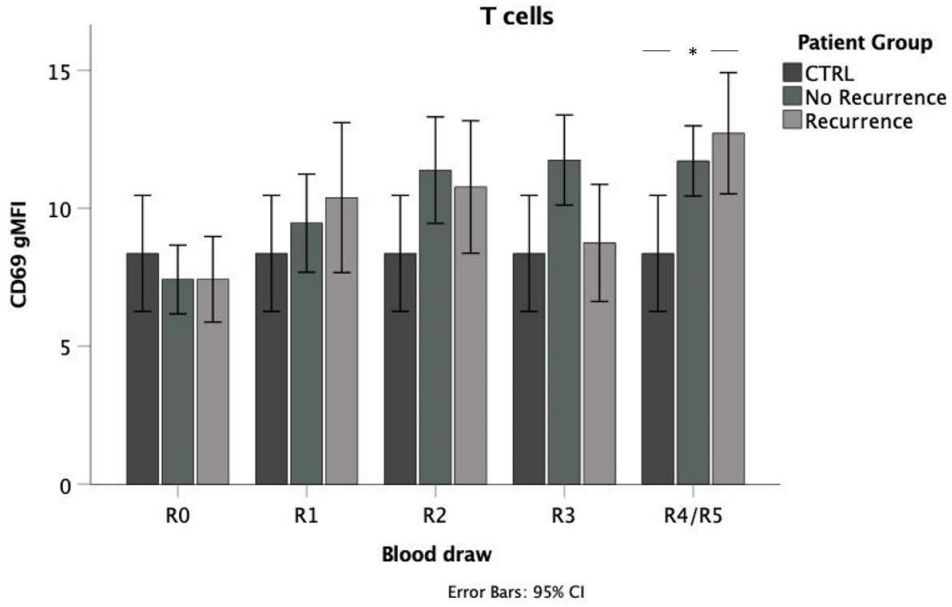

Figure 45: Variances between patient groups in the geometric mean fluorescence intensity of CD69+ T cells for all blood draws R0 to R4/R5 analyzed by univariate analysis (*p ≤ 0.05, **p ≤ 0.01, ***p ≤ 0.001)

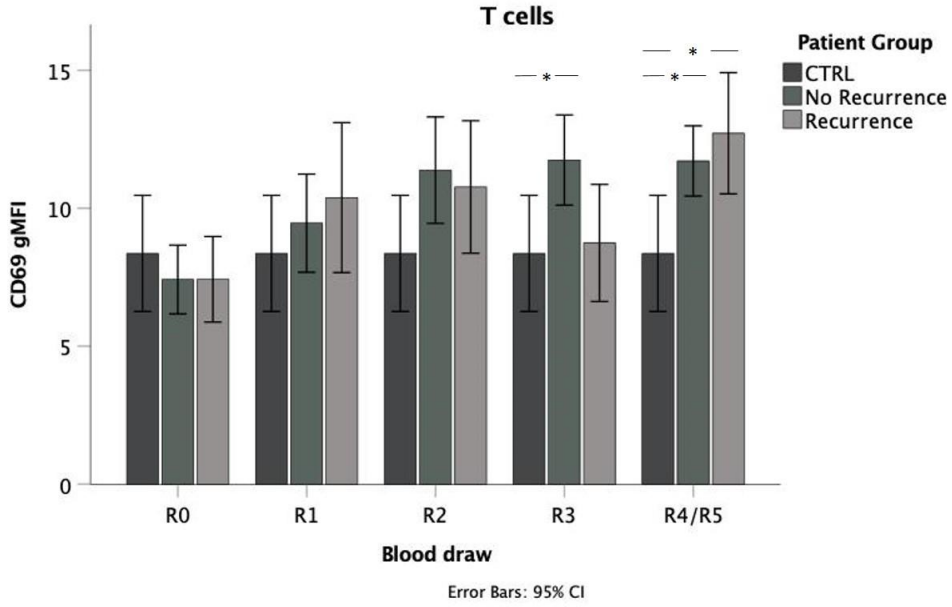

For CD69 gMFI of T cells, multivariate analysis confirms significant differences between the time points of blood draw within the No Recurrence group (Friedman test: χ^2= 22.429, p ≤ 0.001, n = 45). In comparison with the initial blood draw R0, the geometric mean fluorescence intensity is higher at time point R1

(z = -3.367, p_{adj} = 0.008), time point R2 (z = -3.500, p_{adj} = 0.005), time point R3 (z = -4.333, $p_{adj} \leq 0.001$) and time point R4 (z = -3.300, p_{adj} = 0.010). Forementioned results are obtained by a Dunn-Bonnferroni Post-hoc test (see Figure 46). The valid sample size of 4 is too small to draw a meaningful conclusion with the Friedman test for the Recurrence group.

Figure 46: Variances between time points of blood draw in the geometric mean fluorescence intensity of CD69+ T cells for the No Recurrence group analyzed by multivariate analysis (*p ≤ 0.05, **p ≤ 0.01, ***p ≤ 0.001)

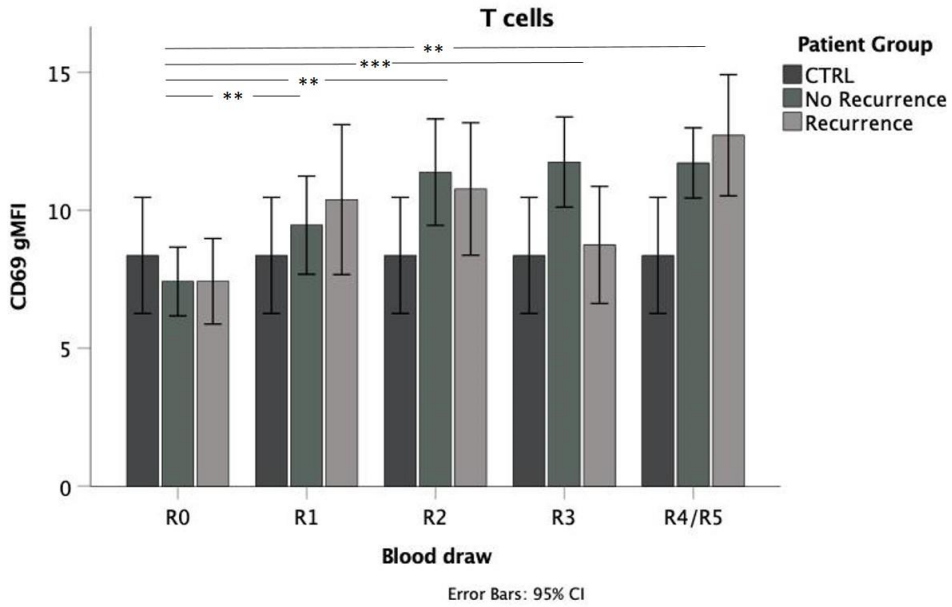

According to the Wilcoxon test, the CD69 gMFI of T cells grows continuously after radiation therapy regarding patients without recurrence. Significant differences can be reported for time point R0 (Mdn = 6.24%) in comparison with time point R1 (Mdn = 7.13%, z = -4.094, p ≤ 0.001, n = 143), time point R2 (Mdn = 9.98%, z = -4.251, p ≤ 0.001, n = 138), time point R3 (Mdn = 10.86%, z = -5.265, p ≤ 0.001, n = 142) and time point R4 (Mdn = 11.60%, z = -5.229, p ≤ 0.001, n = 146). Furthermore, higher geometric mean fluorescence is obvious for time point R3 (Mdn = 10.86%, z = -3.136, p = 0.002, n = 141) and time point R4 (Mdn = 11.60%, z = -2.892, p = 0.004, n = 145) in relation to time point R1 (Mdn = 7.13%) (see Figure 47).

Figure 47: Variances between time points of blood draw in the geometric mean fluorescence intensity of CD69+ T cells for the No Recurrence group analyzed by univariate analysis (*p ≤ 0.05, **p ≤ 0.01, ***p ≤ 0.001)

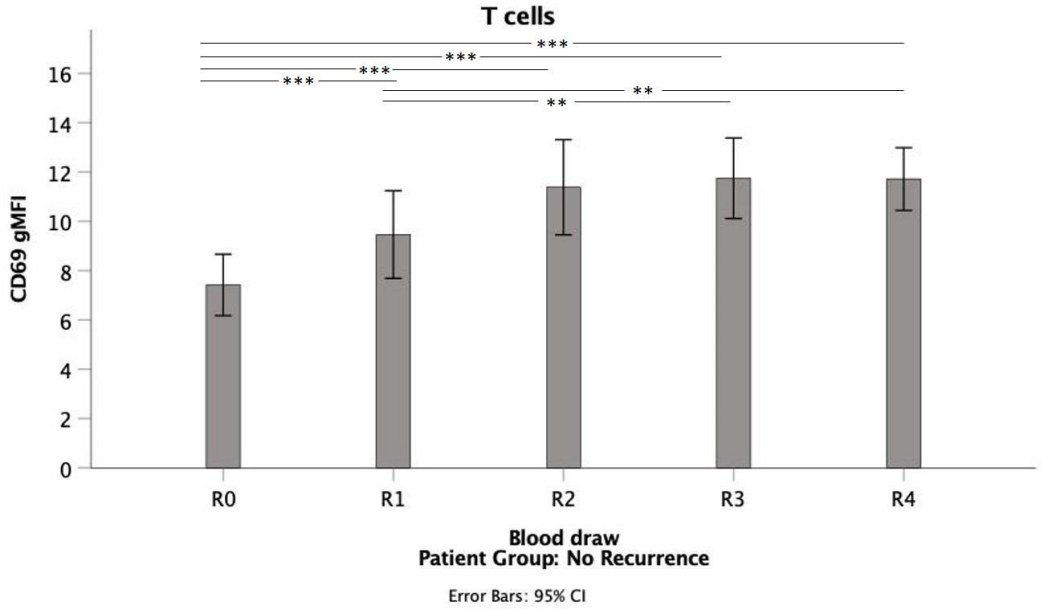

Comparing the blood draw before radiation therapy (Mdn = 7.15%) with time point R2 (Mdn = 11.17%, z = -3.288, p = 0.001, n = 42) and time point R5 (Mdn = 12.83%, z = -4.010, p ≤ 0.001, n = 48), Wilcoxon test confirms a significant increase in the geometric mean fluorescence intensity for the Recurrence group. Furthermore, significant differences for time point R2 (Mdn = 11.17%, z = -2.045, p = 0.041, n = 36), time point R3 (Mdn = 7.94%, z = -2.201, p = 0.031, n = 29) and time point R5 (Mdn = 12.83%, z = -2.689, p = 0.007, n = 42) in relation to blood draw R1 (Mdn = 9.54%) can be stated (see Figure 48).

Collectively, solely the final blood draws R4 and R5 of HNSCC patients present with increased geometric mean fluorescence intensity regarding CD69+ T cells. This elevation can also be confirmed for patients without recurrence in relation to healthy donors at time point R3. Initial levels rise during and after radiation therapy within patients without recurrence, after irradiation gMFI persists at this level. Regarding patients with recurrent disease, a similar observation is made. In comparison with the blood draw during treatment, levels fall at time point R3 before they rise up again at the time of blood draw R5.

Figure 48: Variances between time points of blood draw in the geometric mean fluorescence intensity of CD69+ T cells for the Recurrence group analyzed by univariate analysis (*p ≤ 0.05, **p ≤ 0.01, ***p ≤ 0.001)

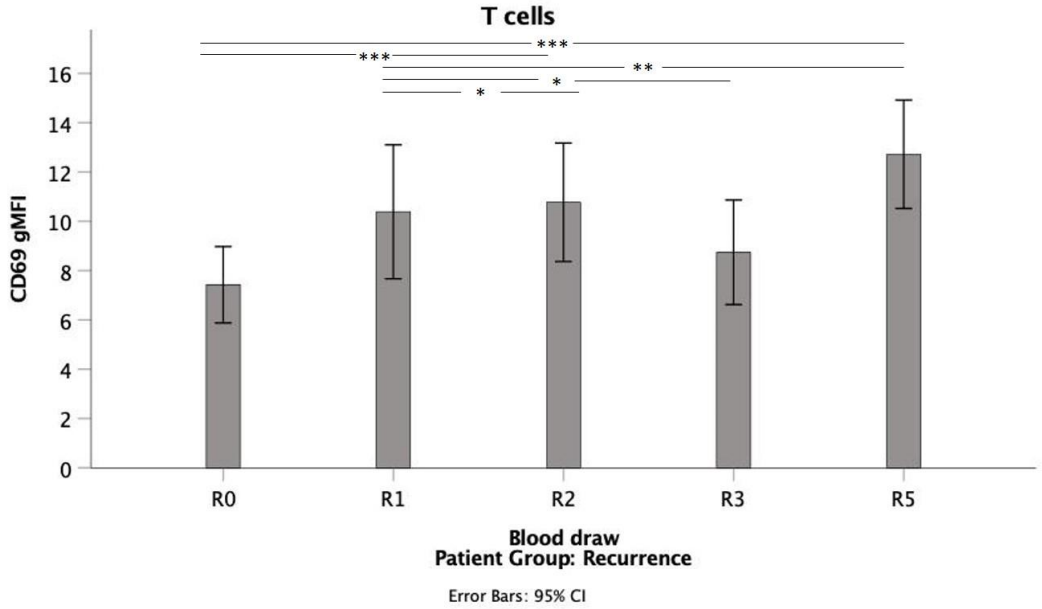

3.2.3. NK-like T cells

Percentage of CD69+ NK-like T cells

At last, we focused on the CD69 expression profile on NK-like T cells. Significant differences between patient groups cannot be detected with the Kruskal-Wallis test for the mean percentage of CD69+ NK-like T cells, respectively.

Performing a Mann-Whitney-U-Test, merely the R5 blood draw of patients suffering from recurrence (Mdn = 27.38%, z = -2.086, p = 0.037) shows a statistically significantly higher CD69+ NK-like T cell mean percentage in relation to non-recurrent disease at time point R4 (Mdn = 20.95%) (see Figure 49).

Significant differences within the No Recurrence group regarding CD69+ NK-like T cells become obvious after multivariate analysis (Friedman test: χ^2= 19.858, p = 0.001, n = 45). A subsequent Dunn-Bonnferroni Post-hoc test reveals a higher mean percentage at later blood draws R2 (z = -3.000, p_{adj} = 0.027), R3 (z = -4.200, $p_{adj} \leq 0.001$) and R4 (z = -3.200, p_{adj} = 0.014) in comparison with the initial blood draw R0 (see Figure 50). Regarding the Recurrence group, the Friedman Test is renounced in regard of a too small valid sample size of 4.

Figure 49: Variances between patient groups in the mean percentage of CD69+ NK-like T cells for all blood draws R0 to R4/R5 analyzed by univariate analysis (*p ≤ 0.05, **p ≤ 0.01, ***p ≤ 0.001)

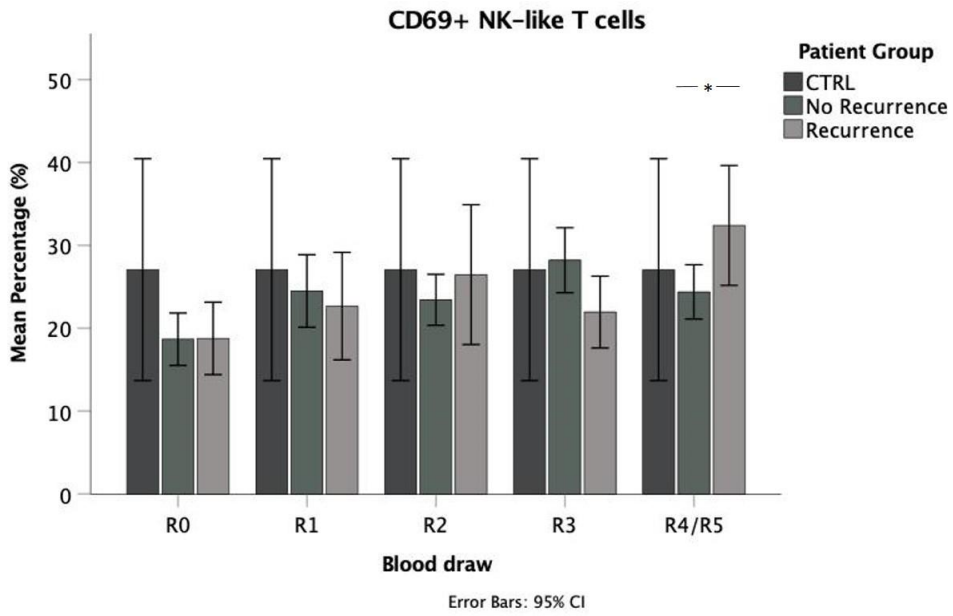

With univariate analysis (Wilcoxon test) within the No Recurrence group, mean percentages of CD69+ NK-like T cells show a higher percentage for all time points (R1: Mdn = 18.80%, z = -3.414, p = 0.001, n = 144, R2: Mdn = 21.48%, z = -3.471, p = 0.001, n = 139, R3: Mdn = 26.16%, z = -4.833, p ≤ 0.001, n = 143, R4: Mdn = 20.95%, z = -3.586, p ≤ 0.001, n = 147) following the initial blood draw at R0 (Mdn = 15.15%). Especially time point R3 (Mdn = 26.16%) presents with a higher value compared with time point R1 (Mdn = 18.80%, z = -2.648, p = 0.008, n = 141) and time point R2 (Mdn = 21.48%, z = -2.007, p = 0.045, n = 136) (see Figure 51).

Comparing the first blood draw R0 (Mdn = 15.79%) with time point R2 (Mdn = 19.76%, z = -2.461, p = 0.014, n = 42) and time point R5 (Mdn = 27.38%, z = -3.815, p ≤ 0.001, n = 48) within the Recurrence group via Wilcoxon test, mean percentage of CD69+ NK-like T cells show a significant lower initial value. Also, mean percentage of blood draw R5 (Mdn = 27.38%, z = -2.792, p = 0.005, n = 42) is significantly higher in comparison with time point R1 (Mdn = 19.68%) (see Figure 52).

Figure 50: Variances between time points of blood draw in the mean percentage of CD69+ NK-like T cells for the No Recurrence group analyzed by multivariate analysis (*p ≤ 0.05, **p ≤ 0.01, ***p ≤ 0.001)

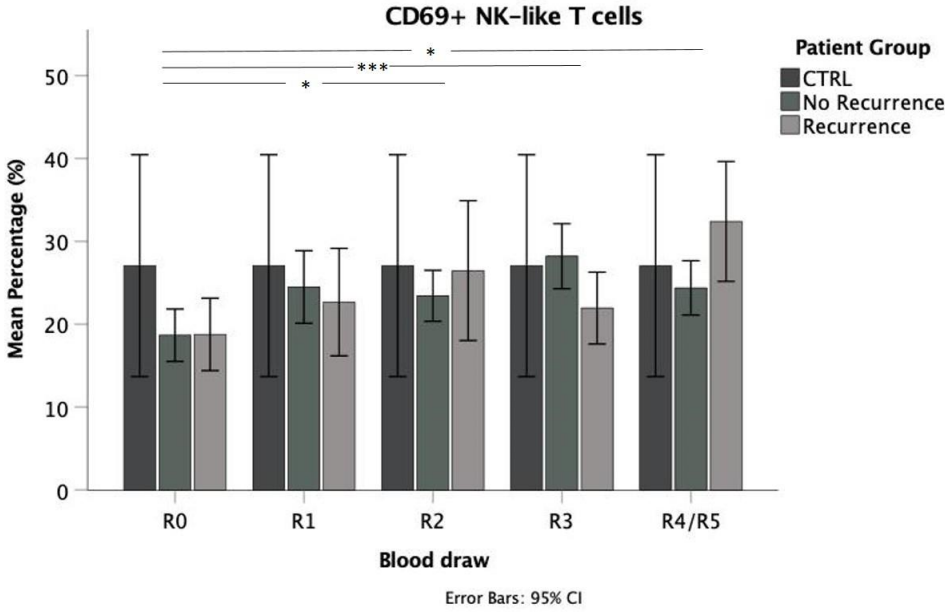

Figure 51: Variances between time points of blood draw in the mean percentage of CD69+ NK-like T cells for the No Recurrence group analyzed by univariate analysis (*p ≤ 0.05, **p ≤ 0.01, ***p ≤ 0.001)

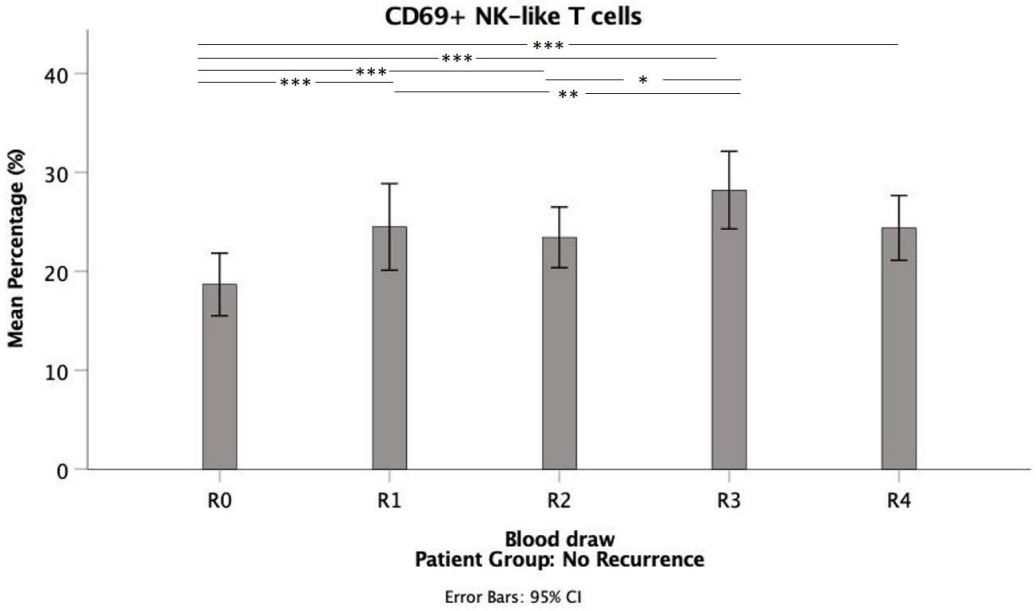

To sum up, mean percentage of CD69+ NK-like T cells is solely significantly elevated for patients with recurrent disease at the time point of final blood draws R4 and R5 in relation to patients without recurrence. Comparing initial mean percentage with consecutive blood draws, levels rise up during and after radiation therapy

regarding patients without tumor recurrence. For patients with recurrent disease, the same conclusion can be drawn. Additionally, levels present with the highest mean percentage at the time of recurrence (blood draw R5).

Figure 52: Variances between time points of blood draw in the mean percentage of CD69+ NK-like T cells for the Recurrence group analyzed by univariate analysis (*p ≤ 0.05, **p ≤ 0.01, ***p ≤ 0.001)

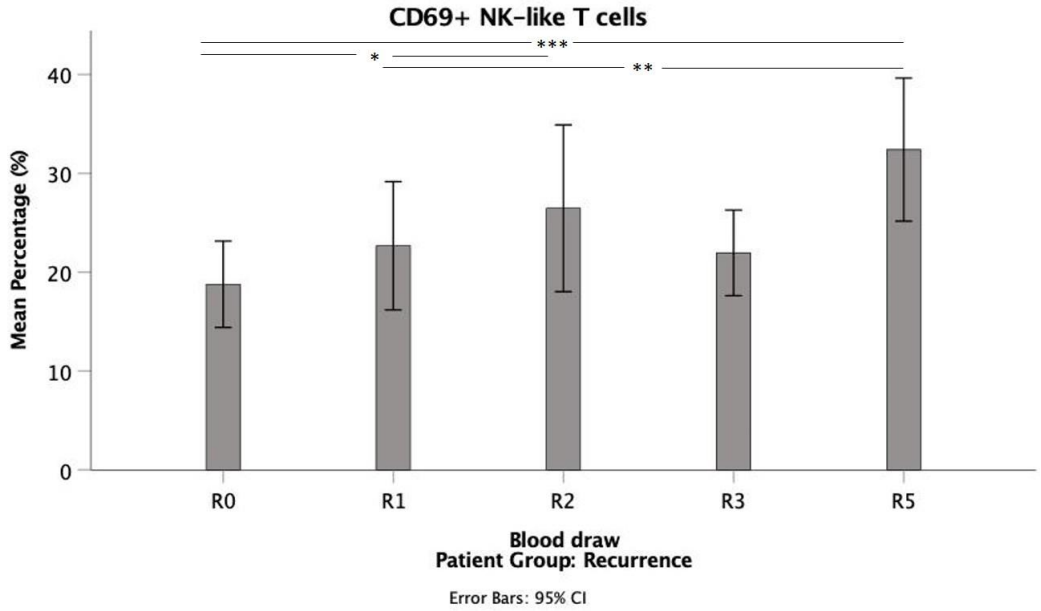

Geometric mean fluorescence intensity (gMFI) of CD69 on NK-like T cells

Conducting a Kruskal-Wallis test, no meaningful results between the patient groups are revealed for the CD69 gMFI of NK-like T cells. With univariate analysis between patient groups a significantly higher CD69 gMFI of NK-like T cells is detected for the Recurrence group (Mdn = 36.40%, Mann-Whitney-U-Test: z = -1.996, p = 0.046) compared with the No Recurrence group (Mdn = 27.33%) at the time of the final blood draw (see Figure 53).

After radiation therapy, CD69 gMFI of NK-like T cells is significantly higher in the No Recurrence group (Friedman test: χ^2 = 17.742, p = 0.001, n = 45). Dunn-Bonnferroni Post-hoc test confirms this observation comparing time point R0 with time point R1 (z = -2.933, p_{adj} = 0.034), time point R2 (z = -3.667, p_{adj} = 0.002), time point R3 (z = -2.933, p_{adj} = 0.034) as well as time point R4 (z = -3.467, p_{adj} = 0.005) (see Figure 54). Regarding the Recurrence group, the Friedman Test is renounced in regard of a too small valid sample size of 4.

Figure 53: Variances between patient groups in the geometric mean fluorescence intensity of CD69+ NK-like T cells for all blood draws R0 to R4/R5 analyzed by univariate analysis (*p ≤ 0.05, **p ≤ 0.01, ***p ≤ 0.001)

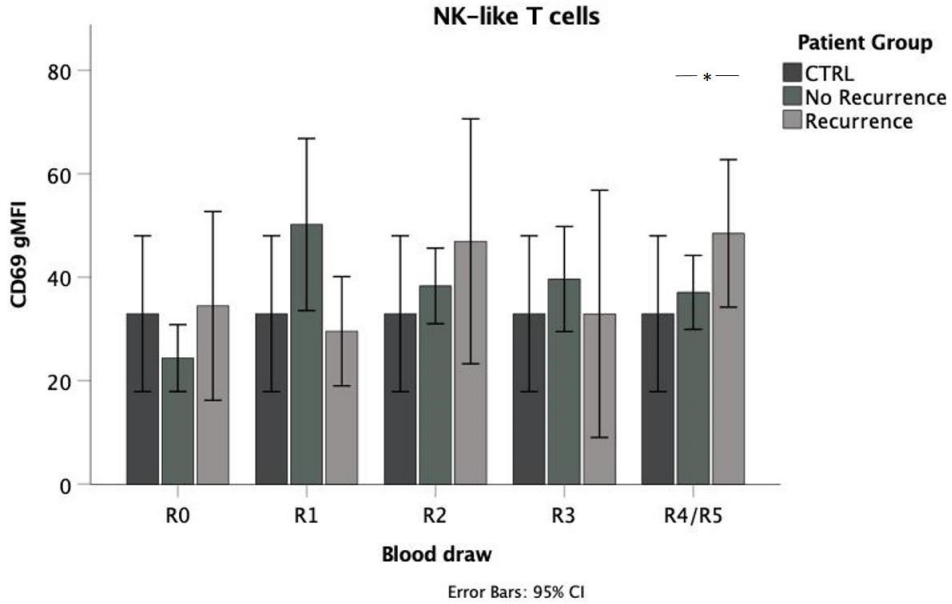

Figure 54: Variances between time points of blood draw in the geometric mean fluorescence intensity of CD69+ NK-like T cells for the No Recurrence group analyzed by multivariate analysis (*p ≤ 0.05, **p ≤ 0.01, ***p ≤ 0.001)

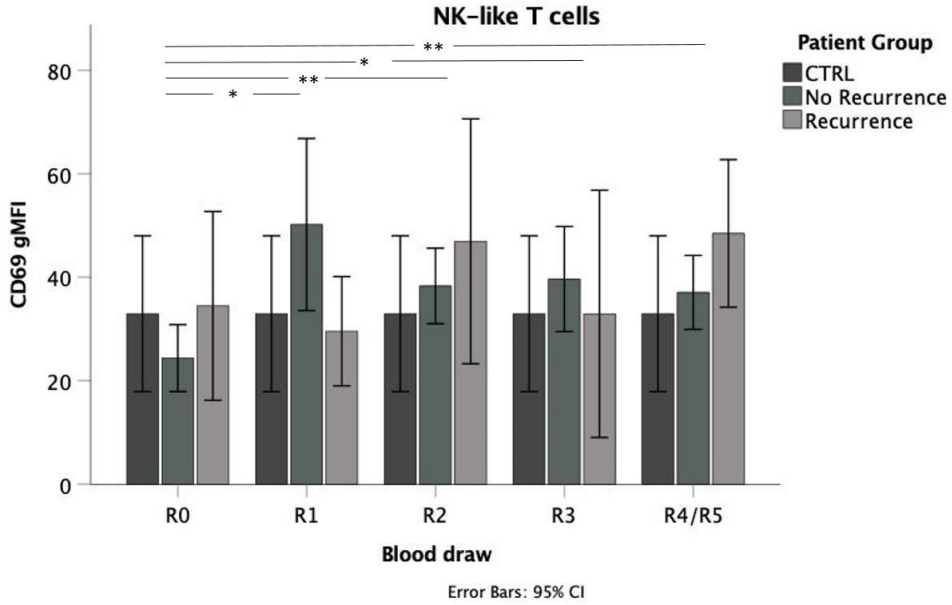

The Wilcoxon test aids to determine significant differences in the CD69 geometric mean fluorescence of NK-like T cells between single time points in the peripheral blood of patients. Regarding the No Recurrence group, CD69 gMFI of NK-like T cells is lower at the time point of initial blood draw (Mdn = 18.10%) compared with time

point R1 (Mdn = 24.23%, z = -3.887, p ≤ 0.001, n = 144) time point R2 (Mdn = 30.87%, z = -4.176, p ≤ 0.001, n = 139), time point R3 (Mdn = 28.96%, z = -4.813, p ≤ 0.001, n = 143) and time point R4 (Mdn = 27.33%, z = -4.229, p ≤ 0.001, n = 147) (see Figure 55).

Concerning the Recurrence group, CD69 gMFI of NK-like T cells is significantly elevated at time point R5 (Mdn = 36.40%) in comparison with time point R0 (Mdn = 16.06%, z = -2.321, p = 0.020, n = 48) and time point R1 (Mdn = 24.56%, z = -3.051, p = 0.002, n = 42). In addition, values at time point R2 (Mdn = 27.02%, z = -1.956, p = 0.050, n = 36) are significantly higher in relation to time point R1 (Mdn = 24.56%) (see Figure 56).

Figure 55: Variances between time points of blood draw in the geometric mean fluorescence intensity of CD69+ NK-like T cells for the No Recurrence group analyzed by univariate analysis (*p ≤ 0.05, **p ≤ 0.01, ***p ≤ 0.001)

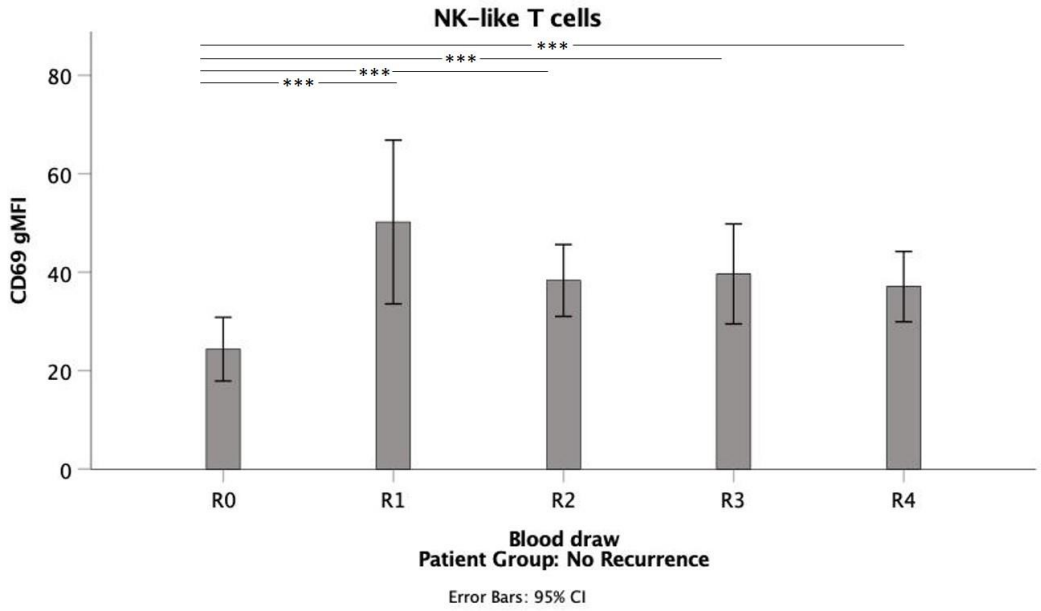

In conclusion, the geometric mean fluorescence intensity (gMFI) of CD69+ NK-like T cells is merely significantly elevated for patients with tumor recurrence during final blood draws R4 and R5 compared with patients without recurrence. For patients without recurrence, initial gMFI values are lower in relation to all consecutive blood draws. Patients suffering from recurrent disease show their highest gMFI at time point of recurrence (blood draw R5).

Figure 56: Variances between time points of blood draw in the geometric mean fluorescence intensity of CD69+ NK-like T cells for the Recurrence group analyzed by univariate analysis (*p ≤ 0.05, **p ≤ 0.01, ***p ≤ 0.001)

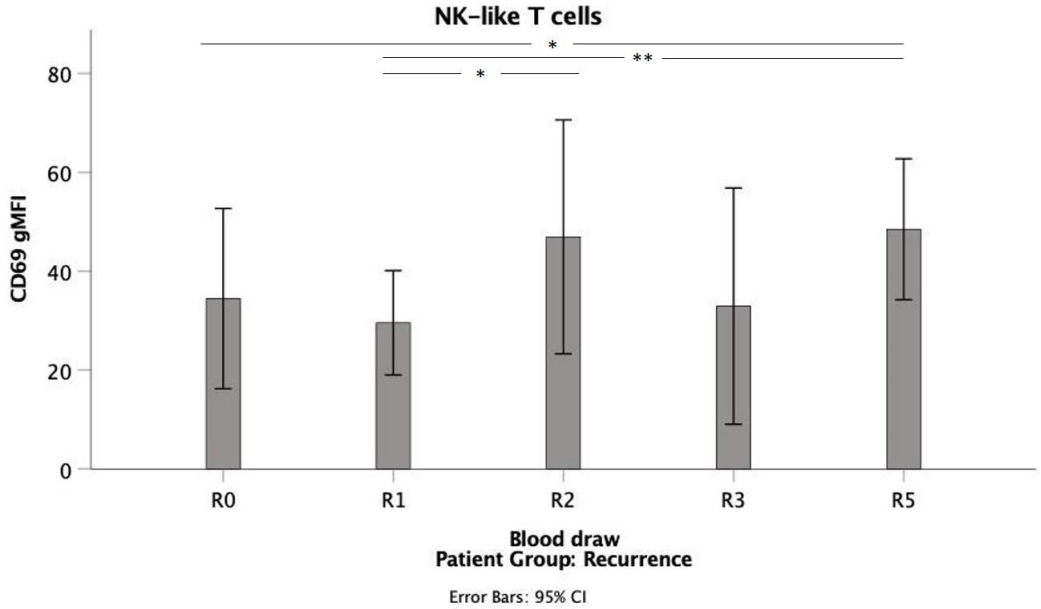

3.3. Programmed cell death protein 1 (PD-1) as a potential prognostic biomarker

Conducting a prefabricated Human PD-1 ELISA, we researched the concentration level of programmed cell death protein 1 (PD-1) within patients' plasma samples. Kruskal-Wallis test shows that the concentration of PD-1 differs significantly between patient groups for time point R0 (χ^2 = 8.469, p = 0.014) and time point R1 (χ^2 = 13.011, p = 0.001). A following Dunn-Bonnferroni Post-hoc test was conducted and reveals a significant higher concentration for healthy donors in relation to patients without recurrent disease at time point R0 (z = 2.563, p = 0.031) and time point R1 (z = 3.019, p = 0.008). For patients experiencing recurrent disease, concentration significantly differs from the CTRL group at time point R1 (z = -2.602, p = 0.028) (see Figure 57).

The concentration of PD-1 is significantly lower for the No Recurrence group (Mdn = 84.86pg/µL) in comparison with the CTRL group (Mdn = 4076.69pg/µL, Mann-Whitney-U-Test: z = - 2.387, p = 0.017) and Recurrence group (Mdn = 126.25pg/µL, Mann-Whitney-U-Test: z = - 1.997, p = 0.046) at time point R0. The same observation can be drawn for time point R1 (No Recurrence: Mdn = 57.93pg/µL, CTRL: Mdn = 4076.69pg/µL, Mann-Whitney-U-Test: z = -2.842,

p = 0.004, Recurrence: Mdn = 118.62pg/µL, Mann-Whitney-U-Test: z = -2.693, p = 0.007). Regarding time point R4/R5 merely the concentration of PD-1 within the No Recurrence group (Mdn = 110.80pg/µL, Mann-Whitney-U-Test: z = -2.121, p = 0.034) is significantly reduced in comparison with healthy donors (Mdn = 4076.69pg/µL) (see Figure 58).

Figure 57: Variances between patient groups in the concentration of PD-1 for all blood draws R0 to R4/R5 analyzed by multivariate analysis (*p ≤ 0.05, **p ≤ 0.01, ***p ≤ 0.001)

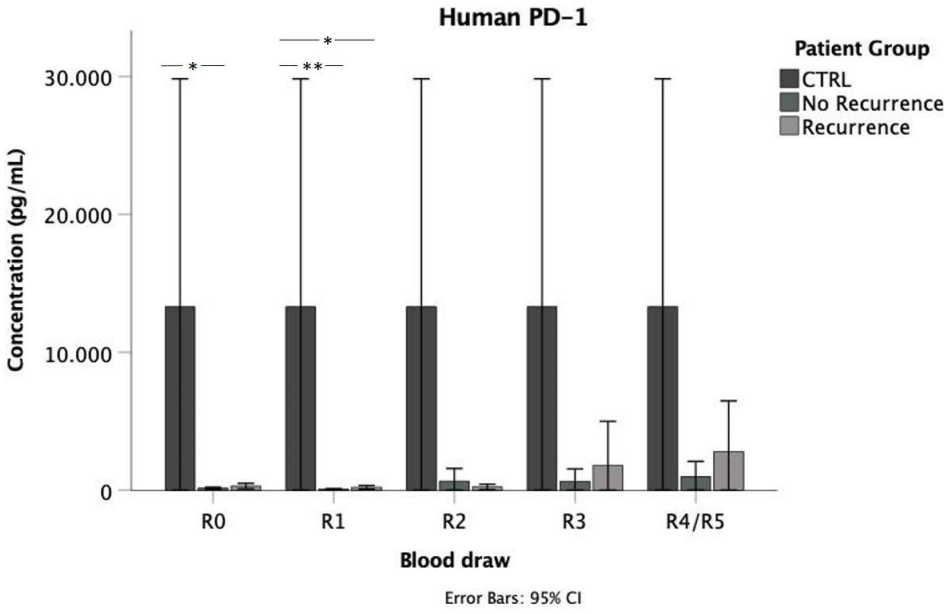

Looking at the changes over the time points of blood draw, the concentration of PD-1 differs significantly within the No Recurrence group (Friedman test: χ^2= 13.754, p = 0.008, n = 25). A Dunn-Bonnferroni Post-hoc test confirms significant results of the PD-1 concentration when comparing time point R1 with time point R2 (z = -3.086, p_{adj} = 0.020) as well as time point R1 to time point R4 (z = -3.399, p_{adj} = 0.007) (see Figure 59). Regarding the Recurrence group, the Friedman Test is renounced in regard of a too small valid sample size of 4.

When comparing the concentration of PD-1 for each blood draw within the No Recurrence group, the Wilcoxon test confirms significances between time point R0 (Mdn = 84.86pg/µL) and time point R1 (Mdn = 57.93pg/µL, z = -3.332, p = 0.001, n = 66), as well as time point R4 (Mdn = 110.80pg/µL, z = -2.067, p = 0.039, n = 68). Also, concentration at time point R1 (Mdn = 57.93pg/µL) differs significantly from time point R2 (Mdn = 141.39pg/µL, z = -2.730, p = 0.006, n = 65),

time point R3 (Mdn = 119.30pg/µL, z = -2.952, p = 0.003, n = 65) and time point R4 (Mdn = 110.80pg/µL, z = -3.486, p ≤ 0.001, n = 66) (see Figure 60). For patients with recurrence no significant results can be reported (see Figure 61).

Figure 58: Variances between patient groups in the concentration of PD-1 for all blood draws R0 to R4/R5 analyzed by univariate analysis (*p ≤ 0.05, **p ≤ 0.01, ***p ≤ 0.001)

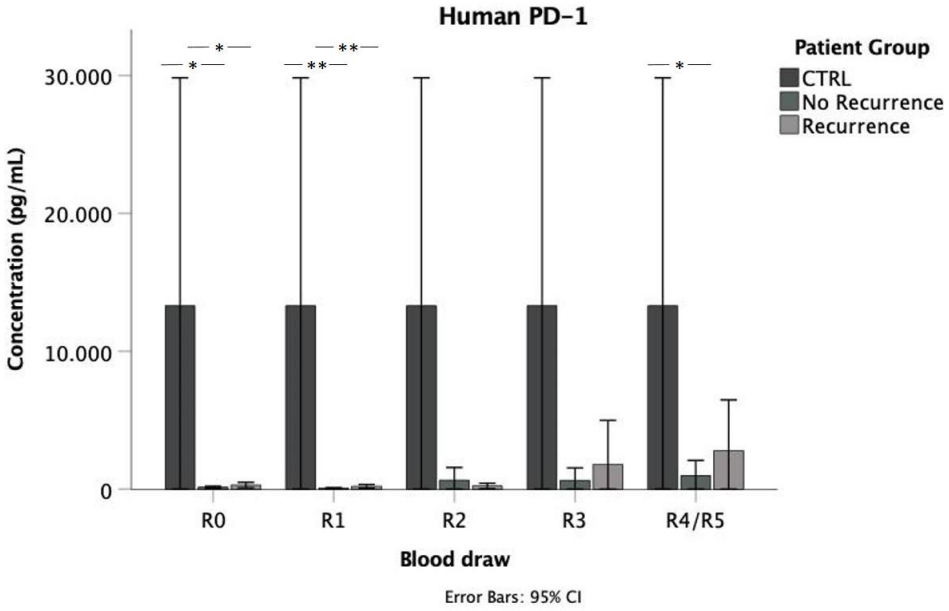

Figure 59: Variances between time points of blood draw in the concentration of PD-1 for the No Recurrence group analyzed by multivariate analysis (*p ≤ 0.05, **p ≤ 0.01, ***p ≤ 0.001)

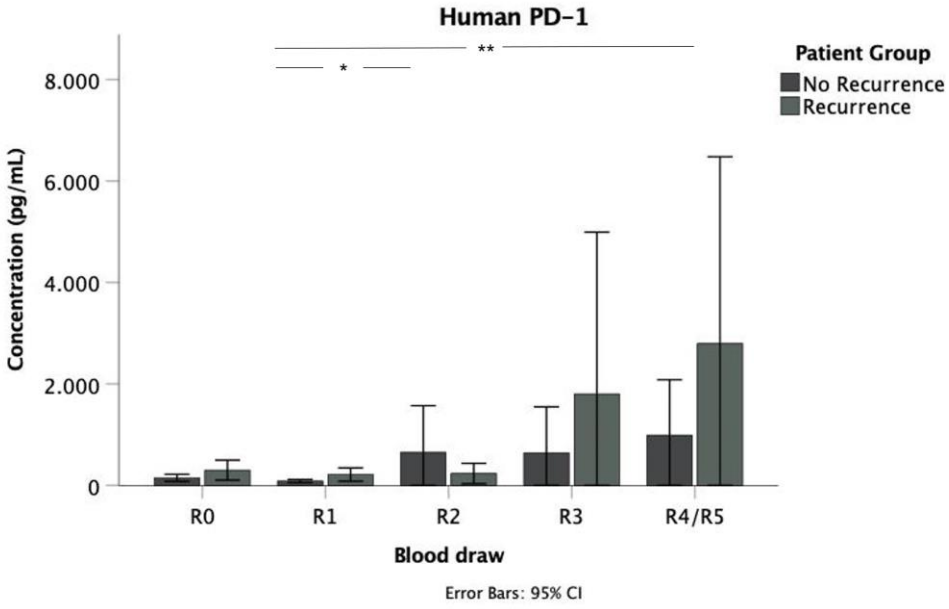

Figure 60: Variances between time points of blood draw in the concentration of PD-1 for the No Recurrence group analyzed by univariate analysis (*p ≤ 0.05, **p ≤ 0.01, ***p ≤ 0.001)

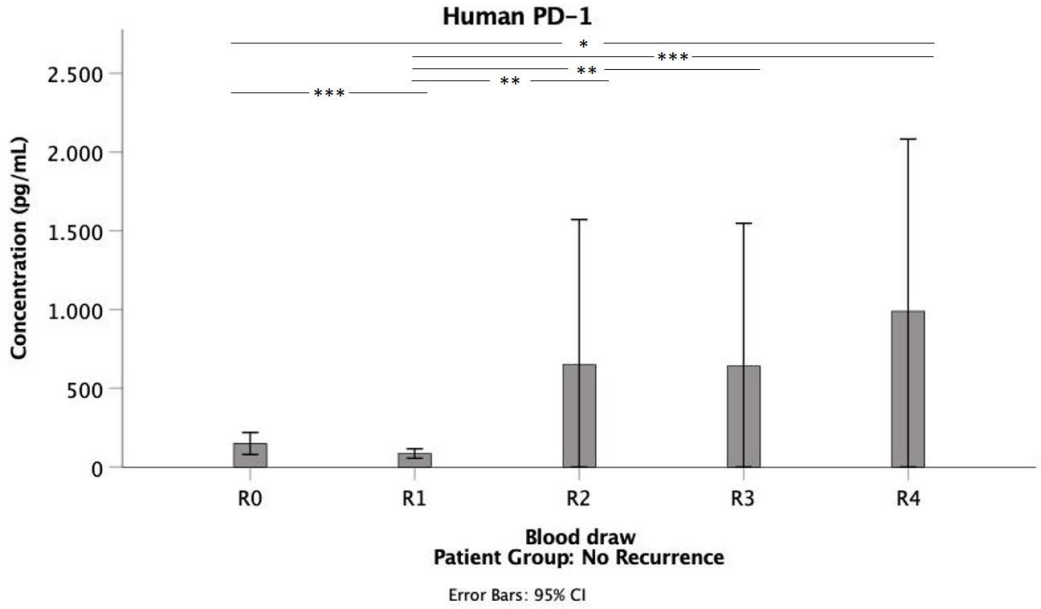

Figure 61: Variances between time points of blood draw in the concentration of PD-1 for the Recurrence group analyzed by univariate analysis (*p ≤ 0.05, **p ≤ 0.01, ***p ≤ 0.001)

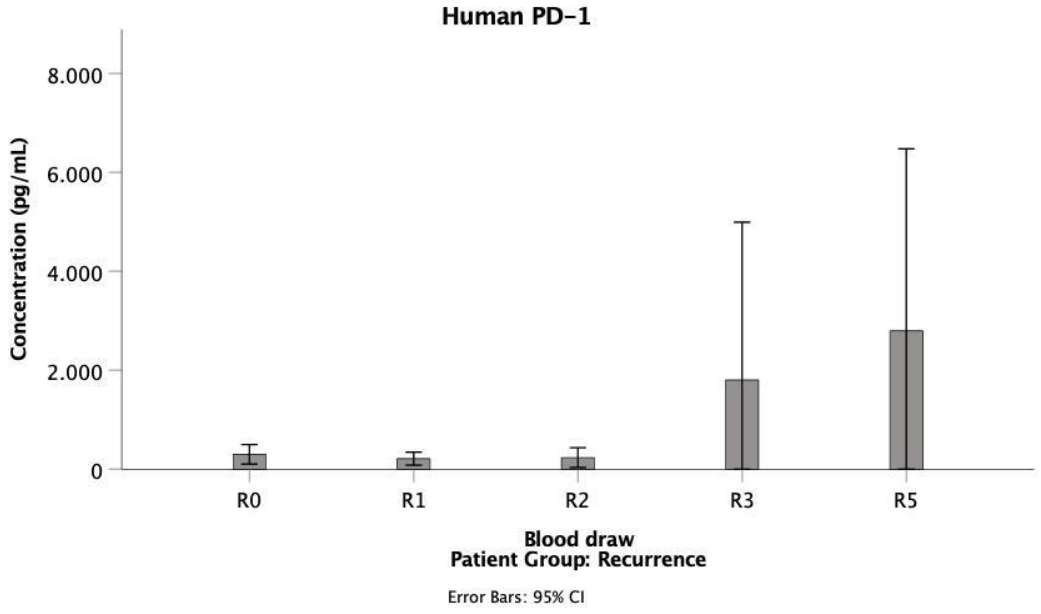

Before and during radiotherapy, especially patients without tumor recurrence show a lower PD-1 concentration compared with healthy donors and patients with recurrent disease. Within the No Recurrence group, concentration of PD-1 sinks during irradiation before it consecutively grows after treatment completion. Levels are especially high at the time of the final blood draw R4. Regarding patients

with tumor recurrence, some individuals also seem to present with a higher PD-1 concentration starting 6 months after undergoing irradiation (blood draw R3). This change cannot be statistically verified.

3.4. Programmed cell death ligand 1 (PD-L1) as a potential prognostic biomarker

In addition to Human PD-1, we want to gain information about the receptor's ligand programmed cell death ligand 1 (PD-L1) by measuring the concentration within plasma samples. Performing a Kruskal-Wallis test, differences in the concentration of PD-L1 between patient groups are detected at time points R0, R1, R2, R3 and R4/R5 (R0: $\chi^2 = 39.466$, $p \leq 0.001$, R1: $\chi^2 = 41.911$, $p \leq 0.001$, R2: $\chi^2 = 37.927$, $p \leq 0.001$, R3: $\chi^2 = 31.431$, $p \leq 0.001$, R4/R5: $\chi^2 = 46.550$, $p \leq 0.001$). A subsequent Dunn-Bonnferroni Post-hoc test can confirm higher concentration for patients suffering from recurrence in relation to the No Recurrence group (R0: $z = -6.281$, $p \leq 0.001$, R1: $z = -6.474$, $p \leq 0.001$, R2: $z = -6.154$, $p \leq 0.001$, R3: $z = -5.592$, $p \leq 0.001$, R4/R5: $z = -6.789$, $p \leq 0.001$) as well as healthy donors (R0: $z = -2.449$, $p = 0.043$, R1: $z = -2.633$, $p = 0.025$, R2: $z = -2.748$, $p = 0.018$, R3: $z = -2.425$, $p = 0.046$, R4/R5: $z = -3.064$, $p = 0.007$) (see Figure 62).

Concentration of PD-L1 is significantly elevated for patients suffering from recurrence (Mdn = 4470.13pg/µL) when comparing with the control group (Mdn = 413.95pg/µL, Mann-Whitney-U-Test: $z = -3.449$, $p = 0.001$) and No Recurrence group (Mdn = 292.35pg/µL, Mann-Whitney-U-Test: $z = -5.977$, $p \leq 0.001$) at time point R0. The same conclusion can be drawn for time point R1 (Recurrence: Mdn = 3554.98pg/µL, CTRL: Mdn = 413.95pg/µL, Mann-Whitney-U-Test: $U = 5.000$, $p \leq 0.001$, No Recurrence: Mdn = 293.69pg/µL, Mann-Whitney-U-Test: $z = -6.181$, $p \leq 0.001$), time point R2 (Recurrence: Mdn = 3875.08pg/µL, CTRL: Mdn = 413.95pg/µL, Mann-Whitney-U-Test: $U = 5.000$, $p \leq 0.001$, No Recurrence: Mdn = 303.81pg/µL, Mann-Whitney-U-Test: $z = -5.889$, $p \leq 0.001$), time point R3 (Recurrence: Mdn = 4369.23pg/µL, CTRL: Mdn = 413.95, Mann-Whitney-U-Test: $U = 2.000$, $p \leq 0.001$, No Recurrence: Mdn = 310.91pg/µL, Mann-Whitney-U-Test: $z = -5.290$, $p \leq 0.001$) as well as time point R4/R5 (Recurrence: Mdn = 3948.51pg/µL, CTRL: Mdn = 413.95pg/µL, Mann-Whitney-U-Test: $z = -3.963$, $p \leq 0.001$, No Recurrence:

Mdn = 318.16pg/µL, Mann-Whitney-U-Test: z = -6.509, p ≤ 0.001). Additionally, at time point R0 PD-L1 concentration in the peripheral blood of patients without recurrent disease (Mdn = 292.35pg/µL, Mann-Whitney-U-Test: z = -2.032, p = 0.042) is significantly lower compared with healthy donors (Mdn = 413.95pg/µL). Also, at time point R1, concentration differs significantly between the CTRL group (Mdn = 413.95pg/µL) and the No Recurrence group (Mdn = 293.69pg/µL, Mann-Whitney-U-Test: z = -2.064, p = 0.039). For blood draw R3 solely a trend towards a lower concentration for the No Recurrence group (Mdn = 310.91pg/µL, Mann-Whitney-U-Test: z = -1.942, p = 0.052) in comparison with healthy donors (Mdn = 413.95pg/µL) is detected (see Figure 63).

Figure 62: Variances between patient groups in the concentration of PD-L1 for all blood draws R0 to R4/R5 analyzed by multivariate analysis (*p ≤ 0.05, **p ≤ 0.01, ***p ≤ 0.001)

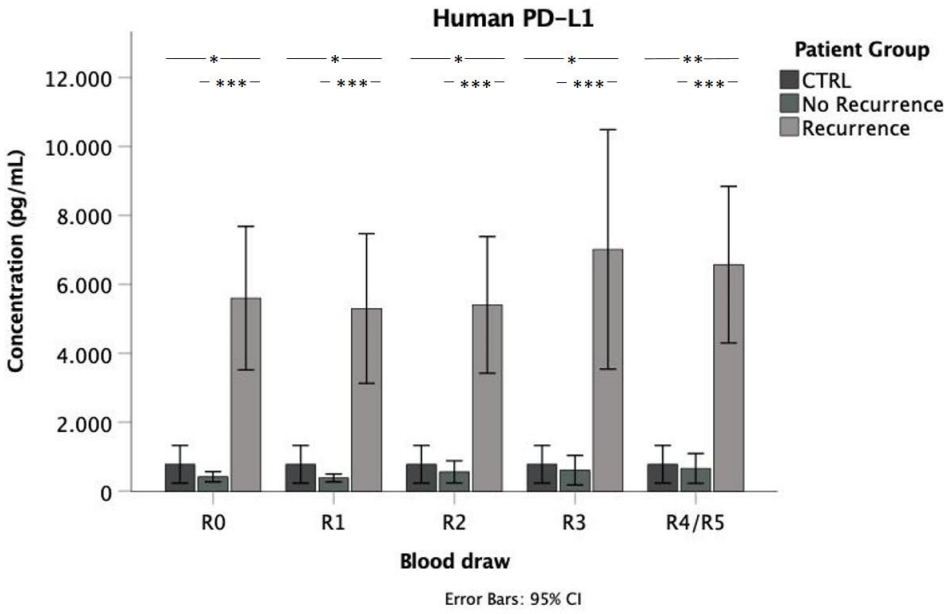

A Friedman test reveals significant differences between the time points of blood draw within the No Recurrence group (Friedman test: χ^2 = 11.696, p = 0.020, n = 37). A subsequent Dunn-Bonnferroni Post-hoc test fails to further specify significant differences (see Figure 64). Regarding the Recurrence group, the valid sample size of 6 is too small to draw a proper conclusion with the Friedman test.

According to the Wilcoxon test, the concentration of PD-L1 solely shows a significant difference between time point R0 (Mdn = 292.35pg/µL) in comparison with time point R1 (Mdn = 293.69pg/µL, z = -2.205, p = 0.027, n = 79)

(see Figure 65). There are no significant results within the Recurrence group (see Figure 66).

Figure 63: Variances between patient groups in the concentration of PD-L1 for all blood draws R0 to R4/R5 analyzed by univariate analysis (*p ≤ 0.05, **p ≤ 0.01, ***p ≤ 0.001)

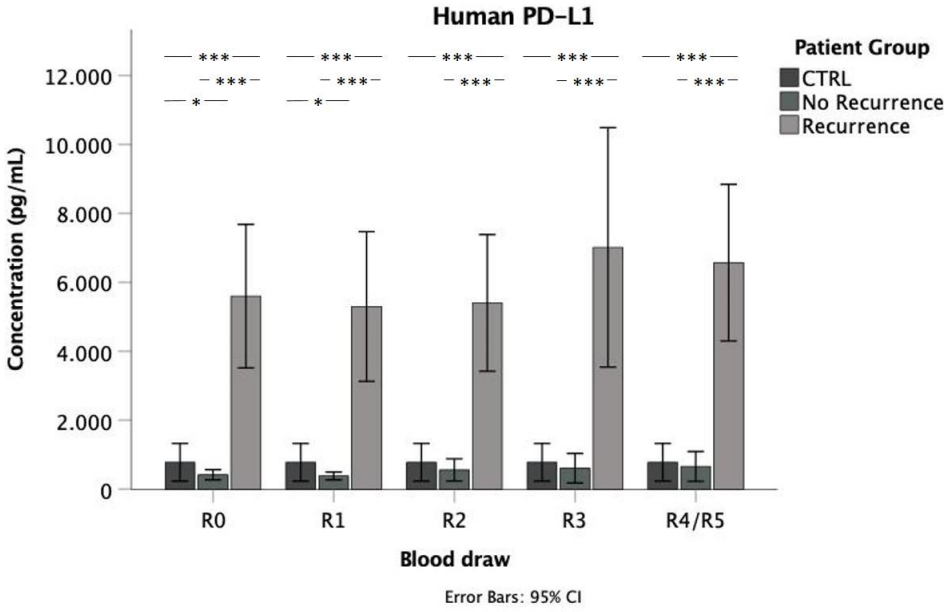

Figure 64: Variances between time points of blood draw in the concentration of PD-L1 for the No Recurrence group analyzed by multivariate analysis (*p ≤ 0.05, **p ≤ 0.01, ***p ≤ 0.001)

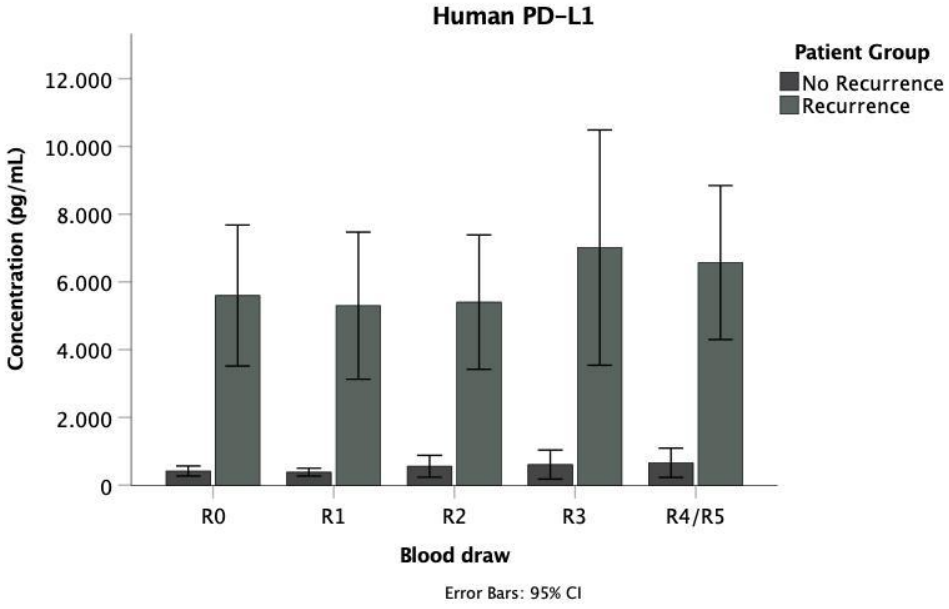

For patients with tumor recurrence, higher concentration throughout all blood draws in comparison with healthy donors and patients without recurrent disease

is remarkable. Patients with tumor recurrence approximately show a 10-fold increase of PD-L1 concentration in peripheral blood in relation to patients without recurrence, the concentration does not change over time within HNSCC patients.

Figure 65: Variances between time points of blood draw in the concentration of PD-L1 for the No Recurrence group analyzed by univariate analysis (*p ≤ 0.05, **p ≤ 0.01, ***p ≤ 0.001)

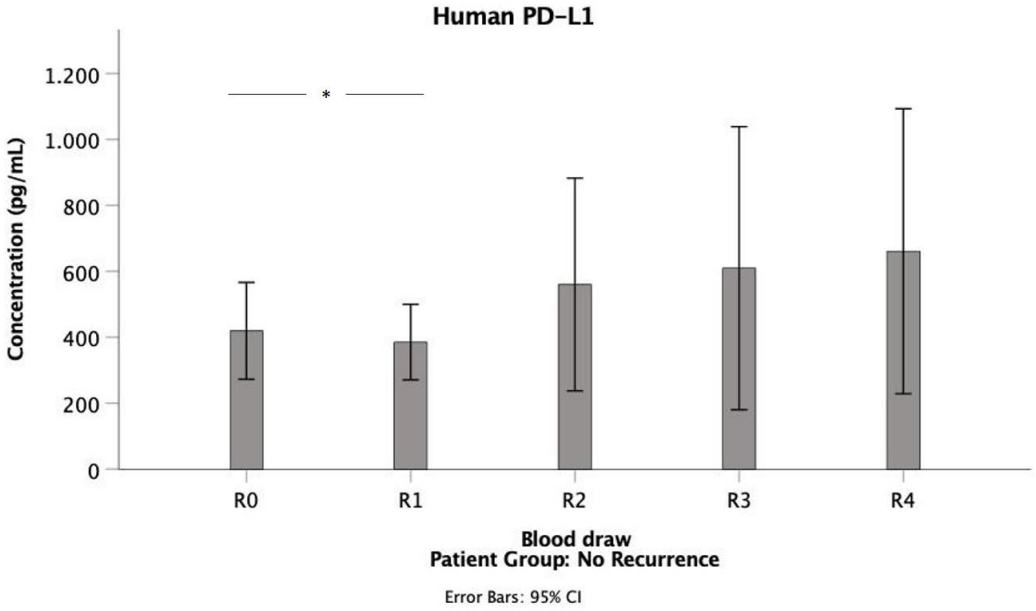

Figure 66: Variances between time points of blood draw in the concentration of PD-L1 for the Recurrence group analyzed by univariate analysis (*p ≤ 0.05, **p ≤ 0.01, ***p ≤ 0.001)

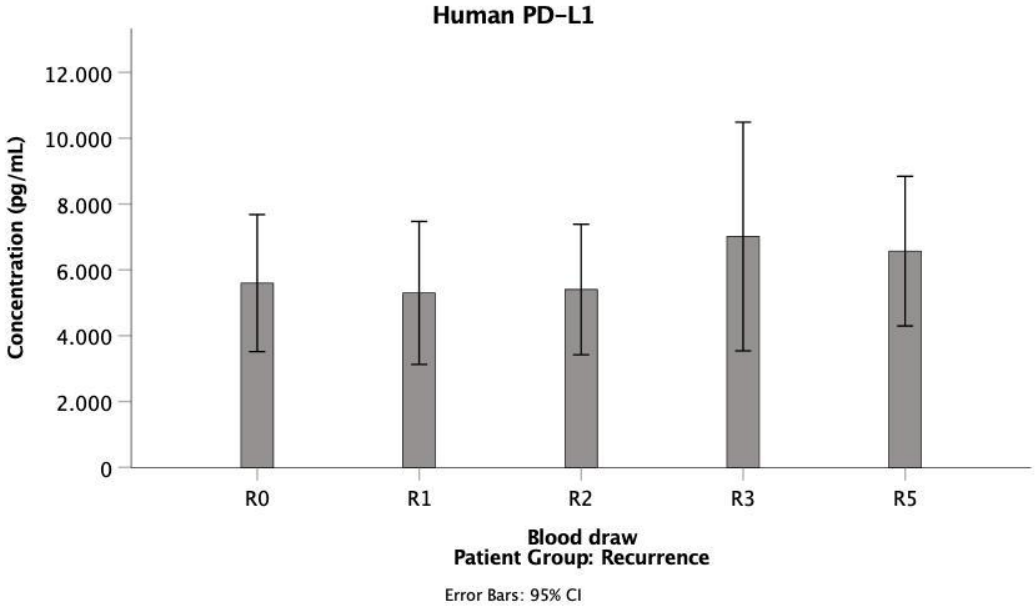

4. Discussion

With nearly 25 million new cancer diagnoses and 10 million cancer deaths each year, diagnosis and management of the disease is worldwide of utter importance. [1, 2] Around three out of a hundred cancer cases arise from oral or pharyngeal subsites with an increasing incidence throughout the United States among middle-aged men and women. [3, 4] While major risk factors such as smoking, alcohol consumption and HPV infection are well known causes, new therapeutic approaches have failed to substantially improve overall survival rates in the past decades. [5, 6, 11, 18] Diagnosis of HNSCC commonly occurs at an advanced stage of the disease, which might impede a successful tumor remission. [49] A cost-effective, non-invasive diagnostic method may lead to earlier detection of the disease and thus to substantially improved treatment outcomes.

Prospectively, research is striving for a more personalized approach of cancer care in order to choose the most suitable therapeutic approach for each patient. [9] Assessment of the patient's prognosis is a critical factor for cancer management since some patients are at higher risk for suffering from recurrence. Those patients are in need of intensified therapeutic approach and cancer screening. [9] Tumoral behavior of HNSCC shows major differences in regard of its aetiology. Whereas cigarette consumption is connected to more aggressive tumoral behavior and worse survival rates, HPV-related HNSCC holds a more favorable prognosis. [22, 71] Side effects of combined treatment approaches including surgery, radiotherapy and chemotherapy might be severe and cause lifelong functional impairment as well as reduced quality of life. [125, 126] For example, de-escalation of radiation dosage may be in favor of patients suffering from less aggressive HNSCC and with reduced risk for recurrence. Improved patient stratification based on suitable prognostic biomarkers could lead to a sparing of healthy tissue and lymphocytes for patients with reduced risk of HNSCC recurrence undergoing radiotherapy. Irradiation has an impact on the composition of the immune system, especially lymphocyte subpopulations are sensitive to ionizing radiation to a significant degree. [131] These changes within the lymphocyte subpopulations may have an impact on the patient's prognosis.

In this study, patients with locally advanced HNSCC treated with a chemoradiotherapy schedule are observed within a time frame of two years. Blood samples taken at five time points before, during and after therapy are thoroughly analyzed. Within EDTA blood samples, especially radiation-induced effects on certain lymphocyte subpopulations (NK cells, T cells and B cells) are verifiable as well as distinctive expression of the early activation marker CD69 on the surface of T cells. Limitations to our study assessing the lymphocyte subpopulations and expression profile of CD69 upon certain lymphocyte subsets are missing or invalid blood samples at certain time points as well as a relatively small number of healthy donors in relation to HNSCC patients. Furthermore, no blood sample is taken directly after radiotherapy completion. Those samples might have added additional valuable information and provided better comparability with other studies which base the alteration of lymphocyte subpopulation on values shortly taken after irradiation. Furthermore, treatment and irradiation schedules might differ broadly when comparing our experiment with other studies leading to restricted comparability.

Considering the differences between patients diagnosed with cancer and healthy individuals within lymphocyte subpopulations and changes during and after radiotherapy, as opposed to our experiment, heparinized blood or EDTA samples of HNSCC patients are seldomly utilized to directly assess lymphocytes by flow cytometry. [198-200] Studies are rather conducted by isolating peripheral blood mononuclear cells (PBMC) from peripheral blood samples [136, 201-205] before conducting further analysis, i.e. flow cytometry. Other approaches to assess changes within lymphocyte subpopulations are analysis of tumor tissue samples [204-206], i.e. by flow cytometry of single cell suspensions, and identification of gene expression referring to certain lymphocyte subpopulations. [206, 207] Also, rather counts than mean percentages of the lymphocyte subpopulations are coming to use when comparing results. [135, 208-211] Thus, comparability between different approaches for the analysis of the studies' results regarding differences between patients diagnosed with HNSCC and healthy subjects as well as radiation-induced changes within lymphocyte subpopulations might be limited to a certain degree.

Observing total lymphocyte counts of 56 HNSCC patients, numbers diminish by over 70 percent two months after patients started their chemoradiotherapy schedule. Further, patients with HPV-negative tumors experience earlier progression of disease. [210] In another experiment, patients also experience depletion of lymphocytes directly after irradiation, one year after the treatment except for NK cells all evaluated lymphocyte subsets still represent lower levels as compared with levels before treatment initiation. [135] This pronounced lymphopenia several weeks after starting radiation therapy is confirmed by further studies for HNSCC [208, 212] and other malignancies [213, 214] and is conclusively regarded as a frequent characteristic of radiation toxicity, independent of radiotherapy as a sole treatment approach or as a postoperative modality [215]. Indeed, a favorable tumor response to radiation therapy can be linked to improved radiation tolerance of lymphocytes for patients suffering from cervical cancer. [216] Similar behavior in total lymphocyte counts can be assumed for our experiment, even though we solely examine the variances within certain subsets of lymphocytes (NK cells, T cells, NK-like T cells and B cells). Thus, undergoing radiotherapy does not only consist of beneficial properties such as the reduction of tumor volume but also interferes with the patient's tumoral immune response. In a study with patients suffering from esophagal cancer, patients who succeed at recovering their immune composition can be connected to an improved prognosis and elevated median survival time. [217] Furthermore, in various malignancies including HNSCC a reduction of the applied radiation dosage should be the destination for further therapeutic strategies in the field of radiotherapy. To achieve a dosage reduction, suitable biomarkers to identify patients who show a proper radiation response and decline of tumor size in spite of a de-escalated radiation schedule are necessary.

In our study, for patients with or without recurrence we can observe a significant elevation of the mean percentage of NK cells after undergoing radiation therapy. In a small study, several HNSCC patients present with elevated NK cell counts. According to the study, this observation can be rarely observed in patients suffering from solid tumors at an advanced stage. [203] This might serve as a suitable explanation for the rise of NK cells consecutively to radiotherapy within

our study design since we solely examine patients with advanced-staged HNSCC. A study consisting of more than 100 samples of untreated patients, treated patients without recurrence and healthy donors similarly reports an increase in the level of NK cells within the group of treated patients. [201] HNSCC patients who have previously undergone extensive treatment, also confirm this observation in another study design. [218] In other studies, NK cells show no significant reaction to irradiation [136, 219], two further studies cannot find a differentiation of NK cell levels between the stages of the disease [200, 202]. On the contrary, patients suffering from esophagal cancer present with a decrease of NK cells after undergoing radiotherapy. [214] Three months subsequently to radiation therapy, NK cell levels have reached initial levels for patients with esophagal cancer. [217] Especially after surgical approach, NK cell levels seem to drop whereas one year after consecutive radiotherapy NK cell levels have fully recovered in contrast to other lymphocyte subpopulations. [135] For patients with cervical/endometrial carcinoma, NK cells first decline to a little extent shortly after beginning radiotherapy. Some patients though show increasing levels of NK cells upon treatment. [199]

While NK cells presumably are more resistant to radiation induced defects and show faster recovery, T cells and B cells are more radiosensitive. While T cells decline three months after irradiation, B cells already start to diminish during radiotherapy. The significant decline of T cells and B cells shortly after irradiation is consistent with many other studies with patients suffering from HNSCC. Forementioned declines of B cells and T cells might also be influenced by the disease itself or cisplatin-based chemotherapy but are more likely to be caused by radiotherapy alone. Studies with patient cohorts of various squamous cell carcinomas including HNSCC present the same decline in B cell and T cell levels. [208, 220] A small study examining 8 women with a cervical or endometrial carcinoma can detect similar results. [199] Studying HNSCC patients who received different treatment schedules, i.e., surgery and radiotherapy or radiation alone, similar conclusions regarding B cell and T cell levels can be drawn. [135, 136, 201, 203, 212, 215, 220] The decrease in T cells can also be confirmed by irradiating isolated T cells in blood bags. [221] Confirmed by gene

expression analysis, the decrease in T cells also affects tumor-infiltrating lymphocytes (TIL), whereas infiltration of T cells shows high variability. [204, 207] Assessment of B cell reactivity by stimulating peripheral blood lymphocytes with polyclonal B cell activator pokeweed mitogen additionally shows a reduction in B cell reactivity. [222] Furthermore, a decrease in CD4+ T cells occurs more predominantly whereas CD8+ T cells are rather unaffected by irradiation. [136, 203, 212] Often a decreased CD4+/CD8+ T cell ratio is reported after patients of various malignancies undergo irradiation. [135, 214] In cases of esophagal cancer, an increase in CD8+ T cell levels upon radiotherapy is reported. [214] A different study of HNSCC patients states a significant increase for the activation status of both circulating CD4+ and CD8+ T cells. [223] In our experiment we merely analyze the whole T cell population without further dividing into its subpopulations.

After radiotherapy T cells continuously shrink further and even after 12 months, they show no signs of recovery in our set-up. On the contrary, a study with patients treated by radiotherapy alone or postoperative irradiation reports starting recovery one month after radiotherapy. [215] In a study examining esophagal cancer, T cell and NK cell levels have reached initial levels after three months. [217] After initiation of radiation therapy, B cells shrink drastically within patients without recurrence before starting to recover directly after radiotherapy. One year after therapy, B cell levels for the No Recurrence group are higher compared with the initial mean percentage. Though values are still lower compared with healthy donors, 12 months after the treatment B cells tend to recover to comparable values. Consistent with our findings for patients without recurrence, a study reports a strong decline in B cells upon 6 months following radiotherapy, initial B cell reactivity levels are reached at 12 months after irradiation. [222] We detect that B cells of patients suffering from recurrence show a less pronounced decrease upon the start of irradiation. A strong interindividual variation can be noted as in an experiment concerning cervical/endometrial carcinoma [199], this might be due to the smaller sample size in relation to the No Recurrence group. Opposed to forementioned study of 8 women, B cell levels show an increase shortly after irradiation and at the time of recurrence are comparable with initial

levels for patients with recurrent disease. A pronounced decrease in B cells upon the start of the irradiation schedule might be correlated with a better treatment response and aid as a positive prognostic parameter for disease-free survival. This notion needs to be confirmed in further studies with a larger cohort and similar group sizes for No Recurrence and Recurrence. For T cells, differences between disease-free patients and patients suffering from recurrence cannot be confirmed. Mean percentage of T cells is inappropriate to stratify patients into groups. In conclusion, except for NK cells, lymphocyte subpopulations rather do not fully recover within a surveillance period of 12 months. [135, 201] In another study, lymphocytes have not reached initial values even after a period of 60 months. [208]

When comparing lymphocyte subpopulations of healthy donors with cancer patients, initial NK cell mean percentage is slightly higher for HNSCC patients. These findings cannot be verified as significant by statistical analysis. Comparing oral SCC patients with healthy individuals, no differences between NK cell levels can be noted. [198] In a large study design comparing HNSCC patients with healthy individuals, a decline of NK cells within HNSCC patients can be identified via demethylated copies of NKp46. [200] In relation to healthy donors, lower numbers of the CD56bright NK cell subpopulation are quantified for HNSCC patients. [202] Diminished cytotoxicity of NK cells correlates with development of regional or distant metastases as well as subsequent death related to tumors of the upper aerodigestive tract in a different experiment. [224] Another study from 1986 simultaneously states a higher risk for individuals with decreased NK cell activity to develop distant metastases. Furthermore, diminished NK cell activity can be conferred to patients consuming alcohol or already suffering from nodal metastases. [225] Before radiotherapy, the mean percentage of T cells for HNSCC patients is in the same range as of healthy donors. Additionally, comparing only CD4+ T cell levels, no difference becomes obvious in a study based on immune-phenotyped PBMCs. [136] Adversely, a study design of various squamous cell carcinomas including HNSCC can detect higher circulating T cell levels for healthy subjects compared with initial levels of patients. [220] Oral SCC patients with a tobacco-chewing history reveal decreased levels of T cells, especially of the

CD4+ T cell subpopulation, as well as a decreased CD4+/CD8+ T cell ratio in comparison with healthy subjects. [198] In contrast to our findings regarding T cells, mean percentage of B cells is already significantly reduced for HNSCC patients in relation to healthy subjects before undergoing radiation therapy. Another study cannot find any differences between patients suffering from squamous cell carcinoma and the control group. [220] Analyzing patients with advanced HNSCC and contraindication for cisplatin-based chemotherapy, levels of naïve B cells are initially higher only for patients experiencing disease progression. [212] Interestingly, HPV-positive patients suffering from HNSCC present with higher levels of B cells in comparison with healthy donors or HPV-negative patients within single cell suspensions of cancerous tissue. [205] Hence, reduced B cell levels may be an indicator of locally advanced HNSCC.

CD69 is known as an early activation marker expressed on T lymphocytes amongst other cells and involved in the proliferation as well as functioning of T cells. [226] Other experiments investigate the expression of CD69 on T cells seldomly directly within PBMCs [176, 177, 227] while most studies are based on the levels of CD69+ T cells within the tumor microenvironment [226, 228, 229] or use a combined approach [175, 230, 231]. In our experiment, mean percentage of CD69+ T cells does not reveal any significant difference between HNSCC patients and healthy donors within peripheral EDTA blood. A study measuring CD69 positivity of T cells within PBMCs of 62 HNSCC patients and 15 healthy subjects confirms our observation. [177] Opposed to our findings, in another study CD69+ activation marker is more frequently detected on T cells within tumorous epithelial in comparison with healthy tissue. [175] Patients at an advanced stage of HNSCC show diminished CD69+ levels after stimulation with PHA compared with healthy donors. [176] Regarding other malignant diseases, patients suffering from prostate cancer show higher mean percentages of CD69+ T cells in peripheral blood in relation to patients diagnosed with benign prostatic hyperplasia. [232] These observations may lead to the conclusion, that differences within levels of CD69+ T cells cannot be determined within peripheral blood alone.

When comparing CD69 expression levels on T cells of tissue samples of either HNSCC or healthy mucosa with peripheral blood lymphocytes, tissues present with

higher expression levels. [229, 230] In a mouse model mimicking HNSCC induced by classical risk factors (i.e., smoking and consumption of alcohol) elevated expression levels of CD69 on CD8+ T lymphocytes emerge in premalignant lesions whereas mice with HNSCC present with less immune stimulation including CD69 expression. [226] In another mouse model examining oral squamous cell carcinoma, the expression of CD69 shows elevated levels for T cells within lymph nodes and the spleen of Stat1-/- mice suffering from HNSCC when comparing with Stat1+/+ mice. [228] Concludingly, CD69 expression levels within tumor tissue seem to have more validity in relation to peripheral blood. Also, behavior of CD69 expression may vary regarding the type and location of the malignancy as indicated by the forementioned prostate cancer study. [232]

After initiation of radiotherapy, levels of CD69+ T cells begin to rise within the peripheral blood of HNSCC patients. For patients without recurrence, CD69+ T cells reach a consistent level 6 months after undergoing radiation therapy. In contrast, patients experiencing recurrent disease present with lower levels of CD69+ T cells 6 months after the treatment while CD69+ T cells are significantly higher in comparison with patients with non-recurrent disease at the time of recurrence. While shrinkage of the CD69+ T cell mean percentage is not significant between 3 months and 6 months after radiotherapy, the elevation of the mean percentage between 6 months after undergoing therapy and incidence of recurrence is slightly significant. The decline of CD69+ T cells 6 months after the treatment may be more distinct when investigating a larger test series of patients with recurrent disease. If the decline can be confirmed, this finding may aid to detect recurrent disease at an earlier point in time. An earlier treatment approach of recurrent HNSCC might improve disease control and quality of life. According to several studies including mouse models, high CD69 expression on T cells can be linked to progression of disease, elevated risk for metastatic disease and therefore worse prognosis and poor overall survival, supporting our thesis. [174, 177, 227] Also for other malignancies, higher values of CD69 T cell expression might constitute a risk factor for the development of prostate cancer and are connected to decreased disease-free survival as well as recurrent disease of colorectal cancer. [232, 233] This process might find its reason in the exhaustion of T cells induced by PD-1 and

TIM3 as well as in the down-regulation of tumor-infiltrating T lymphocytes leading to a diminished secretion of anti-cancerous cytokines, for example IFN-γ and IL-10. [174, 175, 228] In conclusion, the ascertained increase of CD69+ T cells upon recurrence may aid to assess and confirm the patient's progression of disease. On the other hand, a study examining 28 patients suffering from oral squamous cell carcinoma reports worse disease-free survival rates for patients with lower levels of CD69+ CD4+ T cells located in the sentinel nodes. [231] As a potential explanation, CD69 levels of T cells may differ depending on the type of specimen which is used for analysis. Additionally, monoclonal antibodies targeting CD69 are linked to decreased CD8+ T cell exhaustion and elevation of tumor-infiltrating T cells within the tumor microenvironment leading to lessened progression of disease in a mammary cancer mouse model. [174] In another experiment with renal cell carcinoma bearing mice, the subjects can benefit from additional anti-CD69 therapy. [234] An earlier study states the benefits of anti-CD69 therapy regarding an improved anti-tumor response based on an elevation of tumor-infiltrating NK cells and T cells. [235] Patients with recurrent disease and higher expression of CD69 upon T cells may benefit from adjuvant treatment with anti-CD69 antibodies. Further studies are necessary to research the eligibility and mechanism of anti-CD69 in humankind as well as to define suitable patients for anti-CD69 treatment. Little is known about the geometric mean fluorescence intensity of CD69 upon T cells. In our study group, mean fluorescence intensity does not differ between HNSCC patients and healthy donors. Solely 12 months after radiotherapy gMFI of CD69 is slightly higher for HNSCC patients. A constant elevation of CD69 gMFI after starting radiotherapy might be causal. Similarly to the mean percentage of CD69+ T cells, gMFI displays unsignificant lower levels at the time of the blood draw 6 months after treatment. Also, mean fluorescence intensity shows higher values at the time point of recurrence though differences regarding patients without HNSCC recurrence cannot be confirmed. We hypothesize that the CD69 gMFI presents with a similar pattern in relation to the mean percentage of CD69+ T cells. For future investigations mean percentage of CD69 positivity might be more suitable since the changes over time are more distinct.

The exclusive view of CD69+ T cells might not be the most expedient solution since expression of CD69 is intertwined with many regulatory mechanisms of the patient's immune system involved in the activation and presence of T cells. [236] For instance, HNSCC patients have been investigated to understand the connection between the expression of the early activation marker CD69 upon T cells and PD-L1. Results of a study indicate that CD8+ T cells increase the expression of CD69 and PD-1 on their surface after T cell receptor activation. When exosomes with high content of PD-L1 generated from the patients' plasma are added, T cells down-regulate their expression of CD69. Antibodies targeted at PD-1 could prevent the down-regulation of CD69. [236] Regarding T cells in tissues of patients suffering from oral squamous cell carcinoma, high expression levels of PD-1 can be detected. Also, T cells show strong activation and tumor-infiltrating lymphocytes with a low PD-1 expression profile also present with elevated CD69 expression. In contrast to the findings within tumor tissue, tumor-draining lymph node and peripheral blood samples cannot demonstrate high levels of PD-1 and the activation marker CD69. [230]

Substantive results for the immune checkpoint receptor PD-1 and its ligand PD-L1 are gained, especially the observations of PD-L1 are remarkable. Whereas for CD69 no significant differences between the mean percentage of positive T cells or gMFI can be stated, patients experiencing recurrence initially present with a significantly higher concentration level of PD-L1 in plasma compared with patients without disease progression and healthy controls. In comparison with the No Recurrence group, plasma PD-L1 levels of the Recurrence group are approximately 10-fold higher. Initial PD-L1 levels do not change significantly over time, therefore PD-L1 might predict increased risk for relapse before initiating therapy. Another study of 113 patients with locally advanced HNSCC supports these findings. [166] Soluble PD-L1 and PD-1 in plasma or serum are scarcely investigated for head and neck squamous cell carcinoma and other malignancies. In the aforementioned HNSCC study connecting CD69 expression to PD-L1, soluble PD-L1 concentration cannot be linked to progression of disease while circulating exosomes with high PD-L1 expression correlate with further progression. [236] Looking at other malignancies including non-small cell lung cancer, multiple

myeloma and myeloid leukemia, higher levels of soluble PD-L1 are found in plasma samples of patients suffering from cancer compared with healthy subjects. Also, PD-1 concentration is elevated in the patients' plasma samples. Furthermore, concentration of soluble PD-1 and PD-L1 is dependent on the type of tumor. [237] Therefore, conclusions for HNSCC based on different malignancies might be difficult to draw. Regarding soluble PD-L1, further studies investigating lung cancer, thyroid cancer and pancreatic adenocarcinoma state that high PD-L1 expression has a negative impact on the patients' outcomes. [238-240] Evaluating PD-L1 expression within tumor tissue, some HNSCC studies can also connect high PD-L1 levels with negative outcomes. [166, 241, 242] Clinical studies with Nivolumab, a PD-1 checkpoint inhibitor, discover improved response rates for PD-L1 expressing tumors, though significance cannot be reached presumably due to the small number of patients. [243] Another study surveilling patients after Nivolumab therapy states improved progression-free survival as well as reduced adverse events grade 3/4 in comparison with standard therapy. [244] While checkpoint inhibitors targeted at PD-L1 cannot prevent further tumor growth, promising results are achieved when used as an adjuvant agent. [206, 245] Interestingly, cisplatin at low dosage might be able to increase PD-L1 expression on tumor cells in an experiment based on mouse and human HNSCC cell lines. [245] Since patients in our clinical study receive cisplatin-based chemotherapy, the agent might have an influence on the elevation of PD-L1 in peripheral blood. It is uncertain to which extent chemotherapy might influence our findings regarding PD-1 and PD-L1.

When comparing radioresistant and radiosensitive cell lines of HNSCC, PD-L1 expression is almost increased 3-fold in relation to radiosensitive cell lines. [246] A huge study researching PD-L1 can connect elevated levels of PD-1 and PD-L1 expression to better radiosensitivity. Radioresistant patients with elevated expression levels of PD-L1 can be connected to worse prognosis regarding overall survival. [247] Further on, patients with higher PD-1 expression can be related to improved recurrence-free survival rates when undergoing radiotherapy, presumably connected to the finding of increased PD-1 expression for HPV-positive HNSCC. [191, 247] Additionally to PD-1, high tumoral levels of PD-L1

are frequently detected in HPV-positive HNSCC. [191, 248-250] In contrast, patients suffering from pancreatic adenocarcinoma presenting with high soluble PD-1 levels have an inferior median overall survival compared with patients expressing low soluble PD-1 levels. [239] Applied methods of this study are significantly variable and the result might be different for other malignancies than HNSCC. In our experiment, we experience difficulties regarding the PD-1 ELISA assay. Even though experiments have been repeated to rule out laboratory errors, plasma levels of PD-1 of some healthy donors remain questionably high. Furthermore, the sample size of healthy subjects is very small leading to intense measure of variation. Hence, it is virtually impossible to draw reliable conclusions between healthy donors and HNSCC patients. For HNSCC patients the variability of PD-1 concentration is less distinct in comparison with healthy donors. Nevertheless, results should be interpreted with caution. Concerning patients with recurrence, higher average values can be measured in comparison with non-recurrent patients. Furthermore, PD-1 expression is significantly elevated for patients within the No Recurrence group. For recurrent disease, some patients present with elevated PD-1 levels 6 months after radiotherapy though this finding cannot be statistically verified presumably due to the smaller sample size compared with the No Recurrence group. Three studies state a positive correlation between PD-L1 and PD-1 expression. [191, 247, 251] Next to elevated soluble PD-L1 levels, patients with pancreatic adenocarcinoma have a worse median overall survival when elevated soluble PD-1 levels can be detected. [239] Further investigations are necessary to draw conclusions between expression levels of soluble PD-1 and PD-L1 in plasma samples. In other HNSCC studies, PD-1 or PD-L1 expression do not seem to be related to the patients' overall survival. [249, 252] In several cases, higher expression levels of PD-L1 are connected to improved outcomes regarding progression-free survival and overall survival, as a matter of fact. [191, 209, 248, 251] Two studies though report advanced nodal status or higher grade of disease for patients with higher PD-L1 expression levels. [248, 250] Lower tumoral PD-L1 levels are found in HPV-negative tissue samples, which might lead to the conclusion that PD-L1 expression amounts to an improved prognosis for HPV-positive HNSCC. [251] Nevertheless, not all HPV-positive tumors express high PD-L1 levels. [248] None of the studies supporting the thesis of beneficial

PD-L1 increase investigate soluble PD-L1 levels. Divergent differences between used specimens might be the case and function of the immune system in the tumor microenvironment is multifactorial.

PD-L1 concentration in plasma might be a suitable approach of a less invasive diagnostical method to stratify HNSCC patients. Further studies are necessary to better understand the correlation of immune checkpoint expression patterns in different specimens including tumor tissue, healthy tissue as well as serum and plasma samples. Concludingly, patients with higher PD-L1 plasma concentrations might need a more intense therapeutic approach to improve disease free survival as well as overall survival compared with patients with lower PD-L1 levels. It should be investigated if plasma levels of PD-L1 correlate with the patient's HPV status. Furthermore, larger cohort studies are necessary to confirm our linkage of high PD-L1 expression to disease progression. Patients with initially high PD-L1 levels might also benefit from adjuvant application of immune checkpoint inhibitors.

In veterinary medicine, radiotherapy is often used in a palliative manner and is regarded as a reliable therapeutic approach in veterinary oncology. Treatment success is related to tumor size, therefore earlier diagnosis and initiation of therapy should be focused in order to improve the patient's prognosis for disease-free survival, progression-free survival and overall survival. [104] Clinical response rates for palliative therapy measure up to over 75 percent with a mean survival time of 1 year for gingival squamous cell carcinoma. [253] Fewer patient owners choose a radical therapeutical approach including irradiation, since the procedure is very cost-intensive and patients require anesthesia for each fraction. Hence, studies of small animals with malignancies of the head and neck undergoing radiation therapy are very rare. Acute and late radiation toxicities are also common in dogs, most frequently oral mucositis is a side effect of irradiation of the head and neck area. For canines with extended survival times, late side effects are a concerned risk factor. [104, 253, 254] Similar to humans, dogs experience diminishing lymphocytes upon irradiation though seldomly severe lymphopenia occurs. [255, 256] In a study in 1985, three months after total body irradiation canine lymphocytes and T cells do not reach numbers within the normal

spectrum. [257] Irradiated blood samples of dogs reveal that lymphocytes of younger dogs show higher frequencies of T cell apoptosis. Furthermore, CD8+ T cells are affected to a greater extent than CD4+ T cells. [258] Interestingly, cats seem to be less affected by radiation damage since fibroblasts and lymphocytes show more effective DNA and chromosome damage repair properties. [259] A study in 1986 with beagles which underwent whole body gamma irradiation states, that radiotherapy might enhance NK cell activity at a lower dosage whereas their activity is diminished at a higher dosage. [260] In our study, NK cell mean percentage rises after irradiation presumably caused by irradiation dosage, yet no conclusions can be drawn regarding NK cell activity. In conclusion, radiation therapy might compromise the immune system to a certain extent and have a negative impact on the patient's elimination of tumor cells. To ameliorate the patient's immune response within the tumor microenvironment, a reduction of radiation dosage should be aspired after assessment of the individual risk factor for progression of disease. Therefore, small animals with lower risk of recurrence might benefit from de-escalation of radiation dosage as well as mankind.

Immunotherapy is also applied in veterinary medicine, for example mast cell tumors are frequently treated with a tyrosine kinase inhibitor. Since squamous cell carcinoma in cats can hardly be controlled by radiotherapy alone and is considered as resistant to chemotherapy, adjuvant therapeutic options are necessary. Future experiments are needed to evaluate possible immunotherapeutic approaches in canine and feline oncology. Canine T cells also express several activation markers and immune checkpoint molecules including PD-1. [261] Same as for humans, functional exhaustion of lymphocytes might lead to high PD-1 expression. [262] For instance, elevated PD-1 expression is found on TILs or PBMCs in canine patients suffering from oral melanoma or B cell lymphoma. [262, 263] Another study could not locate PD-1 expression in all evaluated canine tumor cell lines. [264] PD-L1 expression is also detected in several canine tumor cell lines and malignant tumor tissues such as oral melanoma, mast cell tumor, mammary adenocarcinoma, prostate adenocarcinoma, osteosarcoma, lymphoma and hemangiosarcoma. [262, 264, 265] Initial levels of PD-L1 show high variability

which can be confirmed by our observations. [265] Stimulation by IFN-γ leads to upregulation of PD-L1 expression in almost all cancer cell lines. [264, 265] Regarding lymphoma, higher PD-L1 expression is solely seen in B cell lymphoma, whereas no PD-1 and PD-L1 expression is observed for T cell lymphoma. Interestingly, tumor-infiltrating cells show high PD-1 and PD-L1 expression for both T cell and B cell lymphoma. Especially cell lines with resistance towards chemotherapy are highly elevated whereas contrary to our observations, expression levels between untreated and recurrent lymphoma show no distinction. [266] In another lymphoma study, PD-L1 expression levels present with a 6-fold increase in lymphoma cells in comparison with ordinary PBMCs and other leukemic cells as well as a up to 3.5-fold increase within lymphoma tissue in comparison with tissue of healthy lymph nodes. [267] Patients suffering from B cell high grade lymphoma have improved overall survival rates when PD-1 levels of lymphonodal CD4+ T cells cells hold lower values. [263] Thus, to properly identify elevated PD-1 and PD-L1 expression and to draw conclusions as to the suspected tumoral behavior, several specimens might need to be evaluated in a larger cohort for each malignancy. Furthermore, high PD-1 and PD-L1 expression might predict chemotherapy-resistant properties in canine lymphoma. A recent study using identical R&D ELISA kits for PD-1 and PD-L1 detection as within our experiment, investigates feline patients with mammary carcinoma. Patients present with elevated serum levels of PD-1 and PD-L1, whereas PD-L1 expression is positively correlated with serum CTLA-4 levels. HER-2 positive feline tumors show more extensive increase of PD-1 expression in serum and PD-L1 expression upon cancer cells and tumor-infiltrating lymphocytes in comparison with triple negative normal-like mammary carcinoma. [268] Due to the positive correlation with PD-L1 expression, CTLA-4 levels might have added further insights and value to our study.

Antibodies used for targeting human PD-1 and PD-L1 presumably are not efficient in the veterinary practice. A study finds that human antibodies cannot properly detect canine PD-1 and PD-L1. Canine PD-1 and PD-L1 antibodies generated with a rat hybridoma can effectively block the binding. [269] Another study with canine oral melanoma and undifferentiated sarcoma patients is conducted with

canine-chimerised anti-PD-L1 antibodies. While the antibody can efficiently improve the production of IFN-γ and IL-2 as well as the proliferation of T cells in the peripheral blood in vitro, treatment leads to a reduction of IL-2 production. Out of 9 dogs, 2 dogs show either a reduction of tumor growth or an enhanced survival rate. [270] Similar to mankind, IFN-γ production in dogs is upregulated upon PD-1 blockade. Antibodies targeting PD-L1 show less upregulation in comparison with antibodies targeting PD-1. [269] In conclusion, treatment with antibodies targeting PD-1 might have a larger impact treating canine malignancies in relation to anti-PD-L1 treatment. PD-1/PD-L1 checkpoint inhibitors might be a useful clinical approach to treat eligible malignant cancer cases in veterinary practice. Further studies investigating canine and feline HNSCC are necessary to identify the most effective therapeutic antibodies as well as patients who might benefit from therapy with immune checkpoint inhibitors.

Dogs and cats might be used as a model of spontaneous head and neck cancer more intensely. The immune system and functions of dogs resemble those of mankind in many ways. For instance, numbers of B cells, T cells, neutrophils and monocytes in the peripheral blood as well as the CD4+ to CD8+ T cell ratio are very similar for dogs and humans. When suffering from cancer, Tregs rise in the peripheral blood and tumor-draining lymph nodes of canine patients. Special features of the canine immune system include circulating γδ T cells, CD4 expression upon neutrophils as well as higher numbers of mast cells at mucosal sites. [261] A study comparing peripheral blood mononuclear cells of younger and older beagles can detect similar age-related transformation of the immune system in comparison with mankind. For example, dogs present with elevated cytokine production levels by T cells and diminished proliferation of T cell subsets at an older age. [271] By now several reagents can be acquired to evaluate canine immune responses to cancerous disease. [261] Though canine and feline cancer studies are more costly in comparison with in vitro studies and mouse models, investigating head and neck cancer in small animals is a valuable approach in translational cancer research and should find room for future clinical studies.

Based on our findings, in human medicine PD-L1 concentration in plasma might function as an early prognostic biomarker to identify patients who are more prone

to recurrent disease. These findings may lead to earlier detection of locally advanced disease as well as an improved patient risk group stratification in order to define a more personalized radiotherapy schedule. Additionally, suitable patients for the use of additional PD-1 or PD-L1 checkpoint inhibitors may be identified and benefit from more promising therapeutic results. In veterinary medicine, adjuvant therapy with immune checkpoint inhibitors may also lead to improved progression free survival and overall survival for canine and feline HNSCC. Continuous investigation of feline and canine HNSCC may lead to additional empirical data in the field of translational research. Further HNSCC studies are necessary to confirm soluble PD-L1 as a robust indicator of more aggressive tumoral behavior before stratifying patients based on their plasma PD-L1 concentration. For instance, measuring PD-L1 simultaneously within tumoral tissue as well as peripheral blood plasma and serum might lead to a better understanding of PD-L1 expression in the peripheral blood and pave the way to finding the most suitable specimen for PD-L1 stratification.

5. Summary

Radiation therapy induced effects on lymphocyte subpopulations and prognostic value of CD69, PD-1 and PD-L1 in the peripheral blood of patients with advanced HNSCC

This doctoral thesis is based on the prospective multicentric observational cohort study *HNprädBio* of the Deutsches Konsortium für Translationale Krebsforschung (DKTK) with patients suffering from locally advanced head and neck squamous cell carcinoma (HNSCC). The thesis covers radiation therapy induced effects on lymphocytes and the prognostic value of the early activation marker CD69, immune checkpoint PD-1 and its ligand PD-L1. The aim of the study comprises the investigation of effects on lymphocyte subsets caused by irradiation and its informative value regarding prognosis for recurrent disease as well as the prognostic value of early activation marker CD69, PD-1 and PD-L1 on locoregional control.

Patients' blood samples are gained before initiating chemoradiotherapy, during treatment, 3 months, 6 months and 12 months post chemoradiotherapy. Another blood sample is taken in case of recurrent disease. Peripheral blood of patients and healthy donors is analyzed by multi-color fluorescence activated cell sorting (FACS) to measure the amount and density of receptors identifying lymphocyte subgroups (NK cells, T cells, NK-like T cells and B cells). Additionally, the expression profile and fluorescence intensity of early activation marker CD69 upon NK cells, T cells and NK-like T cells is investigated by FACS. To evaluate concentration levels of the immune checkpoint PD-1 and its ligand PD-L1, prefabricated enzyme-linked immunosorbent assays (ELISA) detecting human PD-1 and human PD-L1 are conducted.

The evaluation of changes within the lymphocyte subsets of HNSCC patients yields a significant decrease in T cells and B cells upon radiotherapy. Whereas B cells consecutively recover over time to levels below those of healthy donors, T cells do not show any signs of recovery within the surveillance period of two years. Furthermore, NK cells rise after the beginning of treatment. Comparing HNSCC patients with healthy subjects, HNSCC patients initially present with a higher mean

percentage of NK cells and a lower mean percentage of B cells. Regarding the expression of the early activation marker CD69 upon T cells, mean percentage and geometric mean fluorescence intensity (gMFI) start to grow after patients undergo radiotherapy. Patients suffering from recurrence reach their highest values of mean percentage and gMFI at the time of recurrence. For soluble PD-1, the concentration is elevated after irradiation within patients without recurrence whereas patients with recurrent disease present with higher average values in comparison with the other HNSCC patients. Initial concentration values of soluble PD-L1 are approximately ten times higher within patients experiencing recurrence and remain unchanged throughout radiotherapy as well as the ensuing surveillance period.

Further HNSCC studies need to be conducted to confirm soluble PD-L1 as a suitable biomarker for patient stratification.

6. Zusammenfassung

Strahlentherapieinduzierte Effekte auf Lymphozyten-Subpopulationen und prognostischer Wert von CD69, PD-1 und PD-L1 im peripheren Blut von Patienten mit fortgeschrittenem Plattenepithelkarzinom im Kopf- und Halsbereich

Diese Doktorarbeit basiert auf der prospektiven multizentrischen Beobachtungskohortenstudie *HNprädBio* des Deutschen Konsortiums für Translationale Krebsforschung (DKTK) und untersucht Patienten, die an einem lokal fortgeschrittenen Plattenepithelkarzinom des Kopfes und Halses (HNSCC) leiden. Die Arbeit beschäftigt sich mit strahlentherapieinduzierten Effekten auf Lymphozyten und dem prognostischen Wert des Immun-Checkpoints PD-1 und dessen Liganden PD-L1. Das Ziel der Studie umfasst die Untersuchung von bestrahlungsbedingten Effekten auf Untergruppen von Lymphozyten und deren Aussagekraft hinsichtlich der Prognose für eine rezidivierende Erkrankung sowie den prognostischen Wert der frühen Aktivierungsmarker CD69, PD-1 und PD-L1 in Bezug auf die lokoregionäre Kontrolle.

Die Blutproben der Patienten werden vor Beginn der Chemoradiotherapie, während der Behandlung, 3 Monate, 6 Monate und 12 Monate nach der Chemoradiotherapie gewonnen. Eine weitere Blutprobe wird im Falle einer rezidivierenden Erkrankung entnommen. Das periphere Blut von Patienten und gesunden Spendern wird mittels mehrfarbiger fluoreszenzaktivierter Zellsortierung (FACS) analysiert, um die Menge und Dichte von Rezeptoren zu messen, die entsprechende Lymphozyten-Untergruppen (NK-Zellen, T-Zellen, NK-ähnliche T-Zellen und B-Zellen) identifizieren. Zusätzlich werden das Expressionsprofil und die Fluoreszenzintensität des frühen Aktivierungsmarkers CD69 auf NK-Zellen, T-Zellen und NK-ähnlichen T-Zellen mittels FACS untersucht. Um die Konzentrationswerte des Immun-Checkpoints PD-1 und seines Liganden PD-L1 zu ermitteln, werden vorgefertigte Enzyme-linked Immunosorbent Assays (ELISA) zum Nachweis von humanem PD-1 und humanem PD-L1 durchgeführt.

Die Auswertung der Veränderungen innerhalb der Lymphozyten-Untergruppen von HNSCC-Patienten ergibt eine signifikante Abnahme der T-Zellen und B-Zellen

nach Strahlentherapie. Während sich die B-Zellen im Laufe der Zeit konsekutiv auf ein Niveau unterhalb des Niveaus von gesunden Spendern erholen, zeigen die T-Zellen innerhalb des Überwachungszeitraums von zwei Jahren keine Anzeichen einer Erholung. Außerdem steigen die NK-Zellen nach Beginn der Behandlung an. Vergleicht man HNSCC-Patienten mit gesunden Probanden, weisen HNSCC-Patienten zunächst einen höheren Prozentsatz an NK-Zellen und einen niedrigeren Prozentsatz an B-Zellen auf. Der mittlere Prozentsatz der Expression und die geometrische mittlere Fluoreszenzintensität (gMFI) des frühen Aktivierungsmarkers CD69 steigen nach der Strahlentherapie auf T-Zellen an. Patienten, die an einem Rezidiv leiden, erreichen zum Zeitpunkt des Rezidivs die höchsten prozentualen Werte und Fluoreszenzintensitäten. Die Konzentration von löslichem PD-1 ist nach Bestrahlung bei Patienten ohne Rezidiv erhöht, während Patienten mit rezidivierender Erkrankung im Vergleich zu anderen HNSCC-Patienten höhere Durchschnittswerte aufweisen. Die Ausgangswerte von löslichem PD-L1 sind bei Patienten mit einem Rezidiv etwa zehnmal höher und bleiben während der Strahlentherapie und der anschließenden Überwachungsphase unverändert.

Weitere HNSCC-Studien müssen durchgeführt werden, um lösliches PD-L1 als geeigneten Biomarker für die Patientenstratifikation zu bestätigen.

IV. References

1. Global Burden of Disease Cancer Collaboration. Global, Regional, and National Cancer Incidence, Mortality, Years of Life Lost, Years Lived With Disability, and Disability-Adjusted Life-Years for 29 Cancer Groups, 1990 to 2017: A Systematic Analysis for the Global Burden of Disease Study. JAMA Oncology. 2019;5(12):1749-68
2. Bray F, Ferlay J, Soerjomataram I, Siegel RL, Torre LA, Jemal A. Global cancer statistics 2018: GLOBOCAN estimates of incidence and mortality worldwide for 36 cancers in 185 countries. CA: Cancer J Clin. 2018;68(6):394-424
3. Siegel RL, Miller KD, Jemal A. Cancer statistics, 2020. CA: Cancer J Clin. 2020;70(1):7-30
4. Ward EM, Sherman RL, Henley SJ, Jemal A, Siegel DA, Feuer EJ, et al. Annual Report to the Nation on the Status of Cancer, Featuring Cancer in Men and Women Age 20-49 Years. JNCI Natl Cancer Inst. 2019;111(12):1279-97
5. Devaraja K. Current Prospects of Molecular Therapeutics in Head and Neck Squamous Cell Carcinoma. Pharmaceut Med. 2019;33(4):269-89
6. Naghavi M, Abajobir AA, Abbafati C, Abbas KM, Abd-Allah F, Abera SF, et al. Global, regional, and national age-sex specific mortality for 264 causes of death, 1980-2016: a systematic analysis for the Global Burden of Disease Study 2016. Lancet. 2017;390:1151-210
7. Lydiatt WM, Patel SG, O'Sullivan B, Brandwein MS, Ridge JA, Migliacci JC, et al. Head and Neck Cancers-Major Changes in the American Joint Committee on Cancer Eighth Edition Cancer Staging Manual. CA: Cancer J Clin. 2017;67(2):122-37
8. Alibek K, Kakpenova A, Baiken Y. Role of infectious agents in the carcinogenesis of brain and head and neck cancers. Infect Agent Cancer. 2013;8(7):1-9
9. Tsimberidou A-M, Kurzrock R, Anderson KC. Targeted Therapy in Translational Cancer Research. 1 ed. Hoboken: John Wiley & Sons, Inc.; 2016.
10. Harrison LB, Sessions RB, Kies MS. Head and Neck Cancer: A Multidisciplinary Approach. 4 ed. Philadelphia: Lippincott Williams & Wilkins (Wolters Kluwer); 2014.
11. Blot WJ, McLaughlin JK, Winn DM, Austin DF, Greenberg RS, Preston-Martin S, et al. Smoking and Drinking in Relation to Oral and Pharyngeal Cancer. Cancer Res. 1988;48(11):3282-7
12. Anantharaman D, Marron M, Lagiou P, Samoli E, Ahrens W, Pohlabeln H, et al. Population attributable risk of tobacco and alcohol for upper aerodigestive tract cancer. Oral Oncol. 2011;47(8):725-31
13. Hermans R. Squamous Cell Cancer of the Neck. 1 ed. Reznek RH, editor. Cambridge: Cambridge University Press; 2008.
14. Chang ET, Liu Z, Hildesheim A, Liu Q, Cai Y, Zhang Z, et al. Active and Passive Smoking and Risk of Nasopharyngeal Carcinoma: A Population-Based Case-Control Study in Southern China. Am J Epidemiol. 2017;185(12):1272-80

15. Hashibe M, Brennan P, Chuang S-C, Boccia S, Castellsague X, Chen C, et al. Interaction between Tobacco and Alcohol Use and the Risk of Head and Neck Cancer: Pooled Analysis in the International Head and Neck Cancer Epidemiology Consortium. Cancer Epidemiol Biomarkers Prev. 2009;18(2):541-50
16. Adelstein DJ. Squamous Cell Head and Neck Cancer. 1 ed. Totowa, NJ: Humana Press Inc.; 2005.
17. Morse DE, Katz RV, Pendrys DG, Holford TR, Krutchkoff DJ, Eisenberg E, et al. Smoking and Drinking in Relation to Oral Epithelial Dysplasia. Cancer Epidemiol Biomarkers Prev. 1996;5(10):769-77
18. de Martel C, Plummer M, Vignat J, Franceschi S. Worldwide burden of cancer attributable to HPV by site, country and HPV type. Int J Cancer. 2017;141(4):664-70
19. Anantharaman D, Abedi-Ardekani B, Beachler DC, Gheit T, Olshan AF, Wisniewski K, et al. Geographic heterogeneity in the prevalence of human papillomavirus in head and neck cancer. Int J Cancer. 2017;140(9):1968-75
20. Gillison ML, Chaturvedi AK, Anderson WF, Fakhry C. Epidemiology of Human Papillomavirus-Positive Head and Neck Squamous Cell Carcinoma. J Clin Oncol. 2015;33(29):3235-42
21. Pintos J, Black MJ, Sadeghi N, Ghadirian P, Zeitouni AG, Viscidi RP, et al. Human papillomavirus infection and oral cancer: a case-control study in Montreal, Canada. Oral Oncol. 2007;44(3):242-50
22. Shinohara S, Kikuchi M, Tona R, Kanazawa Y, Kishimoto I, Harada H, et al. Prognostic Impact of p16 and p53 Expression in Oropharyngeal Squamous Cell Carcinomas. Jpn J Clin Oncol. 2014;44(3):232-40
23. Khan FM, Gerbi BJ. Treatment Planning in Radiation Oncology

3ed. Philadelphia: Lippincott Williams & Wilkins (Wolters Kluwer); 2012.
24. The Cancer Genome Atlas Network. Comprehensive genomic characterization of head and neck squamous cell carcinomas. Nature. 2015;517(7536):576-82
25. Hayes RB, Ahn J, Fan X, Peters BA, Ma Y, Yang L, et al. Association of Oral Microbiome With Risk for Incident Head and Neck Squamous Cell Cancer. JAMA Oncol. 2018;4(3):358-65
26. Shiga K, Tateda M, Saijo S, Hori T, Sato I, Tateno H, et al. Presence of Streptococcus infection in extra-oropharyngeal head and neck squamous cell carcinoma and its implication in carcinogenesis. Oncol Rep. 2001;8(2):245-8
27. Tateda M, Shiga K, Saijo S, Sone M, Hori T, Yokoyama J, et al. Streptococcus anginosus in head and neck squamous cell carcinoma: Implication in carcinogenesis. Int J Mol Med. 2001;6(6):699-703
28. Sasaki M, Yamaura C, Ohara-Nemoto Y, Tajika S, Kodama Y, Ohya T, et al. Streptococcus anginosus infection in oral cancer and its infection route. Oral Dis. 2005;11(3):151-6
29. Agha-Hosseini F, Sheykhbahaei N, SadrZadeh-Afshar M-S. Evaluation of Potential Risk Factors that contribute to Malignant Transformation of Oral Lichen Planus: A Literature Review. J Contemp Dent Pract. 2016;17(8):692-701
30. De Stefani E, Ronco A, Mendilaharsu M, Deneo-Pellegrini H. Diet and risk of cancer of the upper aerodigestive tract-II. Nutrients. Oral Oncol. 1999;35(1):22-6

31. La Vecchia C, Tavani A, Franceschi S, Levi F, Corrao G, Negri E. Epidemiology and prevention of oral cancer. Oral Oncol. 1997;33(5):302-12
32. Farrow DC, Vaughan TL, Berwick M, Lynch CF, Swanson GM, Lyon JL. Diet and nasopharyngeal cancer in a low-risk population. Int J Cancer. 1998;78(6):675-9
33. Estève J, Riboli E, Péquignot G, Terracini B, Merletti F, Crosignani P, et al. Diet and cancers of the larynx and hypopharynx: the IARC multi-center study in southwestern Europe. Cancer Causes Control. 1996;7(2):240-52
34. Mercante G, Bacciu A, Ferri T, Bacciu S. Gastroesophageal reflux as a possible co-promoting factor in the development of the squamous-cell carcinoma of the oral cavity, of the larynx and of the pharynx. Acta Otorhinolaryngol Belg. 2003;57(2):113-7
35. Langevin SM, Michaud DS, Marsit CJ, Nelson HH, Birnbaum AE, Eliot M, et al. Gastric Reflux Is an Independent Risk Factor for Laryngopharyngeal Carcinoma. Cancer Epidemiol Biomarkers Prev. 2013;22(6):1061-8
36. El-Serag HB, Hepworth EJ, Lee P, Sonnenberg A. Gastroesophageal Reflux Disease Is a Risk Factor for Laryngeal and Pharyngeal Cancer. Am J Gastroenterol. 2001;96(7):2013-8
37. Nicholls JM, Agathanggelou A, Fung K, Xiangguo Z, Niedobitek G. The association of squamous cell carcinomas of the nasopharynx with Epstein-Barr virus shows geographical variation reminiscent of Burkitt's lymphoma. J Pathol. 1999;183(2):164-8
38. Shaw R, Beasley N. Aetiology and risk factors for head and neck cancer: United Kingdom National Multidisciplinary Guidelines. J Laryngol Otol. 2016;130(S2):S9-S12
39. Kutler DI, Auerbach AD, Satagopan J, Giampietro PF, Batish SD, Huvos AG, et al. High Incidence of Head and Neck Squamous Cell Carcinoma in Patients With Fanconi Anemia. Arch Otolaryngol Head Neck Surg. 2003;129(1):106-12
40. Morris Brown L, Moradi T, Gridley G, Plato N, Dosemeci M, Fraumeni JF, Jr. Exposures in the Painting Trades and Paint Manufacturing Industry and Risk of Cancer Among Men and Women in Sweden. J Occup Environ Med. 2002;44(3):258-64
41. Maier H, Tisch M, Enderle G, Dietz A, Weidauer H. [Occupational exposure to paint, lacquer and solvents, and cancer risk in the area of the upper aero-digestive tract]. HNO. 1997;45(11):905-8
42. Azimi S, Rafieian N, Manifar S, Ghorbani Z, Tennant M, Kruger E. Socioeconomic determinants as risk factors for squamous cell carcinoma of the head and neck: a case-control study in Iran. Br J Oral Maxillofac Surg. 2018;56(4):304-9
43. Elwood JM, Pearson JCG, Skippen DH, Jackson SM. Alcohol, smoking, social and occupational factors in the aetiology of cancer of the oral cavity, pharynx and larynx. Int J Cancer. 1984;34(5):603-12
44. Skeel RT, Khlief SN. Handbook of Cancer Chemotherapy. 8 ed. Philadelphia: Lippincott Williams & Wilkins (Wolters Kluwer); 2011.
45. Price T, Montgomery P, Birchall M, Gullane P. A Diagnostic Atlas of Tumors of the Upper Aero-Digestive Tract: A Transnasal Video Endoscopic Approach. London: CRC Press (Taylor & Francis Group, LLC); 2012.

46. Grégoire V, Lefebvre J-L, Licitra L, Felip E. Squamous cell carcinoma of the head and neck: EHNS-ESMO-ESTRO Clinical Practice Guidelines for diagnosis, treatment and follow-up. Ann Oncol. 2010;21 (Supplement 5):v184-v6
47. Zhou H, Zhang J, Guo L, Nie J, Zhu C, Ma X. The value of narrow band imaging in diagnosis of head and neck cancer: a meta-analysis. Sci Rep. 2018;8(1):1-11
48. Budach V, Tinhofer I. Novel prognostic clinical factors and biomarkers for outcome prediction in head and neck cancer: a systematic review. Lancet Oncol. 2019;20(6):e313-e26
49. Liu C, Yu Z, Huang S, Zhao Q, Sun Z, Fletcher C, et al. Combined identification of three miRNAs in serum as effective diagnostic biomarkers for HNSCC. EBioMedicine. 2019;50:135-43
50. Guizard AN, Dejardin OJ, Launay LC, Bara S, Lapôtre-Ledoux BM, Babin EB, et al. Diagnosis and management of head and neck cancers in a high-incidence area in France: A population-based study. Medicine 2017;96(26):e7285-e91
51. Leemans CR, Braakhuis BJM, Brakenhoff RH. The molecular biology of head and neck cancer. Nat Rev Cancer. 2011;11(1):9-22
52. Duprez F, Berwouts D, De Neve W, Bonte K, Boterberg T, Deron P, et al. Distant metastases in head and neck cancer. Head Neck. 2017;39(9):1733-43
53. Vermorken JB, Mesia R, Rivera F, Remenar E, Kawecki A, Rottey S, et al. Platinum-Based Chemotherapy plus Cetuximab in Head and Neck Cancer. N Engl J Med. 2008;359(11):1116-27
54. Burusapat C, Jarungroongruangchai W, Charoenpitakchai M. Prognostic factors of cervical node status in head and neck squamous cell carcinoma. World J Surg Oncol. 2015;13(1)
55. Haksever M, Inançlı HM, Tunçel Ü, Kürkçüoğlu SS, Uyar M, Genç Ö, et al. The effects of tumor size, degree of differentiation, and depth of invasion on the risk of neck node metastasis in squamous cell carcinoma of the oral cavity. Ear Nose Throat J. 2012;91(3):130-5
56. Huang S, O'Sullivan B. Overview of the 8th Edition TNM Classification for Head and Neck Cancer. New York: Springer US; 2017.
57. Amin MB, Edge SB, Greene FL, Schilsky RL, Gaspar LE, Washington MK, et al. AJCC Cancer Staging Manual. 8 ed. Chicago, IL: American College of Surgeons; 2018.
58. Hodler J, Kubik-Huch RA, von Schulthess GK. Diseases of the Brain, Head and Neck, Spine 2020-2023: Diagnostic Imaging. 1 ed. Cham: IDKD Springer Series; 2020.
59. Morikawa K, Walker SM, Nakajima M, Pathak S, Jessup JM, Fidler IJ. Influence of Organ Environment on the Growth, Selection, and Metastasis of Human Colon Carcinoma Cells in Nude Mice. Cancer Res. 1988;48(23):6863-71
60. Tong CCL, Kao J, Sikora AG. Recognizing and reversing the immunosuppressive tumor microenvironment of head and neck cancer. Immunol Res. 2012;54(1-3):266-74
61. Balkwill F, Mantovani A. Inflammation and cancer: back to Virchow? Lancet. 2001;357(9255):539-45
62. Mandal R, Şenbabaoğlu Y, Desrichard A, Havel JJ, Dalin MG, Riaz N, et al. The head and neck cancer immune landscape and its immunotherapeutic implications. JCI Insight. 2016;1(17)

63. Lin W, Chen M, Hong L, Zhao H, Chen Q. Crosstalk Between PD-1/PD-L1 Blockade and Its Combinatorial Therapies in Tumor Immune Microenvironment: A Focus on HNSCC. Front Oncol. 2018;8(532)
64. Miyauchi S, Kim SS, Pang J, Gold KA, Gutkind JS, Califano JA, et al. Immune Modulation of Head and Neck Squamous Cell Carcinoma and the Tumor Microenvironment by Conventional Therapeutics. Clin Cancer Res. 2019;25(14):4211-23
65. de la Iglesia JV, Slebos RJC, Martin-Gomez L, Wang X, Teer JK, Tan AC, et al. Effects of Tobacco Smoking on the Tumor Immune Microenvironment in Head and Neck Squamous Cell Carcinoma. Clin Cancer Res. 2020;26(6):1474-85
66. Coldwell DM. Manual of Interventional Oncology. 1 ed. New York, Stuttgart, Delhi, Rio de Janeiro: Thieme Medical Publishers, Inc.; 2018.
67. Hanoteau A, Newton JM, Krupar R, Huang C, Liu H-C, Gaspero A, et al. Tumor microenvironment modulation enhances immunologic benefit of chemoradiotherapy. J Immunother Cancer. 2019;7(10)
68. National Cancer Institute. [Internet] Cancer Stat Facts: Oral Cavity and Pharynx Cancer [cited 2020 15 Nov]. Available from: https://seer.cancer.gov/statfacts/html/oralcav.html.
69. Huang SH, Xu W, Waldron J, Siu L, Shen X, Tong L, et al. Refining American Joint Committee on Cancer/Union for International Cancer Control TNM Stage and Prognostic Groups for Human Papillomavirus–Related Oropharyngeal Carcinomas. J Clin Oncol. 2015;33(8):836-45
70. Li H, Torabi SJ, Yarbrough WG, Mehra S, Osborn HA, Judson B. Association of Human Papillomavirus Status at Head and Neck Carcinoma Subsites With Overall Survival. JAMA Otolaryngol Head Neck Surg. 2018;144(6):519-25
71. O'Sullivan B, Huang SH, Su J, Garden AS, Sturgis EM, Dahlstrom K, et al. Development and validation of a staging system for HPV-related oropharyngeal cancer by the International Collaboration on Oropharyngeal cancer Network for Staging (ICON-S): a multicentre cohort study. Lancet Oncol. 2016;17(4):440-51
72. Lassen P, Eriksen JG, Hamilton-Dutoit S, Tramm T, Alsner J, Overgaard J. Effect of HPV-Associated p16INK4A Expression on Response to Radiotherapy and Survival in Squamous Cell Carcinoma of the Head and Neck. J Clin Oncol. 2009;27(12):1992-8
73. Sørensen BS, Busk M, Olthof N, Speel E-J, Horsman MR, Alsner J, et al. Radiosensitivity and effect of hypoxia in HPV positive head and neck cancer cells. Radiother Oncol. 2013;108(3):500-5
74. Beynon RA, Lang S, Schimansky S, Penfold CM, Waylen A, Thomas SJ, et al. Tobacco smoking and alcohol drinking at diagnosis of head and neck cancer and all-cause mortality: Results from head and neck 5000, a prospective observational cohort of people with head and neck cancer. Int J Cancer. 2018;143(5):1114-27
75. Price KAR, Cohen EE. Current treatment options for metastatic head and neck cancer. Curr Treat Options Oncol. 2012;13(1):35-46
76. Nordsmark M, Bentzen SM, Rudat V, Brizel D, Lartigau E, Stadler P, et al. Prognostic value of tumor oxygenation in 397 head and neck tumors after primary radiation therapy. An international multi-center study. Radiother Oncol. 2005;77(1):18-24
77. Meuten DJ. Tumors in Domestic Animals. 5 ed. Ames, Iowa: John Wiley & Sons, Inc.; 2017.

78. Morris J, Dobson J. Small Animal Oncology. 1 ed. Osney Mead, Oxford: Blackwell Sciecne Ltd; 2001.
79. Withrow SJ, Vail DM, Page RL. Withrow & MacEwen's small animal clinical oncology. 5 ed. St. Louis, Mo: Saunders (Elsevier Inc.); 2013.
80. Brønden LB, Eriksen T, Kristensen AT. Oral malignant melanomas and other head and neck neoplasms in Danish dogs-data from the Danish Veterinary Cancer Registry. Acta Vet Scand. 2009;51(1)
81. Mikiewicz M, Paździor-Czapula K, Gesek M, Lemishevskyi V, Otrocka-Domagała I. Canine and Feline Oral Cavity Tumours and Tumour-like Lesions: a Retrospective Study of 486 Cases (2015-2017). J Comp Pathol. 2019;172:80-7
82. de Vos JP, Burm AGD, Focker AP, Boschloo H, Karsijns M, van der Waal I. Piroxicam and carboplatin as a combination treatment of canine oral non-tonsillar squamous cell carcinoma: a pilot study and a literature review of a canine model of human head and neck squamous cell carcinoma. Vet Comp Oncol. 2005;3(1):16-24
83. Wypij JM. A Naturally Occurring Feline Model of Head and Neck Squamous Cell Carcinoma. Patholog Res Int. 2013;2013:502197
84. Martin CK, Tannehill-Gregg SH, Wolfe TD, Rosol TJ. Bone-Invasive Oral Squamous Cell Carcinoma in Cats: Pathology and Expression of Parathyroid Hormone-Related Protein. Vet Pathol. 2011;48(1):302-12
85. Lino M, Lanore D, Lajoinie M, Jimenez A, Crouzet F, Queiroga FL. Prognostic factors for cats with squamous cell carcinoma of the nasal planum following high-dose rate brachytherapy. J Feline Med Surg. 2019;21(12):1157-64
86. Reif JS, Bruns C, Lower KS. Cancer of the Nasal Cavity and Paranasal Sinuses and Exposure to Environmental Tobacco Smoke in Pet Dogs. Am J Epidemiol. 1998;147(5):488-92
87. Munday JS, Knight CG, French AF. Evaluation of feline oral squamous cell carcinomas for p16 CDKN2A protein immunoreactivity and the presence of papillomaviral DNA. Vet Sci. 2011;90:280-3
88. Munday JS, French AF, Gibson IR, Knight CG. The Presence of p16CDKN2A Protein Immunostaining Within Feline Nasal Planum Squamous Cell Carcinomas Is Associated With an Increased Survival Time and the Presence of Papillomaviral DNA. Vet Pathol. 2012;50(2):269-73
89. Condjella R, Liu X, Suprynowicz F, Yuan H, Sudarshan S, Dai Y, et al. The canine papillomavirus e5 protein signals from the endoplasmic reticulum. J Virol. 2009;83(24):12833-41
90. Regalado Ibarra AM, Legendre L, Munday JS. Malignant Transformation of a Canine Papillomavirus Type 1-Induced Persistent Oral Papilloma in a 3-Year-Old Dog. J Vet Dent. 2018;35(2):79-95
91. Thaiwong T, Sledge DG, Wise AG, Olstad K, Maes RK, Kiupel M. Malignant transformation of canine oral papillomavirus (CPV1)-associated papillomas in dogs: An emerging concern? Papillomavirus Res. 2018;6:83-9
92. Luff J, Rowland P, Mader M, Orr C, Yuan H. Two Canine Papillomaviruses Associated With Metastatic Squamous Cell Carcinoma in Two Related Basenji Dogs. Vet Pathol. 2016;53(6):1160-3
93. Luff J, Mader M, Rowland P, Britton M, Fass J, Yuan H. Viral genome integration of canine papillomavirus 16. Papillomavirus Res. 2019;7:88-96

94. Munday JS, O'Connor KI, Smits B. Development of multiple pigmented viral plaques and squamous cell carcinomas in a dog infected by a novel papillomavirus. Vet Dermatol. 2010;22(1):104-10
95. Bertone ER, Snyder LA, Moore AS. Environmental and Lifestyle Risk Factors for Oral Squamous Cell Carcinoma in Domestic Cats. J Vet Intern Med. 2003;17(4):557-62
96. Lascelles BDX, Parry AT, Stidworthy MF, Dobson JM, White RAS. Squamous cell carcinoma of the nasal planum in 17 dogs. Vet Rec. 2000;147(17):473-6
97. Avner A, Dobson JM, Sales JI, Herrtage ME. Retrospective review of 50 canine nasal tumours evaluated by low-field magnetic resonance imaging. J Small Anim Pract. 2008;49(5):233-9
98. Armour MD, Broome M, Dell'Anna G, Blades NJ, Esson DW. A review of orbital and intracranial magnetic resonance imaging in 79 canine and 13 feline patients (2004-2010). Vet Ophthalmol. 2011;14(4):215-26
99. Herring ES, Smith MM, Robertson JL. Lymph node staging of oral and maxillofacial neoplasms in 31 dogs and cats. J Vet Dent. 2002;19(3):122-6
100. Wingo K. Histopathologic Diagnoses From Biopsies of the Oral Cavity in 403 Dogs and 73 Cats. J Vet Dent. 2018;35(1):7-17
101. Massari F, Chiti LE, Lisi MLP, Drudi D, Montinaro V, Sommaruga P. Lip-to-nose flap for reconstruction of the nasal planum after curative intent excision of squamous cell carcinoma in cats: Description of technique and outcome in seven cases. Vet Surg. 2020;49(2):339-46
102. Gasymova E, Meier V, Guscetti F, Cancedda S, Roos M, Rohrer Bley C. Retrospective clinical study on outcome in cats with nasal planum squamous cell carcinoma treated with an accelerated radiation protocol. BMC Vet Res. 2017;13(1)
103. Bowles K, DeSandre-Robinson D, Kubicek L, Lurie D, Milner R, Boston SE. Outcome of definitive fractionated radiation followed by exenteration of the nasal cavity in dogs with sinonasal neoplasia: 16 cases. Vet Comp Oncol. 2014;14(4):350-60
104. Théon AP, Rodriguez C, Madewell BR. Analysis of prognostic factors and patterns of failure in dogs with malignant oral tumors treated with megavoltage irradiation. J Am Vet Med Assoc. 1997;210(6):778-84
105. Riggs J, Adams VJ, Hermer JV, Dobson JM, Murphy S, Ladlow JF. Outcomes following surgical excision or surgical excision combined with adjunctive, hypofractionated radiotherapy in dogs with oral squamous cell carcinoma or fibrosarcoma. J Am Vet Med Assoc. 2018;253(1):73-83
106. Fulton AJ, Nemec A, Murphy BG, Kass PH, Verstraete FJ. Risk factors associated with survival in dogs with nontonsillar oral squamous cell carcinoma 31 cases (1990-2010). J Am Vet Med Assoc. 2013;243(5):696-702
107. Dickerson VM, Grimes JA, Vetter CA, Colopy SA, Duval JM, Northrup NC, et al. Outcome following cosmetic rostral nasal reconstruction after planectomy in 26 dogs. Vet Surg. 2018;48(1):64-9
108. Supsavhad W, Dirksen WP, Martin CK, Rosol TJ. Animal models of head and neck squamous cell carcinoma. Vet J. 2016;210:7-16
109. Méry B, Rancoule C, Guy J-B, Espenel S, Wozny A-S, Battiston-Montagne P, et al. Preclinical models in HNSCC: A comprehensive review. Oral Oncol. 2017;65:51-6

110. Costales M, López F, García-Inclán C, Fernández S, Marcos CÁ, Llorente JL, et al. Establishment and characterization of an orthotopic sinonasal squamous cell carcinoma mouse model. Head Neck. 2014;37(12):1769-75
111. Henson B, Li F, Coatney DD, Carey TE, Mitra RS, Kirkwood KL, et al. An orthotopic floor-of-mouth model for locoregional growth and spread of human squamous cell carcinoma. J Oral Pathol Med. 2007;36(6):363-70
112. Carper MB, Troutman S, Wagner BL, Byrd KM, Selitsky SR, Parag-Sharma K, et al. An Immunocompetent Mouse Model of HPV16(+) Head and Neck Squamous Cell Carcinoma. Cell Rep. 2019;29(6):1660-74
113. Cannon CM. Cats, Cancer and Comparative Oncology. Vet Sci. 2015;2(3):111-26
114. Ballegeer EA, Madrill NJ, Berger KL, Agnew DW, McNiel EA. Evaluation of hypoxia in a feline model of head and neck cancer using ^{64}Cu-ATSM positron emission tomography/computed tomography. BMC Cancer. 2013;13
115. Cai S, Zhang T, Forrest WC, Yang Q, Groer C, Mohr E, et al. Phase I/II Clinical Trial of Hyaluronan-Cisplatin Nanoconjugate for the Treatment of Spontaneous Canine Cancers. Am J Vet Res. 2016;77(9):1005-16
116. Liu D, Xiong H, Ellis AE, Northrup NC, Dobbin KK, Shin DM, et al. Canine Spontaneous Head and Neck Squamous Cell Carcinomas Represent Their Human Counterparts at the Molecular Level. PLoS Genet. 2015;11(6)
117. Porcellato I, Brachelente C, Guelfi G, Reginato A, Sforna M, Bongiovanni L, et al. A Retrospective Investigation on Canine Papillomavirus 1 (CPV1) in Oral Oncogenesis Reveals Dogs Are Not a Suitable Animal Model for High-Risk HPV-Induced Oral Cancer. PLoS One. 2014;9(11)
118. Lyman GH, Cassidy J, Bissett D, Spence RAJ, Payne M. Oxford American Handbook of Oncology. 1 ed. New York: Oxford University Press, Inc.; 2009.
119. Boustani J, Grapin M, Laurent P-A, Apetoh L, Mirjolet C. The 6th R of Radiobiology: Reactivation of Anti-Tumor Immune Response. Cancers 2019;11(6)
120. Steel GG, McMillan TJ, Peacock JH. The 5Rs of radiobiology. Int J Radiat Biol. 1989;56(6):1045-8
121. Sharabi AB, Nirschl CJ, Kochel CM, Nirschl TR, Francica BJ, Velarde E, et al. Stereotactic Radiation Therapy Augments Antigen-Specific PD-1-Mediated Antitumor Immune Responses via Cross-Presentation of Tumor Antigen. Cancer Immunol Res. 2015;3(4):345-55
122. Schuler PJ, Harasymczuk M, Schilling B, Saze Z, Strauss L, Lang S, et al. Effects of Adjuvant Chemoradiotherapy on the Frequency and Function of Regulatory T Cells in Patients with Head and Neck Cancer. Clin Cancer Res. 2013;19(23):6585-96
123. Al-Taei S, Banner R, Powell N, Evans M, Palaniappan N, Tabi Z, et al. Decreased HPV-specific T cell responses and accumulation of immunosuppressive influences in oropharyngeal cancer patients following radical therapy. Cancer Immunol Immunother. 2013;62(12):1821-30
124. Dovedi SJ, Adlard AL, Lipowska-Bhalla G, McKenna C, Jones S, Cheadle EJ, et al. Acquired Resistance to Fractionated Radiotherapy Can Be Overcome by Concurrent PD-L1 Blockade. Cancer Res. 2014;74(19):5458-68
125. Sprung CN, Chao M, Leong T, McKay MJ. Chromosomal Radiosensitivity in Two Cell Lineages Derived from Clinically Radiosensitive Cancer Patients. Clin Cancer Res. 2005;11(17):6352-8

126. Haddad RI. Multidisciplinary Management of Head and Neck Cancer. 1 ed. New York Demos Medical Publishing; 2011.
127. Ward EC, van As-Brooks CJ. Head and Neck Cancer: Treatment, Rehabilitation, and Outcomes. 2 ed. San Diego Plural Publishing, Inc.; 2014.
128. Thomas Jr. CR, Heron DE, Tishler RB. Head and Neck Cancer. 2 ed. New York Demos Medical Publishing; 2011.
129. Ferreira BC, Sá-Couto P, Lopes MC, Khouri L. Compliance to radiation therapy of head and neck cancer patients and impact on treatment outcome. Clin Transl Oncol. 2016;18(7):677-84
130. Schmitz A, Bayer J, Déchamps N, Thomas G. Intrinsic susceptibility to radiation-induced apoptosis of human lymphocyte subpopulations. Int J Radiat Oncol Biol Phys. 2003;57(3):769-78
131. Wirsdörfer F, Jendrossek V. The Role of Lymphocytes in Radiotherapy-Induced Adverse Late Effects in the Lung. Front Immunol. 2016;7
132. Sage EK, Schmid TE, Geinitz H, Gehrmann M, Sedelmayr M, Duma MN, et al. Effects of definitive and salvage radiotherapy on the distribution of lymphocyte subpopulations in prostate cancer patients. Strahlenther Onkol. 2017;193(8):648-55
133. Dainiak N. Hematologic consequences of exposure to ionizing radiation. Exp Hematol. 2002;30(6):513-28
134. Gray WC, Chretien PB, Suter CM, Revie DR, Tomazic VT, Blanchard CL, et al. Effects of radiation therapy on T-lymphocyte subpopulations in patients with head and neck cancer. Otolaryngol Head Neck Surg. 1985;93(5):650-60
135. Dovšak T, Ihan A, Didanovič V, Kansky A, Verdenik M, Hren NI. Effect of surgery and radiotherapy on complete blood count, lymphocyte subsets and inflammatory response in patients with advanced oral cancer. BMC Cancer. 2018;18(1)
136. Balázs K, Kis E, Badie C, Bogdándi EN, Candéias S, Garcia LC, et al. Radiotherapy-Induced Changes in the Systemic Immune and Inflammation Parameters of Head and Neck Cancer Patients. Cancers 2019;11(9)
137. Stratton JA, Byfield PE, Byfield JE, Small RC, Benfield J, Pilch Y. A comparison of the Acute Effects of Radiation Therapy, Including or Excluding the Thymus, on the Lymphocyte Subpopulations of Cancer Patients. J Clin Invest. 1975;56(1):88-97
138. Wolf GT, Amendola BE, Diaz R, Lovett EJ, 3rd, Hammerschmidt RM, Peterson KA. Definite vs adjuvant radiotherapy. Comparative effects on lymphocyte subpopulations in patients with head and neck squamous carcinoma. Arch Otolaryngol. 1985;111(11):716-26
139. Kuss I, Hathaway B, Ferris RL, Gooding W, Whiteside TL. Imbalance in absolute counts of T lymphocyte subsets in patients with head and neck cancer and its relation to disease. Adv Otorhinolaryngol. 2005;62:161-72
140. Sage EK, Schmid TE, Sedelmayr M, Gehrmann M, Geinitz H, Duma MN, et al. Comparative analysis of the effects of radiotherapy versus radiotherapy after adjuvant chemotherapy on the composition of lymphocyte subpopulations in breast cancer patients. Radiother Oncol. 2016;118:176-80
141. Cho O, Oh Y-T, Chun M, Noh O-K, Hoe J-S, Kim H. Minimum absolute lymphocyte count during radiotherapy as a new prognostic factor for nasopharyngeal cancer. Head Neck. 2016;38 Suppl 1:E1061-E7

142. Huang J, Kaminski J, Campbell J, Stanton P, Al-Basheer A, Dasher B, et al. Low Baseline Lymphocyte Count May Predict Poorer Overall Survival in Patients With Head and Neck Cancer Treated With Radiation Therapy. Int J Radiat Oncol Biol Phys. 2014;90(1)
143. Cooper LJN, Mittendorf EA, Moyes J, Prabhakaran S. Immunotherapy in Translational Cancer Research. 1 ed. Hoboken, New Jersey: John Wiley & Sons, Inc.; 2018.
144. Sharma P, Allison JP. The future of immune checkpoint therapy. Cancer Immunol Immunother. 2015;348(6230):56-61
145. Ferris RL. Immunology and Immunotherapy of Head and Neck Cancer. J Clin Oncol. 2015;33(29):3293-304
146. Mei Z, Huang J, Qiao B, Lam AK. Immune checkpoint pathways in immunotherapy for head and neck squamous cell carcinoma. Int J Oral Sci. 2020;12
147. Cohen EEW, Bell RB, Bifulco CB, Burtness B, Gillison ML, Harrington KJ, et al. The Society for Immunotherapy of Cancer consensus statement on immunotherapy for the treatment of squamous cell carcinoma of the head and neck (HNSCC). J Immunother Cancer. 2019;7(1)
148. Leemans CR, Snijders PJF, Brakenhoff RH. The molecular landscape of head and neck cancer. Nat Rev Cancer. 2018;18(5):269-82
149. O'Sullivan B, Brierly JD, D'Cruz AK, Fey MF, Pollock R, Vermorken JB, et al. UICC Manual of Clinical Oncology. 9 ed. Hoboken: John Wiley & Sons, Inc.; 2015.
150. Febbo PG, Ladanyi M, Aldape KD, De Marzo AM, Hammond ME, Hayes DF, et al. NCCN Task Force report: Evaluating the clinical utility of tumor markers in oncology. J Natl Compr Canc Netw. 2011;9 Suppl 5:S1-S33
151. Sauerbrei W, Taube SE, McShane LM, Cavenagh MM, Altman DG. Reporting Recommendations for Tumor Marker Prognostic Studies (REMARK): An Abridged Explanation and Elaboration. JNCI Natl Cancer Inst. 2018;110(8):803-11
152. DeVita Jr VT, Hellman S, Rosenberg SA. Cancer: Principles & Practice of Oncology: Annual Advances in Oncology. 1 ed: Lippincott Williams & Wilkins (Wolters Kluwer); 2011.
153. Ow TJ, Pitts CE, Kabarriti R, Garg MK. Effective Biomarkers and Radiation Treatment in Head and Neck Cancer. Arch Pathol Lab Med. 2015;139(11):1379-88
154. Gleber-Netto FO, Rao X, Guo T, Xi Y, Gao M, Shen L, et al. Variations in HPV function are associated with survival in squamous cell carcinoma. JCI Insight. 2019;4(1)
155. Gavrielatou N, Doumas S, Economopoulou P, Foukas PG, Psyrri A. Biomarkers for immunotherapy response in head and neck cancer. Cancer Treat Rev. 2020;84
156. Deng Z, Hasegawa M, Aoki K, Matayoshi S, Kiyuna A, Yamashita Y, et al. A comprehensive evaluation of human papillomavirus positive status and p16INK4a overexpression as a prognostic biomarker in head and neck squamous cell carcinoma. Int J Oncol. 2014;45(1):67-76
157. Topalian SL, Taube JM, Anders RA, Pardoll DM. Mechanism-driven biomarkers to guide immune checkpoint blockade in cancer therapy. Nat Rev Cancer. 2016;16(5):275-87

158. Tsakiroglou AM, Fergie M, Oguejiofor K, Linton K, Thomson D, Stern PL, et al. Spatial proximity between T and PD-L1 expressing cells as a prognostic biomarker for oropharyngeal squamous cell carcinoma. Br J Cancer. 2020;122(4):539-44
159. Goldstein I, Marcel V, Olivier M, Oren M, Rotter V, Hainaut P. Understanding wild-type and mutant p53 activities in human cancer: new landmarks on the way to targeted therapies. Cancer Gene Ther. 2011;18(1):2-11
160. Schmidt H, Kulasinghe A, Perry C, Nelson C, Punyadeera C. A liquid biopsy for head and neck cancers. Expert Rev Mol Diagn. 2016;16(2):165-72
161. Swiecicki PL, Brennan JR, Mierzwa M, Spector ME, Brenner JC. Head and Neck Squamous Cell Carcinoma Detection and Surveillance: Advances of Liquid Biomarkers. Laryngoscope. 2019;129(8):1836-43
162. Diaz Jr LA, Bardelli A. Liquid biopsies: genotyping circulating tumor DNA. J Clin Oncol. 2014;32(6):579-86
163. Lin M-C, Huang M-C, Lou P-J. Anti-C1GALT1 Autoantibody Is a Novel Prognostic Biomarker for Patients With Head and Neck Cancer. Laryngoscope. 2020;00:1-7
164. Tinhofer I, Konschak R, Stromberger C, Raguse J-D, Dreyer JH, Jöhrens K, et al. Detection of circulating tumor cells for prediction of recurrence after adjuvant chemoradiation in locally advanced squamous cell carcinoma of the head and neck. Ann Oncol. 2014;25(10):2042-7
165. Damerla RR, Lee NY, You D, Soni R, Shah R, Reyngold M, et al. Detection of Early Human Papillomavirus-Associated Cancers by Liquid Biopsy. JCO Precis Oncol. 2019;3(3):1-17
166. Strati A, Koutsodontis G, Papaxoinis G, Angelidis I, Zavridou M, Economopoulou P, et al. Prognostic significance of PD-L1 expression on circulating tumor cells in patients with head and neck squamous cell carcinoma. Ann Oncol. 2017;28(8):1923-33
167. Testi R, D'Ambrosio D, De Maria R, Santoni A. The CD69 receptor: a multipurpose cell-surface trigger for hematopoietic cells. Immunol Today. 1994;15(10):479-83
168. Lindsey WB, Lowdell MW, Marti GE, Abbasi F, Zenger V, King KM, et al. CD69 expression as an index of T-cell function: assay standardization, validation and use in monitoring immune recovery. Cytotherapy. 2007;9(2):123-32
169. Barclay AN, Brown MH, Law SKA, McKnight AJ, Tomlinson MG, van der Merwe PA. The Leucocyte Antigen Factsbook. 2 ed. San Diego, CA: Academic Press; 1997.
170. Caruso A, Licenziati S, Corulli M, Canaris AD, De Francesco MA, Fiorentini S, et al. Flow cytometric analysis of activation markers on stimulated T cells and their correlation with cell proliferation. Cytometry. 1997;27(1):71-6
171. Cibrian D, Sanchez-Madrid F. CD69: from activation marker to metabolic gatekeeper. Eur J Immunol. 2017;47(6):946-53
172. Craston R, Koh M, Mc Dermott A, Ray N, Prentice HG, Lowdell MW. Temporal dynamics of CD69 expression on lymphoid cells. J Immunol Methods. 1997;209(1):37-45
173. Simms PE, Ellis TM. Utility of flow cytometric detection of CD69 expression as a rapid method for determining poly- and oligoclonal lymphocyte activation. Clin Diagn Lab Immunol. 1996;3(3):301-4

174. Mita Y, Kimura MY, Hayashizaki K, Koyama-Nasu R, Ito T, Motohashi S, et al. Crucial role of CD69 in anti-tumor immunity through regulating the exhaustion of tumor-infiltrating T cells. Int Immunol. 2018;30(12):559-67
175. Starska K, Głowacka E, Kulig A, Lewy-Trenda I, Bryś M, Lewkowicz P. The role of tumor cells in the modification of T lymphocytes activity--the expression of the early CD69+, CD71+ and the late CD25+, CD26+, HLA/DR+ activation markers on T CD4+ and CD8+ cells in squamous cell laryngeal carcinoma. Part I. Folia Histochem Cytobiol. 2011;49(4):579-92
176. Bose A, Chakraborty T, Chakraborty K, Pal S, Baral R. Dysregulation in immune functions is reflected in tumor cell cytotoxicity by peripheral blood mononuclear cells from head and neck squamous cell carcinoma patients. Cancer Immun. 2008;8
177. Aarstad HJ, Heimdal J-H, Klementsen B, Olofsson J, Ulvestad E. Presence of activated T lymphocytes in peripheral blood of head and neck squamous cell carcinoma patients predicts impaired prognosis. Acta Otolaryngol. 2006;126(12):1326-33
178. Okazaki T, Chikuma S, Iwai Y, Fagarasan S, Honjo T. A rheostat for immune responses: the unique properties of PD-1 and their advantages for clinical application. Nat Immunol. 2013;14(12):1212-8
179. O'Neill RE, Cao X. Co-stimulatory and co-inhibitory pathways in cancer immunotherapy. Adv Cancer Res. 2019;143:145-94
180. Liao P, Wang H, Tang Y-l, Tang Y-J, Liang X-h. The Common Costimulatory and Coinhibitory Signaling Molecules in Head and Neck Squamous Cell Carcinoma. Front Immunol. 2019;10
181. Baumeister SH, Freeman GJ, Dranoff G, Sharpe AH. Coinhibitory Pathways in Immunotherapy for Cancer. Annu Rev Immunol. 2016;34:539-73
182. Rich RR, Fleisher TA, Shearer WT, Schroeder HW, Frew AJ, Weyand CM. Clinical Immunology: Principles and Practice. 5 ed: Elsevier Ltd; 2019.
183. Freeman GJ, Long AJ, Iwai Y, Bourque K, Chernova T, Nishimura H, et al. Engagement of the PD-1 Immunoinhibitory Receptor by a Novel B7 Family Member Leads to Negative Regulation of Lymphocyte Activation. J Exp Med. 2000;192(7):1027-34
184. O'Sullivan D, Sanin DE, Pearce EJ, Pearce EL. Metabolic interventions in the immune response to cancer. Nat Rev Immunol. 2019;19(5):324-35
185. Wherry EJ. T cell exhaustion. Nat Immunol. 2011;12(6):492-9
186. Puntigam L, Jeske S, Brunner C, Hoffmann T, Schuler P. Immune checkpoint expression on lymphocyte populations in head and neck cancer patients. Laryngo Rhino Otol. 2018;97(S02):S122-S3
187. Chemnitz JM, Parry RV, Nichols KE, June CH, Riley JL. SHP-1 and SHP-2 Associate with Immunoreceptor Tyrosine-Based Switch Motif of Programmed Death 1 upon Primary Human T Cell Stimulation, but Only Receptor Ligation Prevents T Cell Activation. J Immunol. 2004;173(2):945-54
188. Lee J-R, Bechstein DJB, Ooi CC, Patel A, Gaster RS, Ng E, et al. Magneto-nanosensor platform for probing low-affinity protein-protein interactions and identification of a low-affinity PD-L1/PD-L2 interaction. Nat Commun. 2016;7
189. Pai SI, Cohen EEW, Lin D, Fountzilas G, Kim ES, Mehlhorn H, et al. SUPREME-HN: a retrospective biomarker study assessing the prognostic value of PD-L1 expression in patients with recurrent and/or metastatic squamous cell carcinoma of the head and neck. J Transl Med. 2019;17

190. Ou D, Adam J, Garberis I, Blanchard P, Nguyen F, Levy A, et al. Clinical relevance of tumor infiltrating lymphocytes, PD-L1 expression and correlation with HPV/p16 in head and neck cancer treated with bio- or chemo-radiotherapy. Oncoimmunology. 2017;6(9)
191. Chen S-W, Li S-H, Shi D-B, Jiang W-M, Song M, Yang A-K, et al. Expression of PD-1/PD-L1 in head and neck squamous cell carcinoma and its clinical significance. Int J Biol Markers. 2019;34(4):398-405
192. Müller T, Braun M, Dietrich D, Aktekin S, Höft S, Kristiansen G, et al. PD-L1: a novel prognostic biomarker in head and neck squamous cell carcinoma. Oncotarget. 2017;8(32):52889-900
193. Shi LZ, Goswami S, Fu T, Guan B, Chen J, Xiong L, et al. Blockade of CTLA-4 and PD-1 Enhances Adoptive T-cell Therapy Efficacy in an ICOS-Mediated Manner. Cancer Immunol Res. 2019;7(11):1803-12
194. Shapiro HM. Practical Flow Cytometry. 4 ed. Hoboken, NJ: John Wiley & Sons, Inc.; 2003.
195. Jahan-Tigh RR, Ryan C, Obermoser G, Schwarzenberger K. Flow cytometry. J Invest Dermatol. 2012;132(10)
196. Wild D. The Immunoassay Handbook: Theory and Applications of Ligand Binding, ELISA and Related Techniques. 4 ed. Oxford: Elsevier Ltd.; 2013.
197. Gan SD, Patel KR. Enzyme Immunoassay and Enzyme-Linked Immunosorbent Assay. J Invest Dermatol. 2013;133(9)
198. Manchanda P, Sharma SC, Das SN. Differential regulation of IL-2 and IL-4 in patients with tobacco-related oral squamous cell carcinoma. Oral Dis. 2006;12(5):455-62
199. Louagie H, M. vE, Philippe J, Thierens H, de Ridder L. Changes in peripheral blood lymphocyte subsets in patients undergoing radiotherapy. Int J Radiat Biol. 1999;75(6):767-71
200. Accomando WP, Wiencke JK, Houseman EA, Butler RA, Zheng S, Nelson HH, et al. Decreased NK Cells in Patients with Head and Neck Cancer Determined in Archival DNA. Clin Cancer Res. 2012;18(22):6147-54
201. Böttcher A, Ostwald J, Guder E, Pau HW, Kramp B, Dommerich S. Distribution of circulating natural killer cells and T lymphocytes in head and neck squamous cell carcinoma. Auris Nasus Larynx. 2013;40(2):216-21
202. Wulff S, Pries R, Börngen K, Trenkle T, Wollenberg B. Decreased Levels of Circulating Regulatory NK Cells in Patients with Head and Neck Cancer throughout all Tumor Stages. Anticancer Res. 2009;29(8):3053-8
203. Melioli G, Semino C, Margarino G, Mereu P, Scala M, Cangemi G, et al. Expansion of natural killer cells in patients with head and neck cancer: detection of "noninhibitory" (activating) killer Ig-like receptors on circulating natural killer cells. Head Neck. 2003;25(4):297-305
204. Lechner A, Schlößer H, Rothschild SI, Thelen M, Reuter S, Zentis P, et al. Characterization of tumor-associated T-lymphocyte subsets and immune checkpoint molecules in head and neck squamous cell carcinoma. Oncotarget. 2017;8(27):44418-33
205. Lechner A, Schlößer HA, Thelen M, Wennhold K, Rothschild SI, Gilles R, et al. Tumor-associated B cells and humoral immune response in head and neck squamous cell carcinoma. Oncoimmunology. 2019;8(3)

206. Kim SS, Shen S, Miyauchi S, Sanders PD, Franiak-Pietryga I, Mell LK, et al. B Cells Improve Overall Survival in HPV-Associated Squamous Cell Carcinomas and Are Activated by Radiation and PD-1 Blockade. Clin Cancer Res. 2020;26(13):3345-59
207. Watermann C, Pasternack H, Idel C, Ribbat-Idel J, Brägelmann J, Kuppler P, et al. Recurrent HNSCC Harbor an Immunosuppressive Tumor Immune Microenvironment Suggesting Successful Tumor Immune Evasion. Clin Cancer Res. 2021;27(2):632-44
208. Verastegui EL, Morales RB, Barrera-Franco JL, Poitevin AC, Hadden J. Long-term immune dysfunction after radiotherapy to the head and neck area. Int Immunopharmacol. 2003;3(8):1093-104
209. Fukushima Y, Someya M, Nakata K, Hori M, Kitagawa M, Hasegawa T, et al. Influence of PD-L1 expression in immune cells on the response to radiation therapy in patients with oropharyngeal squamous cell carcinoma. Radiother Oncol. 2018;129(2):409-14
210. Campian J, Sarai G, Ye X, Marur S, Grossman SA. Association between severe treatment-related lymphopenia and progression-free survival in patients with newly diagnosed squamous cell head and neck cancer. Head Neck. 2014;36(12):1747-53
211. Kobayashi K, Tanaka Y, Horiguchi S, Yamamoto S, Toshinori N, Sugimoto A, et al. The effect of radiotherapy on NKT cells in patients with advanced head and neck cancer. Cancer Immunol Immunother. 2010;59(10):1503-9
212. Weiss J, Sheth S, Deal AM, Grilley Olson JE, Patel S, Hackman TG, et al. Concurrent Definitive Immunoradiotherapy for Patients with Stage III-IV Head and Neck Cancer and Cisplatin Contraindication. Clin Cancer Res. 2020;26(16):4260-7
213. Johnke RM, Edwards JM, Kovacs CJ, Evans MJ, Daly BM, Karlsson UL, et al. Response of T Lymphocyte Populations in Prostate Cancer Patients Undergoing Radiotherapy: Influence of Neoajuvant Total Androgen Suppression. Anticancer Res. 2005;25(4):3159-66
214. Lv Y, Song M, Tian X, Yv X, Liang N, Zhang J. Impact of radiotherapy on circulating lymphocyte subsets in patients with esophageal cancer. Medicine 2020;99(36)
215. Sangthawan D, Phungrassami T, Sinkitjarurnchai W. Effects of Zinc Sulfate Supplementation on Cell-Mediated Immune Response in Head and Neck Cancer Patients Treated with Radiation Therapy. Nutr Cancer. 2015;67(3):449-56
216. Lee S, Cho O, Chun M, Chang SJ, Kong TW, Lee EJ, et al. Association Between Radiation Tolerance of Lymphocytes and Clinical Outcomes in Cervical Cancer. In Vivo. 2019;33(6):2191-8
217. Wang X-B, Wu D-J, Chen W-P, Liu J, Ju Y-J. Impact of radiotherapy on immunological parameters, levels of inflammatory factors, and clinical prognosis in patients with esophageal cancer. J Radiat Res. 2019;60(3):353-63
218. Theodoraki MN, Lorenz K, Lotfi R, Fürst D, Tsamadou C, Jaekle S, et al. Influence of photodynamic therapy on peripheral immune cell populations and cytokine concentrations in head and neck cancer. Photodiagnosis Photodyn Ther. 2017;19:194-201
219. Kaffenberger W, Hölzer-Müller L, Auberger T, Clasen B, Hohlmeier G, van Beuningen D. An immunological outcome predictive score for head and neck carcinoma patients. Strahlenther Onkol. 1995;171(8):444-53

220. Olkowski ZL, McLaren JR, Skeen MJ. Effects of combined immunotherapy with levamisole and Bacillus Calmette-Guérin on immunocompetence of patients with squamous cell carcinoma of the cervix, head and neck, and lung undergoing radiation therapy. Cancer Treat Rep. 1978;62(11):1651-61
221. Góes EG, Borges JC, Covas DT, Orellana MD, Palma PVB, Morais FR, et al. Quality control of blood irradiation: determination T cells radiosensitivity to cobalt-60 gamma rays. Transfusion. 2006;46(1):34-40
222. Sieber G, Zierach P, Herrmann F, Brust VJ, Rühl H. Impaired B lymphocyte reactivity in patients after radiotherapy. Int J Radiat Oncol Biol Phys. 1985;11(4):777-82
223. Andrade MC, Ferreira SB, Gonçalves LC, De-Paula AM, de Faria ES, Teixeira-Carvalho A, et al. Cell surface markers for T and B lymphocytes activation and adhesion as putative prognostic biomarkers for head and neck squamous cell carcinoma. Hum Immunol. 2013;74(12):1563-74
224. Schantz SP, Ordonez NG. Quantitation of natural killer cell function and risk of metastatic poorly differentiated head and neck cancer. Nat Immun Cell Growth Regul. 1991;10(5):278-88
225. Schantz SP, Campbell BH, Guillamondegui OM. Pharyngeal Carcinoma and Natural Killer Cell Activity. Am J Surg. 1986;152(4):467-74
226. Johnson SD, Levingston C, Young MRL. Premalignant Oral Lesion Cells Elicit Increased Cytokine Production and Activation of T-cells. Anticancer Res. 2016;36(7):3261-70
227. Aarstad HJ, Vintermyr OK, Ulvestad E, Aarstad HH, Kross KW, Heimdal JH. Peripheral blood monocyte and T-lymphocyte activation levels at diagnosis predict long-term survival in head and neck squamous cell carcinoma patients. APMIS. 2015;123(4):305-14
228. Ryan N, Anderson K, Volpedo G, Hamza O, Varikuti S, Satoskar AR, et al. STAT1 inhibits T-cell exhaustion and myeloid derived suppressor cell accumulation to promote antitumor immune responses in head and neck squamous cell carcinoma. Int J Cancer. 2020;146(6):1717-29
229. Mazzoni A, Maggi L, Montaini G, Ramazzotti M, Capone M, Vanni A, et al. Human T cells interacting with HNSCC-derived mesenchymal stromal cells acquire tissue-resident memory like properties. Eur J Immunol. 2020;50(10):1571-9
230. Piersiala K, Farrajota Neves da Silva P, Hjalmarsson E, Kolev A, Kågedal Å, Starkhammar M, et al. CD4+ and CD8+ T cells in sentinel nodes exhibit distinct pattern of PD-1, CD69, and HLA-DR expression compared to tumor tissue in oral squamous cell carcinoma. Cancer Sci. 2021;00:1-12
231. Kågedal Å, Hjalmarsson E, Farrajota Neves da Silva P, Piersiala K, Kumlien Georén S, Margolin G, et al. Activation of T helper cells in sentinel node predicts poor prognosis in oral squamous cell carcinoma. Sci Rep. 2020;10(1)
232. Zhang Y, Zhang Z, Zhang L, Zhao S, Zhao J, Ye Q, et al. Clinical Implications of Peripheral CD3+CD69+ T-Cell And CD8+CD28+ T-Cell Proportions in Patients Prior to Radical Prostatectomy. Urol J. 2020;17(3):257-61
233. Taylor ES, McCall JL, Shen S, Girardin A, Munro FM, Black MA, et al. Prognostic roles for IL-2-producing and CD69(+) T cell subsets in colorectal cancer patients. Int J Cancer. 2018;143(8):2008-16

234. Wei S-M, Pan H-L, Wang L, Yin G-L, Zhong K, Zhou Y, et al. Combination therapy with dendritic cell-based vaccine and anti-CD69 antibody enhances antitumor efficacy in renal cell carcinoma-bearing mice. Turk J Med Sci. 2017;47(2):658-67
235. Esplugues E, Sancho D, Vega-Ramos J, Martínez-A C, Syrbe U, Hamann A, et al. Enhanced antitumor immunity in mice deficient in CD69. J Exp Med. 2003;197(9):1093-106
236. Theodoraki M-N, Yerneni SS, Hoffmann TK, Gooding WE, Whiteside TL. Clinical Significance of PD-L1(+) Exosomes in Plasma of Head and Neck Cancer Patients. Clin Cancer Res. 2018;24(4):896-905
237. Goto M, Chamoto K, Higuchi K, Yamashita S, Noda K, Iino T, et al. Analytical performance of a new automated chemiluminescent magnetic immunoassays for soluble PD-1, PD-L1, and CTLA-4 in human plasma. Sci Rep. 2019;9(1)
238. Aghajani MJ, Roberts TL, Yang T, McCafferty CE, Caixeiro NJ, DeSouza P, et al. Elevated levels of soluble PD-L1 are associated with reduced recurrence in papillary thyroid cancer. Endocr Connect. 2019;8(7):1040-51
239. Bian B, Fanale D, Dusetti N, Roque J, Pastor S, Chretien A-S, et al. Prognostic significance of circulating PD-1, PD-L1, pan-BTN3As, BTN3A1 and BTLA in patients with pancreatic adenocarcinoma. Oncoimmunology. 2019;8(4)
240. Okuma Y, Hosomi Y, Nakahara Y, Watanabe K, Sagawa Y, Homma S. High plasma levels of soluble programmed cell death ligand 1 are prognostic for reduced survival in advanced lung cancer. Lung Cancer. 2017;104:1-6
241. Wang H, Mao L, Zhang T, Zhang L, Wu Y, Guo W, et al. Altered expression of TIM-3, LAG-3, IDO, PD-L1, and CTLA-4 during nimotuzumab therapy correlates with responses and prognosis of oral squamous cell carcinoma patients. J Oral Pathol Med. 2019;00:1-8
242. Yoshida S, Nagatsuka H, Nakano K, Kogashiwa Y, Ebihara Y, Yano M, et al. Significance of PD-L1 Expression in Tongue Cancer Development. Int J Med Sci. 2018;15(14):1723-30
243. Ma BBY, Lim W-T, Goh B-C, Hui EP, Lo K-W, Pettinger A, et al. Antitumor Activity of Nivolumab in Recurrent and Metastatic Nasopharyngeal Carcinoma: An International, Multicenter Study of the Mayo Clinic Phase 2 Consortium (NCI-9742). J Clin Oncol. 2018;36(14):1412-8
244. Ferris RL, Blumenschein Jr. G, Fayette J, Guigay J, Colevas AD, Licitra L, et al. Nivolumab for Recurrent Squamous-Cell Carcinoma of the Head and Neck. N Engl J Med. 2016;375(19):1856-67
245. Tran L, Allen CT, Xiao R, Moore E, Davis R, Park S-J, et al. Cisplatin Alters Antitumor Immunity and Synergizes with PD-1/PD-L1 Inhibition in Head and Neck Squamous Cell Carcinoma. Cancer Immunol Res. 2017;5(12):1141-51
246. Schulz D, Stancev I, Sorrentino A, Menevse A-N, Beckhove P, Brockhoff G, et al. Increased PD-L1 expression in radioresistant HNSCC cell lines after irradiation affects cell proliferation due to inactivation of GSK-3beta. Oncotarget. 2019;10(5):573-83
247. Lyu X, Zhang M, Li G, Jiang Y, Qiao Q. PD-1 and PD-L1 Expression Predicts Radiosensitivity and Clinical Outcomes in Head and Neck Cancer and is Associated with HPV Infection. J Cancer. 2019;10(4):937-48
248. Hong AM, Ferguson P, Dodds T, Jones D, Li M, Yang J, et al. Significant association of PD-L1 expression with human papillomavirus positivity and its prognostic impact in oropharyngeal cancer. Oral Oncol. 2019;92:33-9

249. Lilja-Fischer JK, Eriksen JG, Georgsen JB, Vo TT, Larsen SR, Cheng J, et al. Prognostic impact of PD-L1 in oropharyngeal cancer after primary curative radiotherapy and relation to HPV and tobacco smoking. Acta Oncol. 2020;59(6):666-72
250. Steuer CE, Griffith CC, Nannapaneni S, Patel MR, Liu Y, Magliocca KR, et al. A Correlative Analysis of PD-L1, PD-1, PD-L2, EGFR, HER2, and HER3 Expression in Oropharyngeal Squamous Cell Carcinoma. Mol Cancer Ther. 2018;17(3):710-6
251. Birtalan E, Danos K, Gurbi B, Brauswetter D, Halasz J, Kalocsane Piurko V, et al. Expression of PD-L1 on Immune Cells Shows Better Prognosis in Laryngeal, Oropharygeal, and Hypopharyngeal Cancer. Appl Immunohistochem Mol Morphol. 2018;26(7):e79-e85
252. Chang P-H, Wu M-H, Liu S-Y, Wang H-M, Huang W-K, Liao C-T, et al. The Prognostic Roles of Pretreatment Circulating Tumor Cells, Circulating Cancer Stem-Like Cells, and Programmed Cell Death-1 Expression on Peripheral Lymphocytes in Patients with Initially Unresectable, Recurrent or Metastatic Head and Neck Cancer: An Exploratory Study of Three Biomarkers in One-time Blood Drawing. Cancers 2019;11(4)
253. Mosca A, Gibson D, Mason SL, Dobson J, Giuliano A. A possible role of coarse fractionated radiotherapy in the management of gingival squamous cell carcinoma in dogs: a retrospective study of 21 cases from two referral centers in the UK. J Vet Med Sci. 2021
254. Mayer MN, DeWalt JO, Sidhu N, Mauldin GN, Waldner CL. Outcomes and adverse effects associated with stereotactic body radiation therapy in dogs with nasal tumors: 28 cases (2011-2016). J Am Vet Med Assoc. 2019;254(5):602-12
255. Clermont T, LeBlanc AK, Adams WH, LeBlanc CJ, Bartges JW. Radiotherapy-induced myelosuppression in dogs: 103 cases (2002-2006). Vet Comp Oncol. 2012;10(1):24-32
256. Kent MS, Emami S, Rebhun R, Theon A, Hansen K, Sparger E. The effects of local irradiation on circulating lymphocytes in dogs receiving fractionated radiotherapy. Vet Comp Oncol. 2020;18(2):191-8
257. Prümmer O, Raghavachar A, Fliedner TM. Recovery of immune functions in dogs after total body irradiation and transplantation of autologous blood or bone marrow cells. Exp Hematol. 1985;13(9):891-8
258. Stankeová S, Crompton NEA, Blattmann H, Theiler P, Emery GC, Roos M, et al. Apoptotic Response of Irradiated T-Lymphocytes: An Epidemiologic Study in Canine Radiotherapy Patients. Strahlenther Onkol. 2003;179(11):779-86
259. Fujii Y, Yurkon CR, Maeda J, Genet SC, Kubota N, Fujimori A, et al. Comparative study of radioresistance between feline cells and human cells. Radiat Res. 2013;180(1):70-7
260. Dyck JA, Shifrine M, Klein AK, Rosenblatt LS, Kawakami T. Spontaneous Cell-Mediated Cytolysis by Peripheral Blood Cells Obtained from Whole-Body Chronically Irradiated Beagle Dogs. Radiat Res. 1986;106(1):31-40
261. Dow S. A Role for Dogs in Advancing Cancer Immunotherapy Research. Front Immunol. 2019;10
262. Maekawa N, Konnai S, Okagawa T, Nishimori A, Ikebuchi R, Izumi Y, et al. Immunohistochemical Analysis of PD-L1 Expression in Canine Malignant Cancers and PD-1 Expression on Lymphocytes in Canine Oral Melanoma. PLoS ONE. 2016;11(6)

263. Tagawa M, Kurashima C, Takagi S, Maekawa N, Konnai S, Shimbo G, et al. Evaluation of costimulatory molecules in dogs with B cell high grade lymphoma. PLoS ONE. 2018;13(7)
264. Shosu K, Sakurai M, Inoue K, Nakagawa T, Sakai H, Morimoto M, et al. Programmed Cell Death Ligand 1 Expression in Canine Cancer. In Vivo. 2016;30(3):195-204
265. Hartley G, Faulhaber E, Caldwell A, Coy J, Kurihara J, Guth A, et al. Immune regulation of canine tumour and macrophage PD-L1 expression. Vet Comp Oncol. 2017;15(2):534-49
266. Hartley G, Elmslie R, Dow S, Guth A. Checkpoint molecule expression by B and T cell lymphomas in dogs. Vet Comp Oncol. 2018;16(3):352-60
267. Kumar SR, Kim DY, Henry CJ, Bryan JN, Robinson KL, Eaton AM. Programmed death ligand 1 is expressed in canine B cell lymphoma and downregulated by MEK inhibitors. Vet Comp Oncol. 2017;15(4):1527-36
268. Nascimento C, Urbano AC, Gameiro A, Ferreira J, Correia J, Ferreira F. Serum PD-1/PD-L1 Levels, Tumor Expression and PD-L1 Somatic Mutations in HER2-Positive and Triple Negative Normal-Like Feline Mammary Carcinoma Subtypes. Cancers 2020;12(6)
269. Nemoto Y, Shosu K, Okuda M, Noguchi S, Mizuno T. Development and characterization of monoclonal antibodies against canine PD-1 and PD-L1. Vet Immunol Immunopathol. 2018;198:19-25
270. Maekawa N, Konnai S, Takagi S, Kagawa Y, Okagawa T, Nishimori A, et al. A canine chimeric monoclonal antibody targeting PD-L1 and its clinical efficacy in canine oral malignant melanoma or undifferentiated sarcoma. Sci Rep. 2017;7(1)
271. Withers SS, Moore PF, Chang H, Choi JW, McSorley SJ, Kent MS, et al. Multi-color Flow Cytometry for Evaluating Age-Related Changes in Memory Lymphocyte Subsets in Dogs. Dev Comp Immunol. 2018;87:64-74

V. Acknowledgements

Like many scientific papers, my work has been a major undertaking, the success of which is linked to the professional and emotional support of several people.

I am particularly pleased that **Herr Dr. Mathias Gehrmann** took me under his wing and accompanied me on this path with advice and action, good tips, an always open ear and tireless commitment. I have always appreciated your patience while explaining the FACS analysis and supporting the proper evaluation of the obtained data, as well as your emotional support when something did not instantly work out. Thank you very much for the great cooperation and time at the Klinikum Rechts der Isar.

In the same way I would like to thank **Herrn Univ.-Prof. Dr. Thomas Göbel**, who did not hesitate for a second to support my work and answer all of my questions. I am particularly impressed by your deep humanity towards all students and your selfless support in difficult hours. You have often given me the courage I needed to look ahead and not be sidetracked on my path. Thank you dearly for your help.

Furthermore, I would like to thank the other clinics taking part in the DKTK *HNprädBio* study for the seamless sending of the patients' blood samples and my **colleagues at the laboratory** who made the clean running of the experiments possible. Dear thanks to **Susanne Thein** for the pleasant and detailed learning about the practical execution of my experiments. I would also like to thank **Jana Kern** for her always open ear for technical questions as well as the joyful coffee breaks we have had together. I am looking forward to our next coffee.

I am eternally grateful to my **family**, especially my parents, who have always believed in me from childhood, never doubted me for a second and always helped me up. Thank you for always making everything possible, for giving me wings, and for continuously giving me your trust. A dear thank you to my uncle **Melvin L. DePamphilis** for showing me how to be passionate about my work and continuously planting seeds for my curiosity towards biological, chemical and medical subjects as well as scientific work.

I also especially thank my **close friends and my boyfriend** who have always cheered me on, but also provided for emotional relaxation, especially during the turbulent time before the levy. I am glad and truly feel lucky every day to know you in my life.